The Dissertation Committee for Brian Erik Dawes Certifies that this is the approved version of the following dissertation:

Human Neural Stem Cell-Derived Neuron/Astrocyte Co-Cultures as a Model System to Study Emerging Encephalitic Viruses

Committee:

Alexander Freiberg, Ph.D.
Supervisor or Mentor, Chair

Alan Barrett, Ph.D.

Gerald Campbell, M.D., Ph.D.

Benhur Lee, M.D., Ph.D.

Ping Wu, M.D., Ph.D.

Dean, Graduate School

Human Neural Stem Cell-Derived Neuron/Astrocyte Co-Cultures as a Model System to Study Emerging Encephalitic Viruses

by

Brian Erik Dawes, B.S.

Dissertation

Presented to the Faculty of the Graduate School of
The University of Texas Medical Branch
in Partial Fulfillment
of the Requirements
for the Degree of

Doctor of Philosophy

The University of Texas Medical Branch
August 2018

Dedication

This thesis is dedicated to my parents, Gary and Mary Dawes. Their support and encouragement throughout my entire education was essential, especially that of my mother. She instilled in me a love of reading, nature, and science from my earliest memories, and always encouraged me to learn more about whatever I was interested in at that point in time.

Acknowledgements

First, I would like to thank my mentor, Dr. Alexander Freiberg. You have given me so many fantastic opportunities, and been an excellent mentor and teacher. Thank you for being so available to discuss projects and problems, and for all of the advice, insight, feedback which allowed my projects to proceed. Lastly, thank you for making this journey fun and enjoyable. I can honestly say that I loved my time in your lab, and really enjoyed working with you.

I would also like to thank Dr. Ping Wu for her support throughout this collaboration. Thank you for allowing us to use the hNSC system that your lab has developed, and thank you for your help in designing experiments. I would particularly like to thank Dr. Junling Gao for helping provide cells during the early stages of this project, and for his patience in training me on the culture and differentiation of the hNSCs.

Additionally, thanks to my remaining supervisory committee members: Dr. Alan Barrett, Dr. Gerald Campbell, and Dr. Benhur Lee. Thank you all for your willingness to serve on my committee, and for the invaluable feedback you have provided which has helped shape this project. In addition to his role on my committee, I would like to thank Dr. Barrett for the opportunities he provided with the Sealy Institute for Vaccine Sciences internship, and the chance to work on the Zika virus pipeline analysis.

I have to thank all of the members of the Freiberg lab, past and present, who have been excellent mentors, colleagues, and friends. All of you have made the last 4 years very enjoyable. Thank you for all of your time while I was training in the BSL-3 and BSL-4. I would like to thank Terry Juelich for all of her work in making sure that the lab is running as well as possible, and for being able to take care of almost any issue that could possible arise. I must thank Terry, Jennifer Smith, and Dr. Lihong Zhang for all of the work that they did during animal experiments for the favipiravir project. David Perez was a more recent addition to the lab, but has also been extraordinarily helpful and become a good friend. I would also like to thank our postdocs, Dr. Colm Atkins, Dr. Olivier Escaffre, and Dr. Birte Kalveram for their advice and mentoring. I would especially like to thank Dr. Atkins for his frequent help and friendship. Our past postdocs, Dr. Terence Hill, Dr. Tanya Yun, and Dr. Kimberly Roberts deserve thanks as well for all their training on the basics of virology and working in biocontainment.

Lastly, I must thank my family and friends whose support has been unwavering. My parents, to whom this work is dedicated, have been the most constant support throughout my life. Thank you for your help, encouragement, interest, and love throughout this long journey. I would also like to thank my brother Kyle for always being available to talk to and have fun with. Finally, I want to thank my wife, Sofia Fanourakis. Thank you for your companionship and support. I can’t imagine I would have finished this process nearly as sane as I am without you. Thank you for taking such good care of me these last few weeks while I write all day, I owe you when it is your turn!

Human Neural Stem Cell-Derived Neuron/Astrocyte Co-Cultures as a Model System to Study Emerging Encephalitic Viruses

Publication No._____________

Brian Erik Dawes, Ph.D.

The University of Texas Medical Branch, 2018

Supervisor: Alexander Freiberg

Many emerging viral infections target the central nervous system. Such diseases often cause high fatality rates and high rates of neurologic sequelae such as behavioral changes, cognitive deficits, seizures, paralysis, or persistent infection. Relatively little is known about viral infections of cells within the central nervous system such as neurons and astrocytes. One challenge in studying central nervous system infection is the lack of suitable model systems to study infection in neurons and astrocytes. Animal based systems often require immunocompromise and may not be suitable for molecular mechanistic studies. *In vitro* systems often rely on cell lines of cancerous origin, which often have specific signaling defects that may impact cellular responses to infection. This study describes the establishment of a human neural stem cell derived neuron/astrocyte co-cultures system as a model to study encephalitic virus infection. This system provides a more physiologically relevant model that maintains critical interactions between neurons and astrocytes. Two emerging encephalitic viruses were studied using this system, La Crosse virus (LACV) and Nipah virus (NiV). LACV causes pediatric encephalitis in the United States, while NiV causes severe encephalitic and respiratory disease in Southern Asia. Neuron/astrocyte co-cultures were susceptible to LACV infection and displayed apoptotic responses as reported in previous *in vitro* and *in vivo* studies. Neurons and astrocytes were both targets of LACV infection, with neurons becoming the predominant target later in infection possibly due to astrocytic responses to interferon. Additionally, neuron/astrocyte co-cultures responded to LACV infection with strong proinflammatory cytokines and chemokines. In contrast, NiV replicated in both neurons and astrocytes, inhibited inflammatory cytokine/chemokine production, and produced delayed interferon-β responses. Interferon-β was shown to significantly reduce viral titer, apoptosis, and cytotoxicity. Interferon-β preferentially protected astrocytes from NiV infection. Additionally, while the type I interferon response reduced NiV infection, it was not able to fully eliminate it. These results suggest that the type I interferon response may play a role in establishing a persistent NiV infection. Together, these studies demonstrate the ability of this neuron/astrocyte system to respond to viral infection in a manner consistent with *in vivo* observations, and its usefulness in studying encephalitis pathogenesis.

TABLE OF CONTENTS

List of Tables

List of Figures

List of Abbreviations

ADHD	Attention-Deficit-Hyperactivity-Disorder
ANOVA	Analysis of Variance
BBB	Blood-Brain Barrier
BDV	Borna Disease Virus
BSL-4	Biosafety Level 4
CCL2	C-C Motif Chemokine Ligand 2
CCR2	C-C Chemokine Receptor 2
CEPI	Coalition for Epidemic Preparedness and Innovations
CedV	Cedar Virus
CFR	Case Fatality Rate
CNS	Central Nervous System
CPE	Cytopathic Effect
CSF	Cerebrospinal Fluid
CXCL10	C-X-C Motif Chemokine Ligand 10
DAPI	4',6-Diamidino-2-Phenylidole, Dihydrochloride
DC	Dendritic Cell
DC-SIGN	Dendritic Cell-Specific Intercellular Adhesion Molecule-3-Grabbing Non-Integrin
EEEV	Eastern Equine Encephalitis Virus
EGF	Epidermal Growth Factor
ERK1/2	Extracellular Signal Related Kinase 1/2
FACS	Fluorescence-Activated Cell Sorting
FGF	Fibroblast Growth Factor
GAS	Gamma Activated Sequences
G-CSF	Granulocyte Colony Stimulating Factor
GFAP	Glial Fibrillary Acidic Protein
GM-CSF	Granulocyte-Macrophage Colony Stimulating Factor
hESC	Human Embryonic Stem Cell
HeV	Hendra Virus
HIV	Human Immunodeficiency Virus
hMPV	Human Metapneumovirus
hNSC	Neural Stem Cell
HNV	Henipavirus
HPI	Hours Post-Infection
HSV	Herpes Simplex Virus
IFN	Interferon
IFNAR	IFN-Alpha/Beta Receptor
IFN-γR	IFN-γ Receptor
IgG	Immunoglobin G
IL	Interleukin
i.p.	Intraperitoneal

iPCs	Induced Pluripotent Cells
IRF	Interferon Regulatory Transcription Factor
ISG	Interferon Stimulated Gene
ISGF3	IFN-Stimulated Gene Factor Complex 3
JAK1	Janus Kinase 1
JEV	Japanese Encephalitis Virus
KV	Kumasi Virus
LACV	La Crosse Virus
LASV	Lassa Virus
LGP2	Laboratory of Genetics and Physiology 2
LIF	Leukocyte Inhibitory Factor
LPS	Lipopolysaccharide
MAP2	Microtubule Associated Protein 2
MAPK	Mitogen-Activated Protein Kinase
MAVS	Mitochondrial Antiviral-Signaling Protein
MDA5	Melanoma Differentiation-Associated Protein 5
MeV	Measles Virus
MHV	Mouse Hepatitis Virus
MIP-1α	Macrophage Inflammatory Protein 1 Alpha
MMP	Matrix Metallopeptidase
MOI	Multiplicity of Infection
MojV	Mojiang Virus
mTOR	Mammalian Target of Rapamycin
NHP	Non-Human Primate
NiV	Nipah Virus
NiV-B	NiV-Bangladesh Strain
NiV-M	NiV-Malaysia Strain
NLRP3	Nucleotide-Binding Domain and Leucine-Rich Repeat Containing Protein 3
ORF	Open Reading Frame
PDGF	Platelet-Derived Growth Factor
PFU	Plaque Forming Unit
p.o.	Perioral
Poly I:C	Polyinosinic:Polycytidylic Acid
RdRp	RNA-dependent RNA polymerase
RFU	Relative Fluorescence Unit
RIG-I	Retinoic Acid-Inducible Gene-I
RLR	RIG-I-Like Receptor
RLU	Relative Luminescence Unit
rNiV-eGFP	Recombinant NiV Expressing eGFP
rNiV-Gluc-eGFP	Recombinant NiV Expressing Gaussia Luciferase and eGFP
SARM1	Sterile Alpha and TIR Motif Containing 1
s.c.	Subcutaneous
SI	Selective Index
SinV	Sindbis Virus

SLAM	Signaling Leukocyte Activation Molecule
SSPE	Subacute Sclerosing Panencephalitis
STAT	Signal Transducer and Activator of Transcription
TIMP	Tissue Inhibitor of Metalloproteinase
TLR-3	Toll-Like Receptor 3
TNF-α	Tumor Necrosis Factor Alpha
TRIM25	Tripartite Motif-Containing Protein 25
TUNEL	Terminal Deoxynucleotidyl Transferase dUTP Nick-End Labeling
TYK2	Tyrosine Kinase 2
VEEV	Venezuelan Equine Encephalitis Virus
VEGF	Vascular Endothelial Growth Factor
VSV	Vesicular Stomatitis Virus
VZV	Varicella Zoster Virus
WNV	West Nile Virus
ZIKV	Zika Virus

Chapter 1: Introduction

Emerging viruses pose a significant risk to human and animal health across the globe. Many RNA and DNA viruses from diverse families cause severe infection of the central nervous system (CNS) such as West Nile virus (WNV), Zika virus (ZIKV), Japanese encephalitis virus (JEV), Venezuelan equine encephalitis virus (VEEV), Eastern equine encephalitis virus (EEEV), La Crosse virus (LACV), JC virus, human immunodeficiency virus (HIV), Nipah virus (NiV), and Hendra virus (HeV). Despite the widespread morbidity and mortality associated with encephalitic viral infections, severe gaps in knowledge exist in understanding the infection of cells within the CNS such as neurons, astrocytes, microglia, and oligodendrocytes. This chapter will review two examples of emerging encephalitic viruses, LACV and NiV, the role of interferons (IFNs) on the CNS, and current models used to study CNS infection.

LA CROSSE VIRUS

Epidemiology and Clinical Disease

LACV, family *Peribunyaviridae* (genus *Orthobunyavirus*) (previously family *Bunyaviridae*), is a leading cause of pediatric arboviral encephalitis in the United States [1]. LACV was isolated in 1964 from 4 year-old girl from Minnessota who developed meningoencephalitis and subsequently died in La Crosse, Wisconsin in 1960 [2]. Cases of LACV encephalitis were quickly identified across the American Midwest with cases identified in Minnesota, Wisconsin, and Ohio [3,4]. Since these initial studies an additional focus of infection was discovered in Appalachia in the late 1990s beginning in West Virginia and later expanding to Eastern Tennessee and Western North Carolina [5,6]. Currently, LACV remains the most common cause of pediatric arboviral encephalitis in the United States, with most infections occurring in Ohio, West Virginia, North Carolina, and Tennessee [7]. In addition, LACV poses an emergent risk to the Southern and Western United States with cases identified as far South and West as Texas [7]. LACV was responsible for 665 confirmed cases of encephalitis from 2003-2012, although the true incidence of disease is thought to be underestimated due to difficulties in diagnosis and clinical similarities to herpes simplex encephalitis. [7]. Endemic areas of infection can display county level incidence of LACV encephalitis of 0.2-228 cases per 100,000 children under the age of 15 [8].

The primary vector of LACV is the diurnal Eastern tree-hole mosquito (*Ochlerotatus triseriatus*). This mosquito primarily breeds and lays eggs in tree holes, and therefore humans are primarily bitten in wooded areas rather than in or near their homes. The virus is able to overwinter in eggs due to vertical transmission [9]. The primary amplifying hosts of LACV are the Eastern chipmunk (*Tamias striatus*), gray squirrel (*Sciurus carolinensis*), and fox squirrel (*Sciurus niger*) [10,11]. Humans are infected following a bite from an infected mosquito, and are a so-called “dead-end” host as they fail to develop viremia adequate to infect mosquitos via a blood meal. The generalized transmission cycle of LACV is shown in Figure 1.1. While, *O. triseriatus* is present in all endemic areas, *Aedes albopictus* and *Aedes japonicus* may also be relevant vectors, particularly in the Appalachian focus of infection [12–15]. These invasive mosquitos are more closely associated with human habitats and may be a major risk for further emergence of LACV in the Southern United States. As with most arboviral diseases, control of mosquito populations and avoidance of mosquito bites remain the primary methods of prevention for LACV infection.

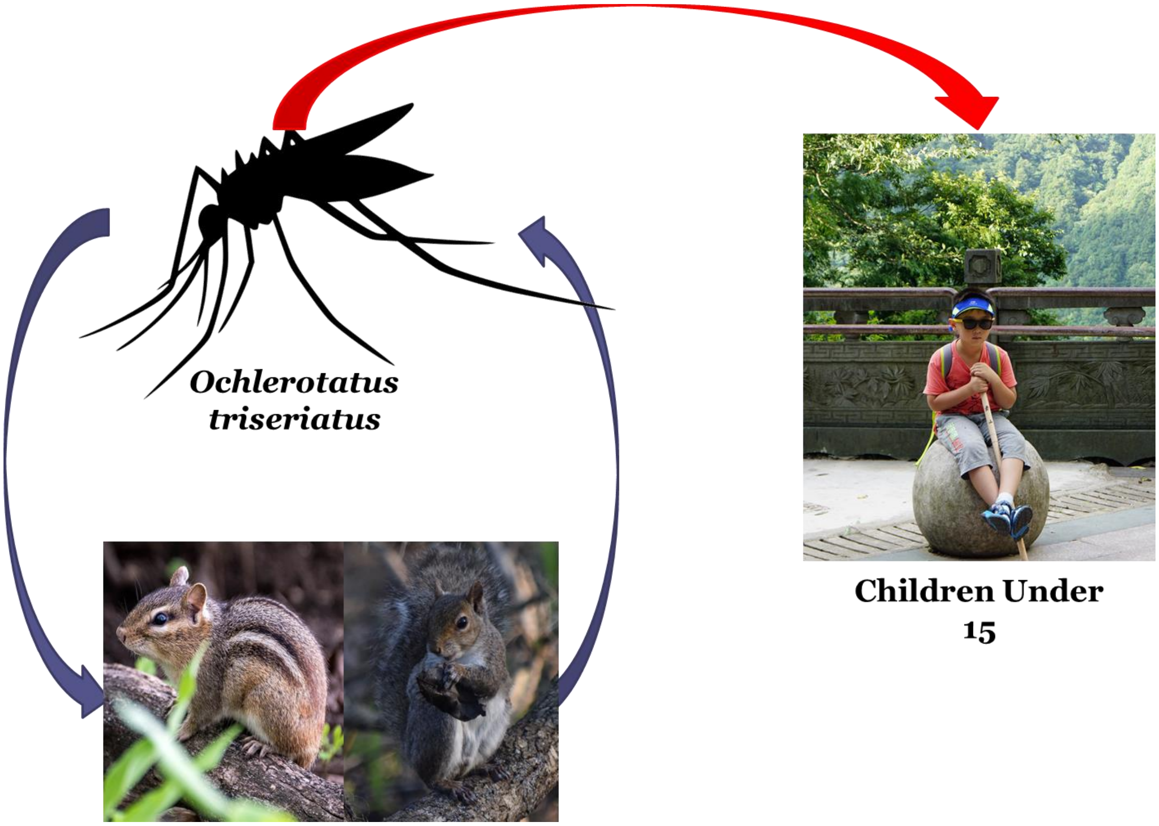

Figure 1.1: Transmission cycle of LACV.

The mosquito *Oclerotatus triseriatus* is the primary vector of LACV transmission. The natural amplifying hosts are small rodents such as chipmunks and squirrels. Occasionally, humans are infected by the bite of an infected mosquito. Generally, this does not result in disease, but in a small percentage of infected children leads to LACV encephalitis. Viral titers do not reach high enough levels in human blood to re-infect mosquitos, therefore making humans dead-end hosts.

LACV encephalitis is almost exclusively found in children under 15 years of age, and more often found in males rather than females [16]. However, it has recently been suggested that adult LACV infection may be an underrecognized cause of morbidity in endemic areas [17]. Like other arboviruses the majority of cases present as mild febrile illness, but in a minority of cases LACV causes severe neuroinvasive disease including encephalitis, meningitis, and meningoencephalitis [18]. To date, no risk factors have been identified for the development of neuroinvasive disease, but risk factors for infection include increased time outdoors, lack of air conditioning or screens on windows, not wearing protective clothing, and proximity to mosquito breeding sites such as tree holes or discarded tires [19]. Neuroinvasive LACV typically presents with fever, headache, and vomiting in greater than 70% of cases [3,16]. In addition, 42% displayed various levels of disorientation, nearly half developed seizures, and 26% had meningeal involvement [3,16]. Of those that developed seizures, a quarter developed status epilepticus, and a third developed seizures with focal components [16]. Additionally, hyponatremia is very common with many patients meeting criteria for syndrome of inappropriate antidiuretic hormone secretion [16]. Perhaps the most severe complication appears to be cerebral herniation [3,16]. Laboratory findings can be misleading with increases in neutrophils in the blood and CNS commonly observed, often a marker for bacterial infection [3,16]. Additionally, electroencephalogram findings can mimic herpes simplex virus (HSV) encephalitis with generalized slowing and temporal lobe disturbances [16]. Imaging studies are generally normal, but cerebral edema can be noted in 12% of cases [16]. While the disease is rarely (<1%) fatal, neurological deficits can cause significant impairment [16]. Epilepsy has been observed to develop in up to a third of cases [18]. Reduced IQ was found in many survivors of severe disease, with many meeting criteria for intellectual disability [16]. Such sequelae have been assessed to cost \$48,000 to \$3,000,000 per case [20]. Attention-deficit-hyperactivity disorder (ADHD) was also noted in 60% of survivors assessed [16]. Additionally, temporary sequelae such as behavioral problems, cranial nerve palsies, speech difficulty and aphasia, ataxia, and memory problems are noted in 10-36% of cases at discharge [3,16].

In human infection cortical and basal ganglia neurons appear to be the primary target of infection in the CNS leading to foci of neuronal necrosis [21]. Within the cortex, lesions can be found in the frontal, parietal, and temporal lobe and appear widely disseminated. Lesions were absent outside of the CNS in human cases [21]. Additionally, inflammatory lesions with largely monocytic infiltration and lymphocytic perivascular cuffing are noted [21]. Leptomeningitis was also noted in one case with a primarily lymphocytic infiltrate [21]. These findings are non-specific and common in viral encephalitis. It also suggests widespread infection of neurons throughout the cortex, and a pathogenic role for inflammation in the development of disease.

Despite the threats posed, there are currently no approved therapeutics or vaccines available against LACV. There are very few results published on LACV vaccine development, but initial studies with vaccinia virus expressing LACV Gc glycoprotein suggest that neutralizing antibodies against Gc are protective in the mouse model of infection [22]. The antiviral drug ribavirin, an guanosine analog which can inhibit RNA virus replication via inhibition of the viral RNA polymerase, was shown to be effective *in vitro* against LACV, but clinical trials were halted due to adverse events reported in children at therapeutic doses [23,24]. More recently, another RNA polymerase inhibitor, the purine analogue favipiravir (Avigan), was shown to be effective against LACV infection *in vitro* but has not been assessed *in vivo* [25].

Basic Virology and Pathogenesis

La Crosse virus is an orthobunyavirus in the California serogroup. Related viruses include California Encephalitis virus, Jamestown canyon virus, Keystone virus, and snowshoe hare virus. California encephalitis virus and Jamestown canyon virus cause mainly febrile illness with occasional encephalitis and Keystone virus was recently associated with mild febrile disease [18,26]. Snowshoe hare virus is very closely related to LACV and associated with encephalitis in Canada [27]. Interestingly, snowshoe hare virus is very similar clinically to LACV, but is generally considered more neurovirulent [18]. The lower numbers of infection by this virus may be due to lower populations in endemic areas or differences in neuroinvasiveness.

LACV shares the same basic virology as other orthobunyaviruses. It contains a tri-segmented negative sense RNA genome composed of a small, medium, and large segment, S, M, and L, respectively [28] (Fig. 1.2). The S segment encodes the nucleocapsid protein (N) as well a nonstructural protein, NSs, via a non-overlapping open reading frame. The M segment encodes the two surface glycoproteins, Gn and Gc, as well as an additional nonstructural gene NSm. Gc and Gn can bind dendritic cell-specific intercellular adhesion molecule-3-grabbing non-integrin (DC-SIGN) for host cell entry [29]. Table 1.1 provides an overview of LACV gene functions. LACV has been shown to enter cells via clathrin-mediated endocytosis and trafficked to early endosomes where viral glycoproteins mediate membrane fusion and release of viral ribonucleoprotein into the cytoplasm [30]. Virus maturation and assembly occurs in the Golgi and virions are released via vesicles similar to the secretory pathway [28].

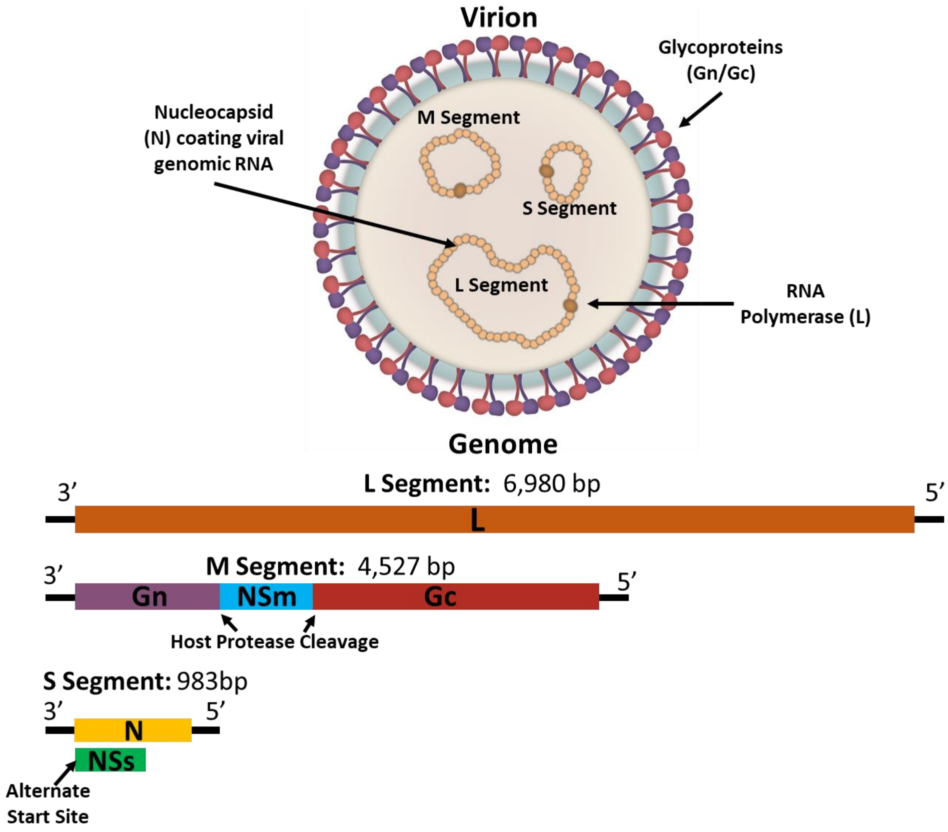

Figure 1.2: La Crosse virus structure and genome

LACV virion structure is typical for bunyaviruses. An envelope comprised of a membrane and viral glycoproteins (Gn/Gc) surrounds a tri-segmented negative sense RNA genome. The genome segments are coated with nucleocapsid (N). Additionally, viral RNA-dependent RNA polymerase (L) is present in the virion, allowing for transcription of genes following infection. The L segment encodes the L protein. The M segment encodes Gn, Gc, and a nonstructural protein NSm. These three proteins are produced as a single polypeptide, which is cleaved by host cell proteases. The S segment encodes N as well as the nonstructural protein NSs via an alternate translational start site.

Protein	Function
L	Viral RNA-dependent RNA Polymerase Transcription & Genome Replication Neurovirulence factor [31]
Gn	Viral glycoprotein Required for efficient attachment and fusion [28]
Gc	Major viral attachment and fusion glycoprotein [28] Neuroinvasive factor [32]
NSm	Unknown Dispensable for viral replication in other orthobunyaviruses [33]
N	Nucleocapsid Coats genomic RNA
NSs	Interferon antagonist Degrades RBP1 leading to inhibition of translation and IFN production

Table 1.1: Functions of LACV proteins

The understanding of LACV neuropathogenesis has been advanced by studies using the suckling mouse model which closely resembles human disease including age related susceptibility [34,35]. Infection of adult mice and rhesus macaques result in asymptomatic infections and antibody responses [34,35]. Additionally, the segmented nature of the genome allows for genomic reassortments with nonpathogenic strains or closely related species, which have been useful in determining virulence factors of LACV infection. Such studies have shown LACV L is an important neurovirulence factor [31,36]. Additionally, the fusion function of Gc is important for neuroinvasion, but dispensable for neuronal infection and neurotoxicity [32]. LACV replicates peripherally in striated muscle, lymph nodes, and nasal turbinates within the first 2-3 days after infection.[34,35]. Robust peripheral replication and higher levels of viremia tend to correlate with neuroinvasiveness around day 4-6, making LACV neuroinvasion a fairly late process during infection [32,37]. Interestingly, control of peripheral infection may be the cause of age related susceptibility to LACV encephalitis in mice as direct intracranial injection of adults results in encephalitis [35]. This hypothesis is further supported by the finding that myeloid dendritic cells (DCs) in adults mount greater interferon (IFN) responses than in suckling pups which prevent neuroinvasion [38]. LACV likely invades the CNS via the capillaries in the olfactory bulb in the mouse model of LACV encephalitis after compromise of the blood-brain barrier (BBB) [34,39].

CNS pathology within the suckling mouse model appears similar to that seen in humans, with neuronal death, inflamed vessels, and infiltrate composed of primarily monocytes and macrophages [34]. Some differences in distribution were noted, with viral antigen found in the spinal cord and in the brainstem, although these were late targets of infection suggesting that virus spreads caudally within the CNS [34]. Most studies agree that neurons comprise the main target cell in the CNS [34,40]. Infected neurons appear to undergo apoptosis via mitochondrial antiviral-signaling protein (MAVS) induced upregulation of sterile alpha and TIR motif containing 1 (SARM1) resulting in oxidative stress [41,42]. Other studies suggest that apoptosis may be caused in part by NSs inhibition of translation [43]. While neurons are the primary CNS cell infected, some groups report low levels of astrocyte infection *in vitro* and *in vivo* [1,40]. There are conflicting reports of microglial infection in the mouse model, but at most infection seems to be rare [34,40]. To date, all studies of LACV neurovirulence have utilized animal models, primary rodent CNS cells, or human neuroblastoma cell lines, and therefore these results have yet to be replicated in primary human tissues.

Innate Immune Responses

Effective type I IFN responses appear to be critical for the control of LACV infection. LACV induces an interferon regulatory transcription factor (IRF) 3 and IRF7 response after being detected by the Retinoic acid-inducible gene-I (RIG-I)-like receptor (RLR) RIG-I [41,44]. Another recent study suggested IRF5 may also be important for prevention of neuroinvasion [45]. At least one interferon stimulated gene (ISG), MxA has been shown to directly inhibit LACV replication by sequestering N, although the role of other ISGs have not been directly studied [46]. IFN production by myeloid DCs appears to be the predominant source of IFN outside of the CNS, and is likely responsible for control during adult infections [38]. To combat host IFN responses, LACV NSs acts as an IFN antagonist by degrading the RBPI subunit of RNA polymerase II, thereby inhibiting translation and IFN production [44,47]. Within the CNS astrocytes and microglia appear to be the primary producers of IFN-β during LACV infection in the mouse model [40]. Neurons also produce IFN-β in response to LACV infection, but to a lesser degree [40,48]. Especially interesting is the finding that when NSs is deleted, astrocytes significantly increase production of IFN, suggesting that IFN production in astrocytes is antagonized by LACV infection [40]. This suggests that astrocytes may be a more important target of infection than previously thought.

Regarding the inflammatory component of disease, a recent study showed that lymphocytes play a protective role during LACV infection of adult mice and do not contribute to pathogenesis of weanling mice [49]. The majority of inflammatory cells noted in human and mouse brains during LACV infection are monocytes and macrophages. Recent work has demonstrated that in the mouse model chemokine (C-C motif) ligand 2 (CCL2) is important for inflammatory monocytic migration within the brain, and that astrocytes are the major source of CCL2 in the brain [21,50]. It is still unclear whether monocytic infiltrate is protective or pathogenic. Importantly, it is becoming increasingly clear that CNS parenchymal cells (neurons, astrocytes, and oligodendrocytes) play a major role in the development of innate immune responses during LACV infection [48,51,52]. Additionally, cytokine responses can also negatively impact BBB integrity and lead to worsened neuroinvasion [53,54]. While knowledge on the pathogenesis and molecular mechanisms of LACV-induced disease using animal models is increasing, there is still a need to verify many of these results with a human based system.

HENIPAVIRUSES

Epidemiology and Clinical Disease

NiV and HeV are highly pathogenic zoonotic viruses of the genus *Henipavirus* (HNV), family *Paramyxoviridae* [55,56]. HeV was the first identified henipavirus, originally designated equine morbillivirus [57]. The first cases were identified in 1994 in Hendra, Brisbane, Australia affecting 20 horses with severe respiratory infections. During this outbreak, three humans were infected with HeV while caring for sick horses [58]. These patients experienced flu like illness followed by signs of neurological disease such as headaches, confusion, and in one of the cases severe respiratory distress and interstitial pneumonia. One case developed meningitis [59]. Since these initial infections, there have been 94 reported cases in horses along the Queensland coast with an 89% case fatality rate (CFR) and 7 human cases with a 57% CFR [60]. After the first outbreak, fruit bats of the *Pteropus* genus were identified as the natural reservoirs of HeV, and a model was proposed in which horses act as intermediate amplifying hosts after being infected by eating half eaten fruit or contact with infected bat urine [61–63]. Several *Pteropus* species are infected in the wild, but *P. Alecto* and *P. conspicillatus* appear to the most relevant reservoirs [60].

NiV first emerged during a 1998-1999 outbreak in peninsular Malaysia and Singapore [64]. The disease was first recognized as a dual outbreak in pigs and pig farmers. Pigs displayed mild febrile illness with respiratory involvement, while humans displayed severe encephalitic illness [64,65]. The incubation period was between 2 days to 2 months, and onset was abrupt with fever, headache, dizziness, and vomiting. Later neurological signs included reduced levels of consciousness, areflexia, hypotonia, and abnormal doll’s eye-reflex [65]. Nearly a quarter of patients had seizures, and almost seizures were all were generalized tonic-clonic [65]. In Malaysia there were few respiratory symptoms other than nonproductive coughs, but 3 cases in Singapore presented with atypical pneumonia [65,66]. Focal signs were common, with the most prominent being segmental myoclonus in 32% of cases [65]. The Malaysian outbreak resulted in the culling of over 1 million pigs and 276 human cases with a 38% CFR [67]. One study estimated that the outbreak resulted in over $2 billion in damages across Malaysia alone due to the disruption of the pig farming industry [68]. Again, *Pteropus* bats were found to be the reservoir of infection, and it is speculated that partially eaten fruits first infected pigs [69]. No other outbreaks have been detected in Malaysia or Singapore. However, there was a suspected NiV outbreak in the Philippines in 2014 associated with sick horses that appears to be NiV-Malaysia strain (NiV-M) [70].

Since 2001 there have been nearly yearly outbreaks in Bangladesh and India associated with approximately 300 human cases, person-person transmission, and a 75% CFR [67,71]. Most of these cases have occurred in Bangladesh or Western Bengal, India, but in 2018 there was an outbreak in Kerala, on the Western coast of India [72,73]. These outbreaks have been associated with various routes of transmission, including the consumption of contaminated date palm sap, human-to-human transmission, exposure to sick cows or pigs, and exposure to bat droppings [74–77]. While these outbreaks are smaller, from 1-66 cases, overall mortality was much higher. Whether differences in mortality are due to differences in virus strains or due to differences in healthcare availability and quality are debated. Additionally, NiV-Bangladesh strain (NiV-B) appears to have a different clinical presentation with more frequent and severe respiratory involvement manifesting as cough and respiratory distress in 75% of cases compared to 14% for NiV-M [76,78]. These differences are interesting, as NiV-M and NiV-B share 91.8% nucleotide homology [79]. Most of these differences are found in the intergenic regions, but the P and V proteins have the largest differences among translated sequences at approximately 92% amino acid similarity [79]. Differences in P and V may be due to the necessity of the virus to overcome the immune response in their reservoir hosts, and these differences may also contribute to differences in pathogenicity related to their ability to inhibit human immune responses. Many patients with respiratory symptoms progress to acute respiratory distress syndrome. However, presentation with neurologic symptoms was still common and similar to that seen in NiV-M cases with fever, altered mental status, headache, and vomiting being found in the majority of cases [78]. The epidemiology of HNV infection is summarized in Fig. 1.3.

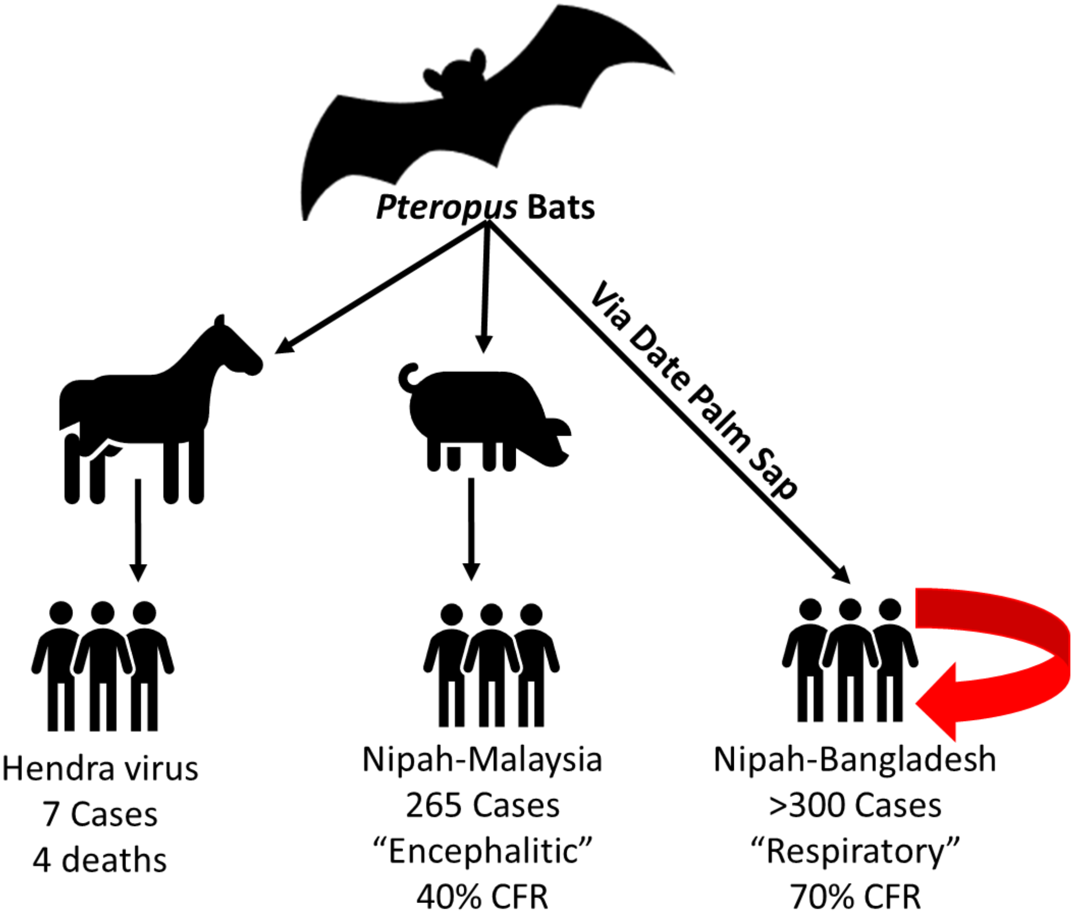

Figure 1.3: Epidemiology of henipavirus infection of humans.

Pteropus fruit bats represent the primary reservoirs of NiV and HeV. HeV infection on the Queensland coast occurs after horses are exposed to HeV from bats, likely via exposure to urine or partially eaten fruits. HeV then is transmitted to humans in close contact to infected horses such as veterinarians or trainers. During the

Malaysia/Singapore outbreak 1998/99, NiV was transmitted to pigs, likely via partially eaten fruits. From pigs the virus infected workers on pig farms and abattoirs. NiV-B has spilled over into humans via numerous routes, but perhaps the most notable is the direct infection of humans via the consumption of date palm sap contaminated by bat urine or saliva. There has also been significant human-human transmission during NiV-B outbreaks.

The pathology of NiV and HeV infection in humans appears similar [59,80]. However, almost all pathological reports of NiV infection are from the initial Malaysia outbreak. Both viruses are characterized primarily by infection of endothelial cells leading to syncytia formation and small vessel vasculitis throughout the body [59,80]. Systemically, HeV vasculitis was noted in the lung, heart, and kidney, and parenchymal inflammation and necrosis was evident in the lung [59]. Type II pneumocytes, alveolar macrophages, and renal tubule cells appeared to be infected with HeV [59]. NiV produced essentially the same pathology in these tissues [80]. In the cited studies the brain appeared to be the most severely affected organ. CNS damage during acute HNV infection seems to arise from a dual pathogenic mechanism of vasculitis and direct neuronal infection. Endothelial infection and vasculitis result in inflammation and thrombi leading to microinfarcts and necrotic plaques in the grey and white matter of the brain [80]. Meanwhile, viral antigen is evident in neurons, but rare in glial and ependymal cells near vascular lesions. While the olfactory nerve has been shown to be a potential route of infection, the locations of neuronal lesions suggest BBB breakdown due to vascular inflammation may be a more relevant mechanism of entry for NiV during human infection [81]. Perivascular cuffing and microglial nodules were also noted along with mononuclear infiltrates [80]. Lesions were found throughout the white and grey matter. Interestingly, this correlates to MRI studies showing that during acute NiV-M infection small hyperintense lesions could be noted throughout the brain [65,66]. These likely reflect necrotic plaques secondary to microinfarcts.

The large range of HNV infections correlates with the range of Pteropus fruit bats, the natural reservoir of HNV infection [62,69]. Due to the large geographic host range, frequent spillover events, high virulence, and potential for human-human transmission, NiV has been proposed as a pandemic potential [82]. The World Health Organization and the Coalition for Epidemic Preparedness and Innovations (CEPI) have listed NiV as one of the pathogens with urgent need for vaccine and antiviral development [83]. There are several vaccine candidates against NiV, and therapeutic options include monoclonal antibodies and antiviral compounds such as favipiravir [84–87]. The most notable vaccine candidates include soluble HeV glycoprotein vaccines and a vesicular stomatitis virus (VSV) vectored vaccine expressing NiV fusion protein and/or glycoprotein [84]. Recent work has identified the wide spectrum antiviral compound favipiravir as a potential antiviral treatment, protecting against lethal NiV infection in hamsters when administered immediately after infection [85]. Favipiravir is a purine analogue targeting viral RNA polymerase initially developed for treatment of influenza but has since been shown to be effective against a wide spectrum of RNA viruses [88]. The monoclonal antibody m102.4 targeting NiV glycoprotein protected African green monkeys from lethal infection even after the onset of clinical disease [87]. Most recently, pre-exposure treatments with lipopeptide fusion inhibitors were shown to be efficacious at preventing NiV respiratory disease in hamsters and African green monkeys [89]. To date, most studies evaluating antiviral treatments have focused on the control of acute systemic HNV infection, and most *in vitro* studies have been conducted using non-CNS tissues. Therefore, an *in vitro* CNS system would be beneficial to demonstrate the efficacy of antivirals within CNS cells. Furthermore, as no models of relapsed encephalitis exist, evaluations of antiviral efficacy against chronic CNS infection have not been conducted. In Bangladesh the use of bamboo-skirts to limit bat contamination of date palm sap has also been implemented as a prevention strategy [90]. In Australia the primary preventative measure against HeV infection is vaccination of horses using a soluble HeV glycoprotein (G) subunit vaccine [91].

Late Onset and Relapsing Encephalitis

In 1994 a patient with exposure to HeV infected horses experienced a brief episode of aseptic meningitis [58]. 13 months later, the same patient presented with mood changes, back pain, and generalized tonic-clonic seizures with no additional exposures to horses. His condition deteriorated with focal motor seizures, low-grade fever, hemiplegia, brainstem signs, loss of conciseness, and death 25 days after admission [58]. PCR of cerebrospinal fluid (CSF) was positive for HeV with a 500 nucleotide sequence of the M gene identical to virus isolated from previous acute cases [58]. MRI revealed high grey matter signal, and anti-HeV Immunoglobin G (IgG) titers were greatly increased. Taken together, the presentation and laboratory findings suggest a recrudescence of HeV. Pathological findings revealed discrete foci of necrosis in the grey matter with viral antigen present in neurons and endothelial cells [58]. Additionally, rare syncytia were observed in the brain, liver, spleen, and lungs, although this finding has not been reported in future cases of henipavirus relapsing encephalitis [58]. No infectious virus was isolated. Further pathologic examination of the CNS revealed extensive inflammation of the cortex, perivascular cuffing, glial proliferation, reactive blood vessels, and severe neuronal necrosis [59]. Importantly, no vasculitis, syncytia (as opposed to earlier analysis), or thrombosis were observed. Viral RNA and antigen were detected in primarily in neurons, with few glial cells also displaying RNA and antigen [59]. Additionally, meningeal inflammation was present, and no syncytia were noted in other organs.

Late-onset cases and relapse were also observed after the 1999 Malaysian outbreak [92]. Late-onset Nipah encephalitis was defined as primary onset of encephalitis 10 or more weeks after exposure to NiV accounting with a prevalence of 5% in Malaysia, and a relapse was defined as neurological presentation after recovery from NiV encephalitis with a prevalence of 9% in Malaysia [93]. Late-onset and relapsed encephalitis appeared similar clinically, pathologically, and radiologically, suggesting that they are a continuum of the same pathologic process [92]. In addition, 18% of 22 patients followed in Bangladesh reported delayed neurological deficiencies, but NiV-B relapse has been studied and followed much less than NiV-M [94]. The overall mortality for these cases was 18%, but a higher rate of neurologic deficits (66%) was seen compared to acute NiV encephalitis [65]. Average time to relapse was generally 7.6 months after primary encephalitis, and the average time between exposure and late-onset encephalitis is 8.4 months, although one case has been reported 11 years after exposure [95]. There were no significant demographic differences between relapsed and non-relapsed populations [92].

Clinically, relapsed/late-onset encephalitis differs from acute NiV encephalitis. Notably, there are no reported respiratory symptoms [92]. Additionally, fever is less common and seizures while focal signs were more common in relapsing encephalitis [92]. In addition, the NiV-B late onset neurologic deficits included ophthalmoplegia and cervical dystonia [94]. MRI findings also differ compared to acute cases. The most common findings were patchy confluent cortical lesions as opposed to small, diffuse, and discrete subcortical and white matter lesions found in acute encephalitis [96]. Pathologically, relapsed/late-onset NiV cases displayed only CNS involvement [80]. Importantly, vasculopathy and demyelination was not noted. The hallmarks of relapsed encephalitis were large confluent lesions with extensive viral inclusions both in neurons and the neuropil [80]. This corresponds with severe neuronal necrosis, gliosis, perivascular cuffing, and inflammatory infiltrate. Glial and ependymal cells were also positive for viral antigen in contrast to acute NiV infection [80]. Overall, the differences in symptoms, radiology, and pathology suggest that relapsed and late-onset NiV encephalitis represent a different pathological process than acute NiV encephalitis.

Basic Virology and Pathogenesis

Henipaviruses share the major molecular and genetic characteristics of other paramyxoviruses with a negative sense non-segmented RNA genome which conforms to the paramyxovirus "rule of six" (Fig. 1.4) [97]. The rule of six is a conserved genome characteristic of paramyxoviruses in which the nucleotide length of viral genomes is always a multiple of six, likely to accommodate binding to nucleocapsid proteins. Henipaviruses contain seven genes which produce nine proteins, the nucleocapsid (N), phosphoprotein (P), matrix (M), fusion (F), glycoprotein (G), and polymerase (L) [98]. Additionally, typical of paramyxoviruses, the P gene contains RNA editing sites which can lead to the production of the proteins V and W as well as an alternate open reading frame (ORF) encoding the C protein (the functions of these proteins will be covered further in the next section). In addition, HeV has been reported to encode an additional ORF in the P gene encoding small basic protein (SB), but the function of this protein remains unknown [98]. The functions of these proteins are similar to those found in other paramyxoviruses (Table 1.2). NiV and HeV G proteins utilize ephrin-B2 and ephrin-B3 as cellular receptors [99,100]. This correlates strongly with the observed tropism of HeV and NiV to endothelial cells and neurons, which express the ephrin receptors [101].

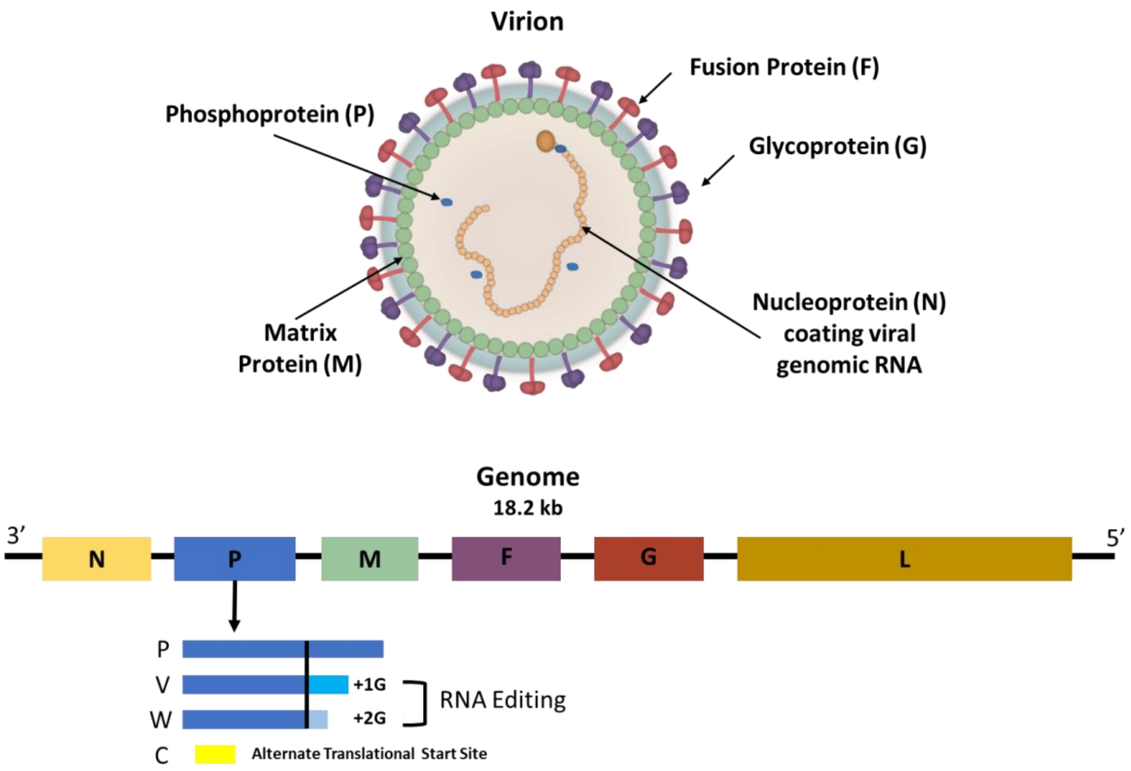

Figure 1.4: Henipavirus structure and genome

HNV virion structure is typical for paramyxoviruses. The lipid envelope is contains the attachement (G) and fusion (F) glycoproteins. Matrix protein (M) forms an ordered structure beneath the membrane. The RNA genome is coated by a ribonucleoprotein complex primarily composed of nucleocapsid protein (N). Additionally, the RNA polymerase (L) and phosphoprotein (P) are present.

The genome of HNVs is also typical of paramyxoviruses. Six genes encode nine proteins. Transcriptional polarity is observed with genes at the 3' end of the genome being transcribed more than those at the 5' end. This is due to the possibility of RNA polymerase release in the intergenic regions. The P gene also encodes V, W, and C proteins. V and W are produced via RNA editing in which one or two guanines are added to mRNAs at an editing site. C is produced by an alternate ribosomal start signal.

Function	Function
N	Nucleocapsid encasing viral genome Prevents STAT1 translocation [102]
P	Component of RNA polymerase complex Sequestration of STAT1/2 [103]
V	Block RIG-I/MDA5 signaling [104,105] Inhibits NLRP3 inflammasome activation [106] Sequestration of STAT1/2 [103]
W	Inhibits IRF3 phosphorylation [107] Sequestration of STAT1/2 [103] Inhibition of inflammatory responses [108]
C	Enhancement of virion budding [109] Blocks IRF7 signaling [110]
M	Virion budding [111,112] IFN antagonism (inhibits TRIM6 mediated IKKε ubiquitination) [113] Reduction of rRNA production [114]
F	Fusion protein responsible for viral entry and syncytia formation
G	Attachment glycoprotein binds to ephrin-B2/B3 [99,100]
L	Viral RNA dependent RNA polymerase

Table 1.2: Henipavirus protein functions

In addition to NiV and HeV, *Henipavirus* contains three other members, Cedar virus (CedV), Mojiang virus (MojV), and Kumasi virus (KV). The relevance of these viruses to human health has not been determined, but it appears that CedV is non-pathogenic at least in part due to impaired signal transducer and activator of transcription 1 (STAT1)/STAT2 antagonism [115]. KV RNA was found in *Eidolon helvum* fruit bats in Ghana [116]. While no human disease has been noted, humans in Cameroon appear to have been exposed to henipaviruses, potentially KV [117]. MojV RNA was isolated in during an investigation of febrile disease in miners in China, but no conclusive link to disease has been shown [118]. MojV appears to be the most divergent of the HNVs, as its presumed reservoir is rats, and it does not use ephrin-B2 or ephrin-B3 as entry receptors [119].

HNVs are difficult to study due to their classification as biosafety level 4 pathogens. However, pathogenesis studies of NiV and HeV have largely been greatly aided by a variety of animal models of infection. Pigs and horses are susceptible to NiV and HeV, respectively, and display similar respiratory and neurological disease secondary to encephalitis as seen in humans, although the course of disease appears more mild in pigs and does not have prominent encephalitic components [120,121]. Interestingly, when lesions were noted in pig brains, glial cells were more prominently infected compared to other models [122]. However, due to their size and cost pigs and horses are not attractive models for pathogenesis studies. Cats were characterized as an early model, developing severe vasculitis and respiratory diseases, but again, encephalitic disease was limited [120,123]. Guinea pigs have also been studied, but disease is more mild without a clear respiratory component, and within the CNS the meninges and ependyma were affected but not the brain parenchyma [124]. The primary animal models used to study HNV pathogenesis have been hamsters, ferrets, African green monkeys, and IFN-α/β receptor (IFNAR) knock out (IFNAR$^{-/-}$) mice [125]. The hamster model has been the most widely used small animal model. Hamsters develop both respiratory and encephalitic disease, but the route and dose of infection bias the disease course [126,127]. A low dose infection tends to lead to encephalitic disease while higher doses lead to rapid development of respiratory disease [126]. One of the major limitations of this model is the lack of available hamster specific reagents, making mechanistic studies difficult. The ferret model is larger, more expensive, and also lacks reagents, but develops disease very similar to humans with consistent respiratory and encephalitic disease occurring [128,129]. The African green monkey remains the gold standard infectious model, very closely resembling human NiV and HeV infection [130,131]. Neurologic disease is apparent in most animals, although respiratory disease seems the more severe. Immunocompetent mice strains are not susceptible to NiV infection, although they can develop lethal infection following direct intracerebral infection [132,133]. IFNAR$^{-/-}$ mice develop encephalitis, meningitis, and pneumonia following intraperitoneal infection [132]. A recent study demonstrated infection of aged immunocompetent mice with HeV led to a more protracted infection confined to the brain parenchyma (largely neurons), and may be a suitable model to study HeV brain parenchymal infection [134]. However, this same model was not susceptible to NiV encephalitis [133]. An interesting new model is the development of human lung xenografts in mice with human immune reconstitution. Such models offer the ability to study human tissue in infections in a more complex *in vivo* setting [135,136].

Few studies have addressed the differences between NiV-M and NiV-B, although one study in the African green monkey model suggests that NiV-B is more pathogenic and causes more severe respiratory lesions, leading to mortality before neurological disease can become apparent [137]. CNS entry appears to be a later phenomenon during NiV infection. While viral RNA can be detected in the lungs hours after infection, it is not present in the CNS for roughly two days [138]. CNS damage during acute HNV infection seems to arise from a dual pathogenic mechanism of vasculitis and direct neuronal infection. Few studies have addressed CNS infection. Therefore, the results of neuronal infection, evasion of immune responses in the CNS, persistence, and relapse remain unknown. The mechanisms of persistence and relapse will need to be addressed for the development of vaccines and antivirals. *In vivo* studies using hamsters have demonstrated that neurons and endothelial cells produce the lymphocytic chemokine C-X-C motif chemokine ligand 10 (CXCL10) which was confirmed in human tissues which may play a pathogenic or protective role in recruiting lymphocytes to sites of infection [139]. Infiltrating lymphocytes may be necessary to clear viral infection and limit disease course, or they may induce neuronal damage and worsen the clinical outcome of disease.

In vitro studies of neuronal and glial NiV infection are lacking. Mouse primary glial cells were susceptible to NiV-M infection, and at low multiplicities of infection (MOIs) the type I IFN response limited viral replication [132]. Glial cells were also shown to produce IFN-β during this study. Several studies have used human neuroblastoma cell lines to study NiV infection to limited degrees. NiV-M failed to induce productive infection in the SK-N-MC, but did induce apoptosis [140,141].

Infection of the M17 neuroblastoma cell line led to highly productive infection, but failed to induce IFN-β or chemokine responses [142,143]. In contrast, primary human endothelial cells and epithelial cells induce IFN and inflammatory cytokine/chemokine responses [108,136,143,144]. Neuroblastoma cell lines are an important model, but cancer derived cell lines often have impaired signaling pathways and genetic regulations. It is still unknown if more physiologic neuronal cells can still respond to NiV infection with IFN and/or chemokine responses.

Relapsed HNV encephalitis has drawn comparison to subacute sclerosing panencephalitis (SSPE) caused by another paramyxovirus, measles virus (MeV). SSPE is a severe, often fatal, episode of demyelinating encephalitis due to MeV infection of neurons and glia months to years after infection [145]. SSPE is most commonly found when children are infected with MeV within the first year of life. Due to waning maternal antibody and the immature immune system found in infants, they may be less likely to clear the virus. Additionally, immunosuppression from a separate viral infection prior to MeV may predispose a patient to SSPE [145]. SSPE occurs despite high concentrations of neutralizing antibodies. Studies have shown the virus-neutralizing antibodies alter expression of MeV P and M in HeLa cells, and a global down regulation of viral gene expression in neurons in a phenomenon known as antibody-induced antigenic modulation [146,147]. Additionally, polymorphisms within the genes encoding interleukin (IL)-2, IL-4, IL-12, MxA, and toll-like receptor 3 (TLR-3) have been implicated in susceptibility to SSPE [148]. Neurons appear to fail to induce a type 1 IFN response or induce MHC I expression when infected with MeV [149–151]. Other studies have shown significant transneuronal spread, likely at the synapses with syncytium like complexes forming which appears to be important for neurovirulence and mediated by the viral Hemagglutinin protein [152]. Expression of the structural genes M, F, and H (encoding the Hemagglutinin protein) are reduced in SSPE, and hypermutations in the coding sequences of these genes, especially M and F, are often found and are thought to contribute to increased RNA replication [153,154]. Furthermore, wild-type MeV expressing SSPE isolate M become neurovirulent, suggesting that these mutations play a functional role in the development of SSPE [154]. Hyperfusogenic F proteins also seem to be important for neurovirulence as well as mutations in the P gene which reduce RNA editing and expression of V [155,156]. Taken together, mutations, neutralizing antibody, and cell-cell spread may explain the lack of isolatable infectious virus during SSPE. While differences in pathology and disease course exist, SSPE is the best studied case of paramyxovirus relapsed encephalitis, and may provide insight into NiV persistence. To date no host factors involved with persistence or relapse of NiV infection have been identified. Unpublished reports claim that no mutations have been identified in viral RNA recovered from relapsed cases [157]. However, recent reports of ferret infection with NiV deficient in P gene products suggest that they may play a role in persistent neurologic infection and will be discussed in the next section [108,158]. The role of the IFN response in neurons with regards to NiV persistence has not yet been addressed.

Innate Immune Responses

IFN-α/β responses are important for control of NiV infection as demonstrated by the susceptibility of IFNAR$^{-/-}$ mice [132]. Additionally, it has been shown that infected primary endothelial, epithelial, and glial cells can produce IFN-β in response to NiV or HeV infection [132,143,144,159]. However, neuroblastoma cells failed to mount a successful IFN response [132]. The ability of HNVs to evade the IFN response is critical for the development of disease and is therefore antagonized by several viral proteins. The most notable IFN antagonists are the P gene products, P, V, W, and C [160]. The basic IFN response can be separated into 3 basic components: recognition of viral RNA by cellular sensors, the signaling pathways activated by theses sensors that lead to IFN production, and the signaling mediated by binding of IFN to the IFNAR complex leading to the production of ISGs. HNVs are able to antagonize all of these components. The role of these proteins in HNVs may be uniquely important as HNVs produce far more RNA edited transcripts than other paramyxoviruses [161].

The HNV V proteins are able to bind and inhibit host dsRNA sensors melanoma differentiation-associated protein 5 (MDA5) and Laboratory of Genetics and Physiology 2 (LGP2) [104,162]. MDA5 is an important sensor of RNA virus infection, while the role of LGP2 is less well understood and may act as a negative regulator of RLR signaling. More recently, NiV V protein was shown to inhibit the ubiquitination of RIG-I by tripartite motif-containing protein 25 (TRIM25), and therefore blocking downstream activation of MAVS and the induction of IFN [105].

Signaling pathways induced by the detection of viral RNA ultimately activate IRF3/IRF7 and induce the transcription of IFN-α/β. NiV W and M have all been shown to disrupt this pathway. M protein has been shown to interact with and degrade the ubiquitin ligase TRIM6 and therefore block the ubiquitination of IKKε which is necessary for the phosphorylation of IRF3 and STAT1 [113]. Additionally, W was shown to traffic to the nucleus where it inhibited TLR-3 signaling induction of IRF3 phosphorylation [107]. There has also been a report that C can inhibit TLR7/TLR9 activation via interactions with IKKα which prevent activation of IRF7 [110]. This strategy would be particularly important in plasmacytoid DCs which are responsible for the majority of IFN production outside of the CNS.

P, V, and W all target IFN-β signal transduction and transcription of ISGs via the inhibition via inhibition of STAT1/STAT2. NiV and HeV V proteins were shown to interact with STAT1 and STAT2 (but only in the presence of STAT1) and lead to their aggregation into high-molecular weight complexes which prevent phosphorylation [163,164]. This can block both the type I and type II IFN responses. P and W share the same STAT1 binding domains, but W appears to primarily sequester STAT1 to the nucleus [103]. P appeared to be less efficient than V or W in inhibiting STAT1 responses

[103]. Recent reports have also described a role for N in blocking nuclear import of STAT1 which may represent a novel paramyxovirus IFN antagonism strategy [102].

Studies using recombinant NiV lacking V, W, and C have provided conflicting results regarding their roles *in vivo*. P knockouts cannot be generated as it is an essential part of the RNA polymerase complex. Two groups have reported attenuation following C deletion in the hamster model [165,166]. One of these groups further demonstrated an increase in inflammatory cytokines and chemokines [166]. The other group also showed a decrease in virulence after V deletion [165]. However, another group with a different reverse genetics system and mutation strategy demonstrated that C deletion had no effect on virulence in the ferret model while V deletion resulted in 100% survival [108,158]. Interestingly, deletions of W (as well as W and C) resulted in protracted disease course with long term neurologic symptoms [108,158]. It was also shown that V more strongly inhibited IFN responses while W appeared to inhibit inflammatory responses via suppression of cytokines/chemokines [108]. These results suggest that V may be necessary for virulent infection, while inflammatory responses, W, and C may be dispensable for persistent/relapsed infection. Additionally, V has recently been shown to inhibit the activation of the nucleotide-binding domain and leucine-rich repeat containing protein 3 (NLRP3) inflammasome [106]. This, together with the effects of W deletion, demonstrate that in addition to being IFN antagonists, the P genes are also potent inhibitors of inflammation.

INTERFERON RESPONSES IN THE CNS

Type I IFN

Type I IFNs include IFN-α and IFN-β along with other less well characterized IFNs which signal though the IFNAR complex. Generally, binding of IFN to the IFNAR1/2 heterodimer induces signaling of tyrosine kinase 2 (TYK2) and Janus kinase 1 (JAK1) to phosphorylate STAT1/STAT2 heterodimers. These heterodimers translocate to the nucleus where together with IRF9 form the IFN-stimulated gene factor complex 3 (ISGF3), which acts as a transcription factor for ISGs. These ISGs establish an antiviral state within the affected cell. However, there are alternate signaling pathways identified such as STAT1 or STAT2 homodimers, heterodimers of various STATS (1, 2, 3, 4,5 or 6), mammalian target of rapamycin (mTOR), and mitogen-activated protein kinase (MAPK) [167].

Type I IFN responses are critical for the control of several viral CNS infections [168–172]. All CNS cell types have been shown to produce type I IFNs including neurons [40,48]. Additionally, all such cell types can respond to IFN signals (Fig. 1.5). However, heterogeneity of responses have been noted. Species differences have been noted. In Borna disease virus (BDV) infection, rat neurons fail to produce the ISG MxA in response to IFN-α and become persistently infected while mouse neurons induce MxA and control viral infection [173]. Interestingly, neurons tend to have delayed and sustained STAT1 phosphorylation after IFN signaling, which may mediate some of the difference in expression patterns [174]. In general astrocytes appear to respond to type I IFN more strongly than neurons. Astrocytes appear to express higher basal levels of ISGs [175,176]. Differences in ISG expression patterns also seem to render neurons less able to control viral infections [176–178]. In addition, neurons from different brain regions respond differently to type I IFN. Specifically, multiple studies have concluded that cortical neurons are less responsive than cerebellar neurons [179–181].

Several recent studies have also highlighted the importance of astrocyte production and response to type I IFNs. One set of studies have shown that abortively infected astrocytes are a major producer of IFN during viral infection [182,183]. In the LACV model astrocytes were the primary producers of IFN-β in the CNS [40]. Additionally, the VSV model has shown that IFN-β production in the olfactory bulb (an initial site of neuroinvasion) by astrocytes is critical to control viral replication and induces IFN responses in distant brain regions [168,184]. Studies in which the IFNAR was knocked out selectively in astrocytes during mouse hepatitis virus (MHV) infection and WNV infection demonstrate that astrocyte IFN signaling is critical for the control of CNS infections [185,186]. Interestingly, some of this response may be due to defective interfering particles [187].

Type II IFN

The type II IFN IFN-γ has been shown to be important for the clearance of virus in neurons via non-cytolytic mechanisms [188–193]. IFN-γ signals via the interferon-gamma receptor (IFN-γR). Signaling then proceeds via JAK1/2 phosporylation and the formation of phosphorylated STAT1 homodimers. These then activate the transcription of gamma activated sequences (GAS). Many of these genes are similar to those induced by type I IFNs and induce an antiviral state while others are unique to IFN-γ. However, noncanonical signaling pathways such as STAT3 and extracellular signal related kinase 1/2 (ERK1/2) have been identified and may play roles in the central nervous system [193–196]. Specifically, ERK1/2 signaling following IFN-γ stimulation was found to be neuroprotective by inhibiting apoptosis in neurons [194]. IFN-γ signaling in CNS cells is summarized in Figure 1.5.

IFN-γ is important for the development of cell mediated adaptive immune responses, and this accounts for some of its importance during viral encephalitis. Indeed it is required for the clearance of BDV and Sindbis virus (SinV) via CD8 T-cells [190,197]. Interestingly, it also was shown to protect neurons form CD8 T-cell mediated cell death during BDV infection [198]. This suggests a neuroprotective role for IFN-γ. Indeed, IFN- γ has been shown to be antiapoptotic in HSV1 and HSV2 infected neurons while also preventing HSV reactivation [199–201]. IFN-γ was also shown to inhibit replication of pseudorabies virus, VSV, cytomegalovirus, and Theiler's murine encephalomyelitis virus [202–205]. IFN-γ has been shown to be critical for the noncytolytic clearance of SinV virus [188,206]. Antibodies appear to be required to clear the virus initially. However, viral RNA persists, and IFN-γ is critical to fully clear viral RNA and ensure that viral infection does not reactivate [170,190]. Of interest is the ability of IFN-γ to control MeV virus CNS infection of neurons via non-cytolytic mechanisms [191–193]. This appears to be via STAT1 independent mechanisms, and one study in organotypic brain cultures demonstrated that IFN-γ was necessary and sufficient to control MeV [192,193]. However, the mechanisms of viral clearance in this model remain unknown but may provide a novel therapeutic target to treat viral infections of the CNS.

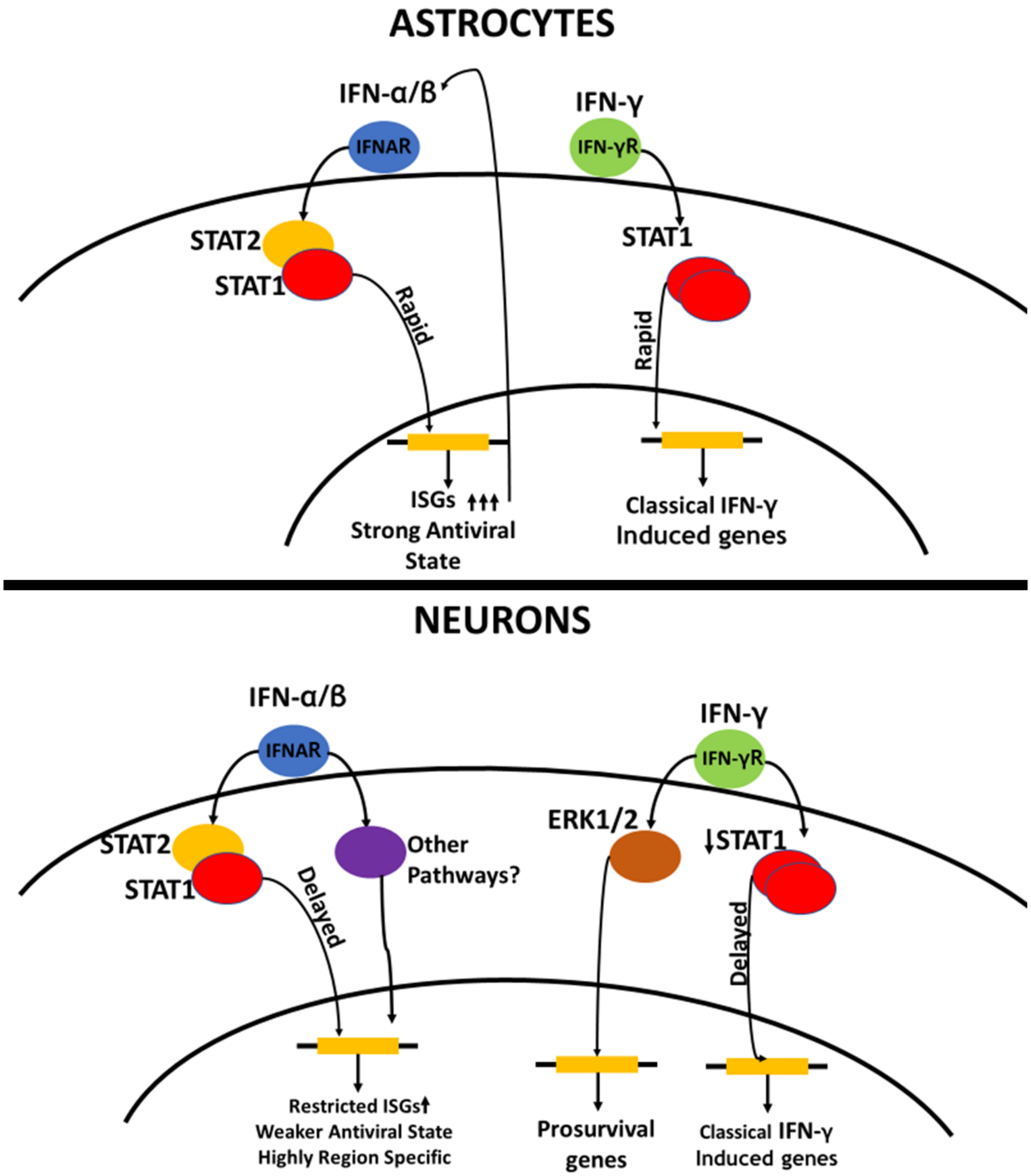

Figure 1.5: IFN signaling in the CNS

The above figure provides a simplified overview of IFN signaling with in the CNS. In general, astrocytes respond to type I and type II IFNs with the classical STAT1/STAT2 pathways. These induce strong antiviral states with large rapid increases in ISG production. Neurons may use alternate signaling pathways and respond to type I IFNs with a more restricted set of ISGs in a region specific manner. This can result in weaker antiviral states. Additionally, STAT1 signaling following IFN-γ stimulation is delayed and weaker in neurons, which allows for other pathways such as ERK1/2 to be more pronounced.

MODEL SYSTEMS OF VIRAL ENCEPHALITIS

ANIMAL MODELS

Several systems exist to study viral infections of the central nervous system. Animal models, which accurately model human disease, remain a gold standard. However, in many cases good animal models either do not exist or have major limitations. Human viruses may not infect animal models. For example, MeV is a human specific virus, and until the advent of human CD46 transgenic mice pathologic studies were limited to human tissue or nonhuman primate models [207]. This example also demonstrates that available models may not use the most relevant viruses, as CD46 is primarily used as a receptor by measles vaccine strains while signaling leukocyte activation molecule (SLAM) is used by wild strains (although recent work has developed SLAM transgenic mice as well) [208]. An additional limitation of animal models is the large differences in host response that exist between animal species, making translation of results to human tissue difficult [209,210]. Differences also exist in the structure and function of human and murine CNS parenchymal cells. For example, astrocytes are much larger and perform more complex signaling in humans than in mice [211]. Specifically for NiV, there are limitations to each animal model. The lack of reagents makes the study of specific CNS cell types difficult in the hamster and ferret model. The NHP model is very expensive and large pathogenesis studies are not be cost effective and ethical. The mouse models require immune system dysfunction, which is not useful for the study of host responses in the context of natural infection.

***In Vitro* Models**

In general, *in vitro* systems are better suited for initial mechanistic studies due to their lower cost, ease of manipulation, and reproducibility. Primary neurons are terminally differentiated, post-mitotic, and difficult to obtain. Most studies of encephalitic viruses rely on primary rat or mouse neuronal cells or human neuroblastoma cell lines. While these models are strong tools for understanding pathogenesis, each has its own limitations. Human primary cells are very difficult to obtain, particularly neurons, and very expensive. Rodent primary cells are very strong models, but the species differences noted in the previous section limit the translation of results to human tissue. For example, the study of NiV infection of mouse CNS cells would be useful, but the susceptibility induced by IFNAR$^{-/-}$ demonstrates that species specific difference in the IFN response during NiV infection exist. Furthermore, most studies rely on the use of a single cell type, although it has been shown that neuronal cells behave differently in co-culture compared to monoculture [212,213]. Astrocytes play a key role in the physiologic support of neuronal health and function such as synaptic development, protection from glutamate toxicity and oxidative stress, and metabolic support [214]. Astrocytes also are increasingly recognized as major contributors to proinflammatory responses during CNS infection. Therefore, the ideal *in vitro* CNS system should be easy to produce, of human origin, non-transformed, and ideally contain more than one cell type.

In recent years, hNSC, embryonic stem cells (hESCs), and induced pluripotent cells (iPCs) have become important tools in studying neurologic diseases, including encephalitic viruses. Varicella zoster virus (VZV) has been extensively studied using such systems, which has provided accurate models for VZV productive infection, latency, and reactivation. [215–219]. Such models have the benefit of begin derived from human primary tissues, being non-transformed, and after initial isolation stem cells can self-renew and divide indefinitely. The lack of donor variation can be a benefit as it can lead to clearer data sets, but variation between individuals does exist and has been reflected in such systems [220].

Other more complex *in vitro* models have been developed in the last several years. Brain organoid models utilize stem cell differentiation into structures that resemble the early stages of brain development [221]. Such systems have been used recently in the study of ZIKV, and they are particularly suited for such studies, as ZIKV's impact is largely on the developing brain [222,223]. A more recent study assessed JEV infection of organoids [224]. However, there are limitations to these studies for other viruses, as the structures are not necessarily phenotypically representative of child or adult brains. Another model is the organotypic brain slice model. In this model, slices of brain from recently deceased animals, or more rarely humans, are maintained at an air liquid interface. Such systems have been successfully used to study SinV, MeV, BDV, and reovirus [173,192,225,226]. This system allows for the study of the CNS in a much more complete 3-dimensional layout and maintains interactions between cell types. However, for NiV studies this system would be limited due to lack of reagents (hamster), innate immune differences (mice), or difficulty in obtaining tissue (humans).

hNSC Derived Neuron/Astrocyte Co-Cultures

The current project utilized a well validated hNSC-derived neuron/astrocyte co-culture system which has previously been used in the study of neurodegenerative diseases [227–229]. NSCs are a multipotent stem cell population capable of differentiating into either neurons, astrocytes, or oligodendrocytes [230]. Through specialized differentiation protocols summarized in chapter 2, hNSC can be differentiated into a co-culture of neurons/astrocytes, which retain important neuron-astrocyte interaction. The maintenance of these interactions leads to greater synaptic development and greater resistance of neurons to toxic insult. Therefore, this system should allow for the study of viral infection in a much more physiologic setting than a monoculture system. It should be noted that microglia, another cell type that is critical for innate immune responses in the CNS can not be generated by this system as they are not derived from NSCs. Importantly, this primary human neural cell system was recently used to assess Zika virus induced changes in hNSC differentiation, although this study mainly focused on the direct infection of hNSCs rather than differentiated neuronal cells [220]. The susceptibility of neuron/astrocyte co-cultures to infection with HNV has been briefly reported, but an in depth characterization of the cellular responses to infection has not been conducted [231].

PROJECT OUTLINE

The hNSC derived neuron/astrocyte co-culture system represents an attractive candidate model system to study encephalitic viruses. The ability to culture human neurons in essentially unlimited numbers has major advantages to the use of primary human neurons. Additionally, the maintenance of neuron/astrocyte interactions will likely lead to a more physiologically normal system. The expectation was that in co-culture both cell types would be more resistant to infection than standard cell culture models and allow for observations that mirror those seen *in vivo.* Therefore, this dissertation aims to assess both the reliability of this system in replicating key aspects of neuronal/astrocytic infection with encephalitic viruses. **The central hypothesis of this dissertation was that hNSC-derived neuron/astrocyte co-cultures systems can provide a novel model to study encephalitic RNA viruses.** Two different viruses, LACV and NiV, were chosen to characterize this system. Both viruses cause encephalitis and pose major public health risks outlined in the preceding sections. In addition, both viruses have differing mechanisms of pathogenesis in the CNS and provide an opportunity to demonstrate that the hNSC co-culture system can respond physiologically in a virus dependent manner (Table 1.3).

Features of CNS Disease	**La Crosse Virus**	**Nipah Virus**
Population Affected	Children younger than 15	Adults and children
Clinical Symptoms/Outcomes	Fever, headache, vomiting, disorientation, seizures 1% CFR, high rates of epilepsy, reduced IQ, ADHD in survivors	Confusion, motor deficets, seizures, hypotonia, myoclonus, coma 40-70%CFR, relapsed encephalitis in 10% of cases
Route of Neuroinvasion	Capillaries in olfactory bulb	Olfactory nerve or disrupted blood vessels
Regions Infected	Cortex and basal ganglia	Acute: Grey and white matter Relapsed: Grey matter (mostly cortical)
Cell Types Infected	Neurons (<1% astrocytes)	Neurons (Rare glial cells, glial infection is more common in relapse)
Pathologic Lesions	Inflammatory lesions, microglial nodules, foci of neuronal necrosis	Acute: Vasculitis/endothelitis, necrotic plaques secondary to microinfarcts, non-specific inflammation Relapsed: Widespread inflammation
Mechanisms of Cell Death	Neuronal Apoptosis	Unknown (One neuroblastoma study suggests apoptosis)
Inflammation	Mostly monocytes and lymphocytes	Acute: Non-specific Relapsed: Macrophages/Lymphocytes

Table 1.3: Key features of LACV and NiV CNS infection

This dissertation will demonstrate the value of this model system in terms of novel insights about the innate immune responses to these viruses in neurons and/or astrocytes, as well as the ability of this system to accurately replicate aspects of human infection *in vitro*. This study was divided into two aims, detailed in chapters 3 and 4, respectively. **The first aim was to determine the susceptibility and responses of primary hNSC-derived neuron/astrocyte co-cultures to infection with LACV**. LACV is a major cause of pediatric encephalitis in the United States, and greater understanding of LACV neuropathogenesis may lead to improved therapeutics to reduce morbidity. Additionally, LACV has a well validated animal model with which to compare results to aid in validation of the neuron/astrocyte co-culture system. The co-culture system was predicted to replicate key aspects of LACV infection such as a primarily neuronal tropism and induction of apoptosis. In addition, because of the high degrees of inflammation observed in human an animal infection, it was predicted that LACV would induce strong proinflammatory responses. **The second aim was to determine the responses of primary hNSC-derived neuron/astrocyte co-cultures to infection with NiV and determine their response to IFN treatment.** NiV is an encephalitic virus with pandemic potential, and the neuropathogenesis of NIV infection is very poorly understood. The current models of NiV infection are poorly suited to mechanistic studies of neuronal infection, and the neuron/astrocyte co-culture system will be useful for such studies. The co-culture system was predicted to be susceptible to NiV infection but have greatly reduced proinflammatory responses due to the highly anti-inflammatory nature of this virus. In addition, after initial characterizations a mechanistic study was conducted to determine the responses of the co-culture system to IFN stimulation during NiV infection. IFN-γ is critical for control of MeV neuronal infection and was predicted to have similar effects against NiV.

Chapter 2: Materials and Methods

CELLS AND VIRUSES

Vero CCL81 cells were acquired from American Type Culture Collection (ATCC, Manassas, VA). Vero cells were propagated using MEM (Corning) supplemented with 10%FBS and maintained at 37ºC and 5% CO_2. Vero cells were used for viral propagation and plaque assays. K048 hNSCs were originally obtained from the cortex of an 9-week-old male fetus and were propagated as described previously [227]. Briefly, hNSCs were cultured as nonadherent neurospheres in DMEM/F12 (Corning) media supplemented with epidermal growth factor (EGF) (20ng/mL) (R&D Systems), fibroblast growth factor (FGF) (20ng/mL) (R&D Systems), leukocyte inhibitory factor (LIF) (10ng/mL) (Chemicon), heparin (5µg/mL) (Sigma-Aldrich), and insulin (25µg/mL) (Sigma-Aldrich). Media was exchanged every 3.5 days. Cells were passaged every 10 days and maintained at 37ºC and 8.5% CO_2 and monitored for mycoplasma contamination routinely. Primary human microglia (ScienCell) were cultured in flasks coated with 2µg/cm^2 poly-L-lysine with complete microglia media (ScienCell).

hNSCs were plated onto wells coated overnight with 0.01% poly-D-Lysine (Sigma-Aldrich) and 1µg/cm^2 laminin. Cells were plated at a density of 1.2x10^5 cell/well in 24-well plates or 2.4x10^5 cells/well in 12 well plates. Cells were primed for 4 days with a priming media of DMEM/F12 containing EGF (20ng/mL), LIF (10ng/mL), and laminin (1µg/mL) (GIBCO). Cells were then differentiated for 9 days in a differentiation media containing N2 basal media supplemented with glutathione (1µg/mL) (Sigma-Aldrich), biotin (0.1µg/mL) (Sigma-Aldrich), superoxide dismutase (2.5µg/mL) (Sigma-Aldrich), DL-α-tocopherol (1µg/mL) (Sigma-Aldrich), DL-α-tocopherol acetate (1µg/mL) (Sigma-Aldrich), and catalase (2.5µg/mL) (Sigma-Aldrich) with media exchanges every 3 days. K048 hNSCs were differentiated into neurons and astrocytes in a roughly 1:1 ratio. The neurons in this system have previously been characterized as being both GABAergic and glutamatergic and the overall composition is similar to that found in the cerebral cortex [232].

LACV (1964 human isolate) was obtained from the World Reference Center for Emerging Viruses and Arboviruses at the University of Texas Medical Branch (kindly provided by R. Tesh). The strain used was isolated from a human brain in Wisconsin in 1964. This strain had undergone 9 passages in suckling mice, and was amplified for one passage in Vero cells.

NiV-M and NiV-B were provided by the Special Pathogens Branch (Centers for Disease Control and Prevention), and HeV (prototype strain) was provided by the Special Pathogens Program (National Microbiology Laboratory, Canadian Science Centre for Human and Animal Health). Recombinant NiV expressing eGFP (rNiV-eGFP) was rescued as previously described [231]. All infectious virus experiments with NiV or HeV were conducted in the Robert E. Shope BSL-4 lab or Galveston National Laboratory BSL-4 lab at the University of Texas Medical Branch.

GROWTH CURVES

Neuron/astrocyte co-cultures were infected with 0.1, 1, or 10 multiplicity of infection (MOI) of LACV for one hour at 37°C and 8.5% CO_2 for LACV experiments. For HNV experiments, 0.01 MOI of virus was used. Viral MOIs were estimated based on titrations performed using Vero cells. Virus inoculum was removed, cells gently washed with PBS 1x, and fresh differentiation medium re-added. Cells only underwent one PBS wash due to the fragility of the neurons to avoid their detachment. Supernatant aliquots were then collected at various time points after infection. Samples were titrated via standard plaque assay. Briefly, cell culture supernatant aliquots were serially diluted in MEM supplemented with 2% FBS and used to infect Vero CCL81 cells for 1 hour. Cells were washed with PBS and given a media overlay of MEM with 0.8% tragacanth

(Sigma-Aldrich) for LACV plaque assays or MEM with 0.5% methylcellulose (Thermo Fisher) for NiV and HeV plaque assays. Cells were fixed in 10% formalin (Thermo Fisher) and stained using crystal violet (Thermo Fisher), and plaques were counted at 4 days post-infection for LACV assays and 3 days post-infection for NiV and HeV assays.

For microglial infections, microglia (ScienCell) were plated at a density of $4x10^4$ cells/well. Cells were infected similarly to the hNSCs, with 1 MOI of LACV or 0.01 MOI of NiV-M for one hour with one PBS wash. Supernatant was collected and titrated on Vero cells.

IMMUNOFLUORESCENCE

Neuron/astrocyte co-cultures on glass coverslips were infected with 0.1, 1, or 10 MOI of LACV or 0.01 MOI of rNiV-eGFP as described above. Infected cells were fixed in formalin at various times post-infection. Cells were stained with primary antibodies and fluorophore conjugated secondary antibodies along with 4',6-diamidino-2-phenylidole, dihydrochloride (DAPI) (Sigma Aldrich) as previously described [212]. Antibodies used were rabbit-anti-microtubule associated protein 2 (MAP2) polyclonal (Millipore, AB5622) used at 1:500, rabbit-anti-glial fibrillary acidic protein (GFAP) polyclonal (Millipore, AB5804) used at 1:2,000, and mouse-anti-LACV Gc monoclonal (ThermoFisher), MA1-10801) used at 1:1,000. Secondary antibodies were Alexa Fluor goat-anti-rabbit 594 and goat-anti-mouse 488 used at 1:500 (ThermoFisher). Images were acquired on an Olympus IX71 fluorescent microscope and cells were manually quantified visually using 6 random fields per condition with an average of over 200 cells/field. For microglial experiments, cells were stained with rabbit-anti-NiV N antibody (generously provided by Dr. Thomas Geisbert). Alexa Fluor goat-anti-rabbit 488 was used as a secondary antibody.

CYTOTOXICITY AND APOPTOSIS ASSAYS

Neuron/astrocyte co-cultures were grown in 96-well plates ($3x10^4$ cells/well) and infected with either 1 MOI of LACV or 0.01 MOI of NiV-M as in other experiments along with media only controls and 10µM staurosporine (Abcam) treatment. Cells were then assayed using the ApoTox-Glo triplex assay (Promega) according to the manufacturer's protocols. Plates were assayed on a BioTek Synergy HT plate reader at $485nm_{Ex}/520nm_{Em}$ for cytotoxicity (extracellular protease activity) and luminescence for apoptosis (caspase 3/7 activity). For NiV infections viability was also measured at $360nm_{Ex}/520nm_{Em}$ (Intracellular live-cell protease activity), and cytotoxicity and apoptosis were normalized to viability measurements to control for well-well variability.

BIOPLEX ASSAYS

Co-cultures were infected as in previous experiments with 0.1, 1, or 10 MOI of LACV or treated with heat inactivated LACV (60ºC for 30 minutes), (1 MOI) or 10µg/mL polyinosinic:polycytidylic acid (poly I:C) (Sigma Aldrich), or 10µg/mL lipopolysaccharide (LPS) (Sigma Aldrich). For NiV experiments Neuron/astrocyte co-cultures were infected with 0.01 MOI of NiV-M as described previously, mock infected, infected with 0.01 MOI of heat inactivated NiV-M, or 1µg/mL poly I:C. During some experiments 0.01 NiV-B or HeV infections or 0.1 MOI NiV-M infections were also carried out. Supernatant samples were collected at various time points post infection and γ-irradiated with a dose of 5 Mrad to inactivate infectious virus. Cells treated with poly I:C or heat inactivated virus were collected at 48 hours post infection (HPI) only for LACV experiments. Samples were then used for BioPlex assay analysis (Bio-Plex Pro Human Cytokine, Group 1, 27-Plex, Bio-Plex, Bio-Plex Pro Human MMP, 9-Plex, Bio-Plex, or Bio-Plex Pro Human TIMP, 4-Plex, Bio-Plex) according to manufacturer's protocols on low PMT settings with undiluted samples. Standard curves were developed using fresh standards provided in each kit. Microglial experiments used a custom made

BioPlex kit (BioRad). The assays were run on a Bio-Plex 200 system (Bio-Rad) and data was analyzed using Bio-Plex Manager (Bio-Rad).

QRT-PCR

Co-cultures were grown and infected with 0.1, 1, 10 MOI or treated with heat inactivated virus, or 10µg/mL poly I:C. For NiV experiments co-cultures were infected with 0.01 MOI of NiV-M as described previously, mock infected, infected with 0.01 MOI of heat inactivated NiV-M, or 1µg/mL poly I:C. Cells were lysed and collected in TRIzol (Thermo Fisher) reagent and RNA was isolated using Direct-zol RNA Miniprep kits (Zymo Research). cDNA was obtained using High Capacity RNA-to-cDNA kit (ThermoFisher). cDNA was then amplified using SYBR green mix (Bio-Rad) on a Bio-Rad CFX384 instrument using manufactures suggested cycle settings. Data was analyzed using CFX Manager (Bio-Rad), and mRNA expression differences were determined via change in threshold cycle (ΔC_T) and normalized to 18S RNA (ΔΔCT). PrimePCR PCR primers (Bio-Rad) were used to target IL-6, IL-8, CXCL10, CCL2, CCL4, CCL5, TIMP1, and tumor necrosis factor alpha (TNF-α) the sequences for these primers are proprietary and unavailable. PrimeTime qPCR primers (IDT) were used to target matrix metallopeptidase 7 (MMP7), MMP2, and tissue inhibitor of metalloproteinases 2 (TIMP2). Additional primers (IDT) were used to target 18S, IFN-α, IFN-β, and LACV N. Primer sequences are available in table 2.1.

Primer	Sequence
18S	F=GTA-ACC-CGT-TGA-ACC-CCA-TT R=CCA-TCC-AAT-CGG-TAG-TAG-CG
IFN-α	F=GAC-TCC-ATC-TTG-GCT-GTG-A R=TGA-TTT-CTG-CTC-TGA-CAA-CCT
IFN-β	F=TCT-GGC-ACA-GGT-AGT-AGG-C R=GAG-AAG-CAC-AAC-AGG-AGA-GCA-A
MMP7	F= GAA-TGT-CCC-ATA-CCC-AAA-GAA-TG R=GAT-GAG-GAT-GAA-CGC-TGG-A
MMP2	F= GTG-CAG-CTG-TCA-TAG-GAT-GT R= TCC-ACC-ACC-TAC-AAC-TTT-GAG
TIMP2	F= TGT-GGT-TCA-GGC-TCT-TCT-TC R= GAC-GTT-GGA-GGA-AAG-AAG-GA
LACV-(N)	F=ATT-CTA-CCC-GCT-GAC-CAT-TG R=GTG-AGA-GTG-CCA-TAG-CGT-TG

Table 2.1: Primer sequences

INTERFERON AND POLY I:C INHIBITION ASSAYS

For NiV experiments studying the effects of IFN or poly I:C treatments, all cells were treated at day 9 post-differentiation and infected on day 10 post-infection. Unless otherwise state 100U/ml doses were used for IFN-γ and IFN-β (PBL Assay Science), and poly I:C was used at 1μg/mL. For multiple addition experiments treatments were repeated at the same dose once daily. rNiV-eGFP was used instead of NiV-M for rapid visual assessment of infection and immunofluorescence experiments. After 24 hour pretreatment, cells were infected with 0.01 MOI of rNiV-eGFP. Following PBS washes, media containing IFN or poly I:C was re-added to the cells (this was not fresh media, but the same media the cells had been treated with overnight). Virus titration, cytotoxicity/apoptosis assays, and BioPlex assays were carried out as described above.

STATISTICAL ANALYSES

All experiments were performed in triplicate unless otherwise stated. All statistical analyses and figure preparations were performed with Prism (GraphPad Software). Growth curves were analyzed using 2-way analysis of variance (ANOVA) with Tukey's or Bonferroni's multiple comparisons tests. Cytotoxicity and apoptosis assays were subjected to 2-way ANOVA with Bonferroni's multiple comparisons test for LACV experiments, Dunnett's multiple comparisons test for NiV-M experiments, and Tukey's multiple comparisons test for IFN treatment experiments. The qRT-PCR and BioPlex experiments of the stimulated controls during LACV experiments were subjected to 1-way ANOVA with Dunnett's multiple comparisons test. The qRT-PCR, BioPlex, and immunofluorescence experiments of virus infected samples were subjected to 2-way ANOVA with Tukey's multiple comparisons test for LACV experiments. For NiV-M experiments, RT-PCR data was analyzed using 2-way ANOVA with Dunnet's multiple comparisons test. NiV BioPlex data was analyzed using 2-way ANOVA with Tukey's multiple comparisons test. Lastly, rNiV-eGFP immunofluorescence data was analyzed using 2-way ANOVA with Tukey's multiple comparisons test and for the percentage of cell types infected analysis with Bonferroni's multiple comparisons test.

Chapter 3: LACV Infection of hNSC Derived Neuron/Astrocyte Co-Cultures

ABSTRACT

This chapter will describe the establishment of hNSC derived neuron/astrocyte co-cultures as a model system to study LACV encephalitis. To date no published studies on LACV have been completed using primary human CNS cells. This model will allow for the study of LACV infection in human neurons and astrocytes without the influence of signaling and gene expression perturbations that may be induced by transformed cell lines. It was hypothesized that this co-culture system would be susceptible to LACV infection, and that neurons would be the primary cell type infected as seen *in vivo*. Furthermore, it was hypothesized that this co-culture system would have intact IFN and proinflammatory responses, which may influence the recruitment of leukocytes as seen in human cases and in animal models. To accomplish these goals neuron/astrocyte co-cultures were infected with LACV and viral titers and viral RNA were measured. The RNA and protein expression of cytokines and chemokines were also assessed via qRT-PCR and BioPlex assays of LACV infected or poly I:C stimulated neuron/astrocyte co-cultures. Lastly, infected co-cultures were analyzed via immunofluorescence to determine the cell types infected throughout the course of the infection. Together, these results represent the first experimental infection of human neurons/astrocytes with LACV and demonstrate the usefulness of this system as a model to study viral encephalitis.

HNSC DERIVED NEURON/ASTROCYTE CO-CULTURES ARE SUSCEPTIBLE TO LACV INFECTION

The first goal of this project was to demonstrate that hNSC derived neuron/astrocyte co-cultures were susceptible to LACV infection and accurately replicated key aspects of LACV infection seen in other models including the susceptibility of neurons and apoptosis [32,34,41,42]. Differentiated co-cultures were infected with 0.1, 1, or 10 MOI of LACV and images were taken at 24, 48, and 72 HPI. At 48 HPI, the lytic nature of LACV infection could be observed in the form of rounded detached or detaching cells, which is consistent with human and animal pathology (Fig. 3.1a) [21,34,42]. Cytopathic effect (CPE) was correlated with initial MOI, with 10 MOI infections resulting in maximum cell rounding and cell death as opposed to 1 MOI which had less observable CPE.

Supernatant aliquots were collected and titrated via plaque assay (Fig. 3.1b). High initial titers are due to the fragility of the co-culture system, and the limited ability to wash cells after the initial infection period. Therefore, all infections were only washed once. Regardless, a sharp increase in viral titers was observed within the first 24 HPI. The 10, 1, and 0.1 MOI infections reached peak titers by 24, 48, and 72 HPI, respectively. Peak titers were approximately 10^6-10^7 plaque forming units (PFU)/ml and remained within that range for the duration of the study. Viral replication was confirmed via qRT-PCR (Fig. 3.1c). An increase in viral RNA within the first 24 HPI was also noted, however, there was a decline at 48 HPI. By 72 HPI viral RNA had once again increased. This result confirms that viral replication was taking place in infected cells throughout the course of the infection. These results indicate that the hNSC derived neuron/astrocyte co-culture system is susceptible to LACV infection and supports replication, and that viral infection leads to noticeable cytopathic effect.

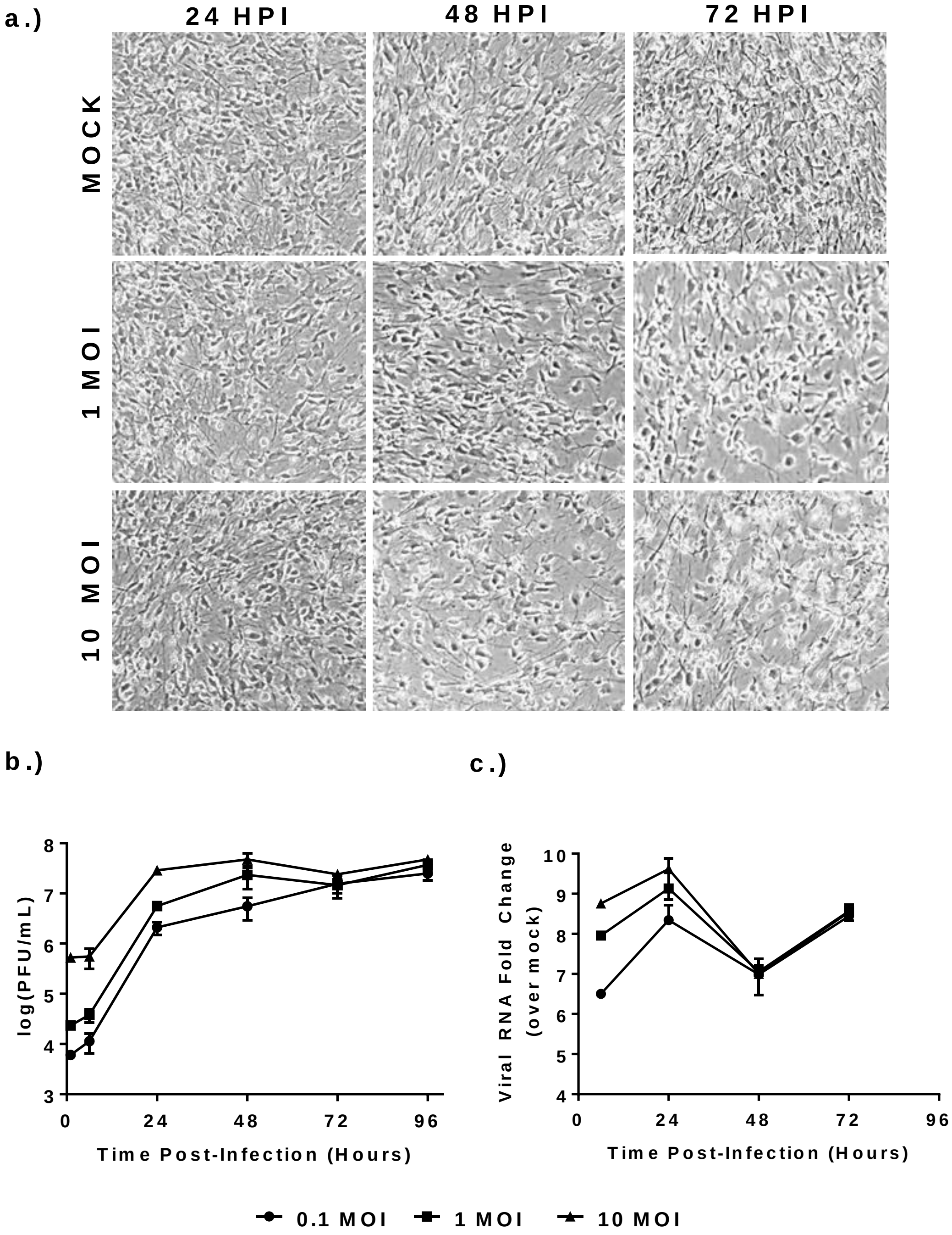

Figure 3.1: Susceptibility and replication kinetics in differentiated hNSC neuron/astrocyte co-cultures.

hNSCs were primed and differentiated into mature neuron/astrocyte co-cultures for 9 days prior to infection with mock, 0.01, 1, or 10 MOI of LACV. **(a)** Co-cultures were imaged at various times post-infection via phase contrast microscopy. **(b)** Supernatant was collected at various times post-infection and titrated via plaque assay **(c)** Cells were lysed, RNA was collected, and qRT-PCR was used to determine viral replication. Anti-

LACV N gene primers were used, and levels were determined as fold change relative to mock infected background.

NEURONS AND ASTROCYTES BOTH SUPPORT LACV REPLICATION

Next the cell types infected with LACV in the neuron/astrocyte co-cultures were measured. Infected cells were fixed in formalin and stained with antibodies specific to LACV glycoprotein and either an astrocytic marker (GFAP) or a neuronal marker (MAP2) with a DAPI counterstain (Fig. 3.2a). These experiments demonstrated that both neurons and astrocytes were infected as virus antigen was detectable in both GFAP and MAP2 positive cells. Interestingly, different intracellular distribution patterns were noted, particularly at 96 HPI. Neurons either had small punctuate patterns or cell wide distribution of viral antigen, while in astrocytes antigen was much more apparent in larger clusters. To further quantify the cell types infected, fields with evident infection were counted and the percentage of cells infected (Fig. 3.2b), the ratio of infected neurons:astrocytes (Fig. 3.2c), and the overall ratio of neurons:astrocytes (Fig. 3.3) were determined. The data indicate that, as previously reported, there is an approximate 1:1 ratio of neurons:astrocytes present in the co-cultures and this ratio does not change throughout infection (Fig. 3.3) [220,227]. As early as 12 HPI, virus was detectable in both cell types, and the percentage of cells infected increases in a time and dose dependent manner (Fig. 3.2b). By 96 HPI about 50% of cells are infected in all conditions. In the 1 MOI infection group at early time points neurons and astrocytes appear to be infected at an approximate 1:1 ratio (Fig. 3.2c). However, by 48 HPI neurons became the more prevalent infected cell type. By 96 HPI the ratio of neurons to astrocytes infected was nearly 2:1. This trend was also observed for 1 and 10 MOI infections (Fig. 3.4). Taken together, these data indicate that in the hNSC derived neuron/astrocyte co-culture system neurons and astrocytes are both susceptible to LACV infection, but neuronal infection is enriched later during the course of infection.

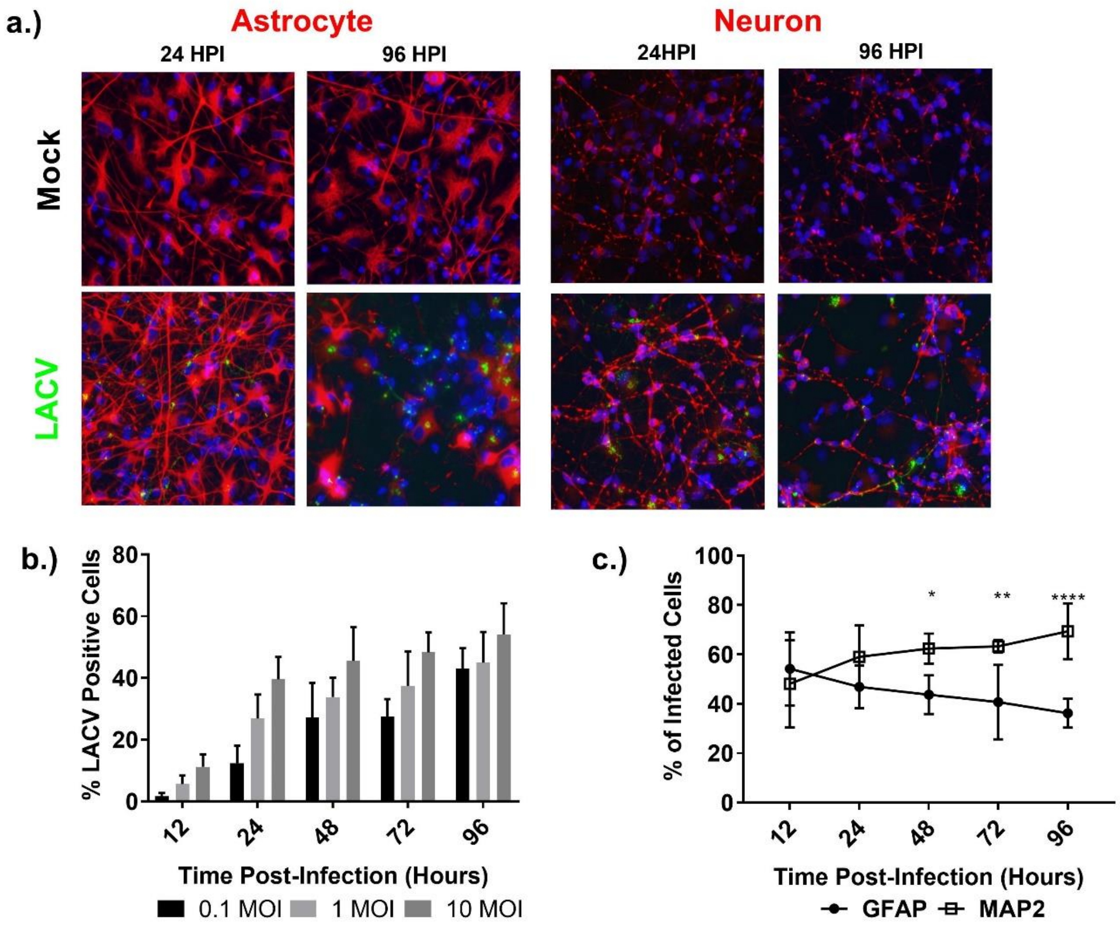

Figure 3.2: Identification of LACV target cells in neuron/astrocyte co-cultures.

Neuron/astrocyte co-cultures were infected with 0.1, 1, and 10 MOI of LACV and formalin fixed at various times post-infection. **(a)** Cells were then stained for DAPI (blue), LACV Gc protein (green), and either neuronal marker MAP2 or astrocytic marker GFAP (red). Representative images from the mock infected and 1 MOI LACV infected group are shown. **(b)** The total percentage of cells infected was determined over the course of infection for all three MOIs. **(c)** The percentage of infected cells expressing either MAP2 or GFAP was quantified for the set of cells infected with 1 MOI. The 0.1 and 10 MOI have similar trends and are available in Figure 3.4. *P<0.05, **P<0.01, ****P<0.0001

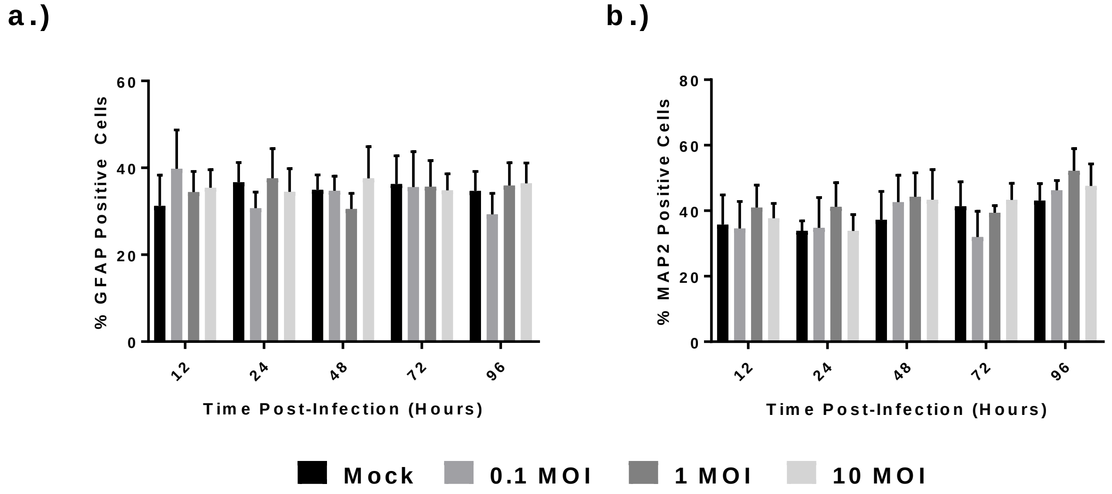

Figure 3.3: Frequency of neurons and astrocytes in neuron/astrocyte co-cultures

Neuron/astrocyte co-cultures were either mock infected or infected with 0.1, 1, or 10 MOI of LACV. Cells were formalin fixed and stained for MAP2 or GFAP with DAPI counterstain. Percentages of GFAP or MAP2 positive cells were calculated across 6 fields of at least 200 cells.

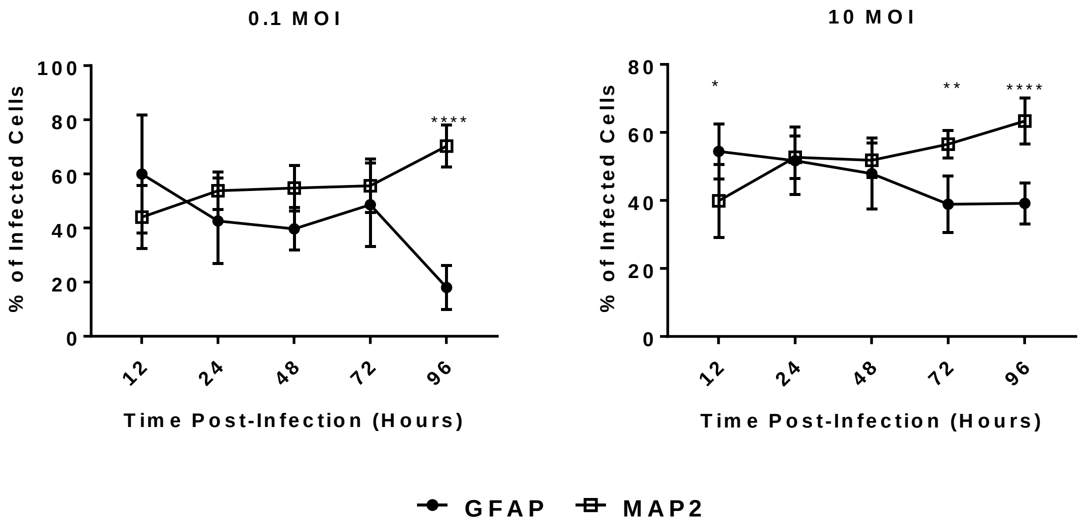

Figure 3.4: Infected cell types of high and low MOI LACV infection of neuron/astrocyte co-cultures

Neuron/astrocyte co-cultures were either mock infected or infected with 0.1 or 10 MOI of LACV. Cells were formalin fixed and stained for MAP2 or GFAP, LACV antigen and with DAPI counterstain. Percentages of infected cells positive for GFAP and MAP2 were calculated.

LACV INDUCES APOPTOSIS IN HNSC DERIVED NEURON/ASTROCYTE CO-CULTURES

Previous studies have demonstrated that neurons in the mouse model and *in vitro* undergo apoptosis in response to LACV infection [34,41,42]. To further validate this system, cytotoxicity and apoptosis assays were performed to confirm apoptotic cell death. Neuron/astrocyte co-cultures were either mock infected, infected with LACV, or treated with staurosporine as a positive control for apoptosis induction. A single dose of LACV (1 MOI) was selected because at this MOI CPE is apparent, titers are comparable to 10 MOI infections, and cells remain viable for longer which allowed us to assay later time points. A cytotoxicity assay (Fig. 3.5a) assessed supernatant for cell-impermeable proteases via fluorescence, and an apoptosis assay (Fig. 3.5b) detected caspase 3/7 activity via luminescence after cell lysis. As expected, mock infected controls displayed low levels of cytotoxicity and caspase activation throughout the course of the experiment. Staurospoine controls were only measured for the first 24 hours but demonstrated significant cytotoxicity and caspase 3/7 activation at that time point indicating an apoptotic response. LACV infected co-cultures began displaying significant cytotoxicity at 48 HPI (Fig. 3.5a) consistent with CPE observed in Fig. 3.1a. Additionally, at 48 HPI significant increases in caspase 3/7 activity were measured in LACV infected neuron/astrocyte co-cultures (Fig. 3.5b). Taken together, these results suggest that apoptosis is a primary mediator of cytotoxicity in LACV infected neuron/astrocyte co-cultures.

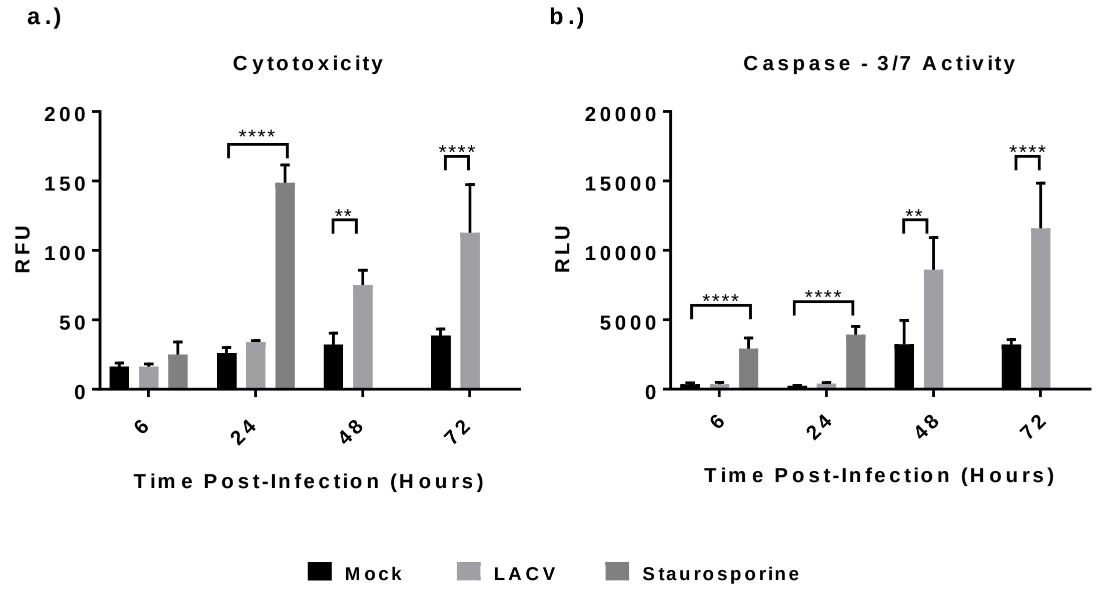

Figure 3.5: Apoptosis of LACV infected neuron/astrocyte co-cultures.

Neuron/astrocyte co-cultures were infected with 1MOI of LACV and assayed for **(a)** cytotoxicity or **(b)** apoptosis at various time points. Staursporine treatment was included up to 24 HPI as a positive control for apoptosis. Cytotoxicity was measured via fluorescence activity of a non-permeable protease substrate, and apoptosis was measured via luminescence from a caspase 3/7 substrate. Measurements are reported as relative fluorescence units (RFUs) or relative luminescence units (RLUs). **P<0.01. ****P<0.0001

hNSC DERIVED NEURON/ASTROCYTE CO-CULTURES ARE RESPONSIVE TO PROINFLAMMATORY STIMULI

After demonstrating that the hNSC derived neuron/astrocyte co-culture system reproduced the known features of LACV infection such as apoptosis and neuronal infection, innate immune responses of these primary human cells to inflammatory stimuli was assessed [21,34,42]. For these studies neuron/astrocyte co-cultures were either mock treated or treated with heat inactivated LACV or poly I:C (Fig. 3.6a). At 48 hours post-treatment, RNA was collected and analyzed using qRT-PCR (Fig. 3.6a). No significant increases were noted with inactivated LACV for any of the tested analytes at the transcriptional level. In contrast, most analytes were significantly upregulated after poly I:C exposure including IFN-β, proinflammatory cytokines IL-6 and TNF-α, and proinflammatory chemokines IL-8, CCL2, CCL4, CCL5, and CXCL10 (Fig. 3.6a). IFN-α was not significantly upregulated in response to poly I:C similar to previous studies [233,234].

BioPlex assays were performed to confirm the expression of proinflammatory cytokines and chemokines by neurons/astrocytes at the translational level using supernatant of stimulated cells (Fig. 3.6b). Additionally, for BioPlex experiments co-cultures were treated with lipopolysaccharide (LPS), but no changes were observed except for a small increase in CXCL10 expression. Similar to the qRT-PCR results, no significant responses after treatment with inactive LACV were observed. In contrast, significant increases in nearly all analytes were measured after poly I:C stimulation, confirming qRT-PCR results. Among the upregulated proteins were the proinflammatory cytokines IFN-γ, IL-6, and TNF-α and the proinflammatory chemokines IL-8, CCL4, CCL5, and CXCL10 (Fig. 3.6b). Surprisingly, no significant increase in CCL2 protein expression was detected in comparison to mock and heat inactivated LACV treated cells. For ease of interpretation analytes with the most relevance to viral encephalitis were included in Figure 3.6b. Additional analytes not discussed further are provided as additional files (Appendix A, Fig. 1). These data indicate that neuron/astrocyte co-cultures have the ability to respond to proinflammatory stimuli in a physiologically relevant manner with the production of interferons, cytokines, and chemokines.

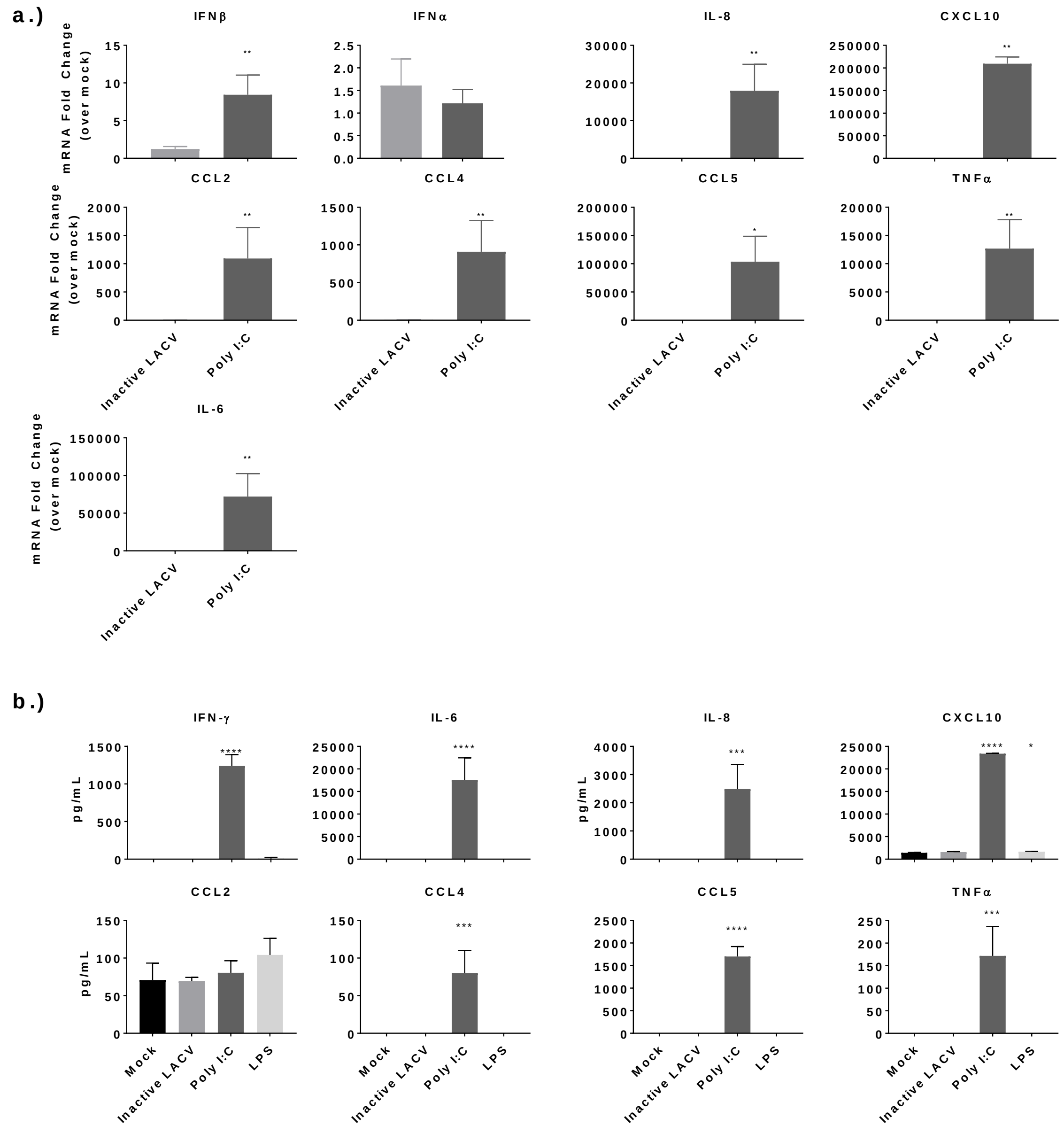

Figure. 3.6: Innate immune responses to inflammatory stimuli in neuron/astrocyte co-cultures.

RT-PCR and BioPlex assays were performed to determine the cytokine and chemokine responses of neuron/astrocyte co-cultures. (**a**) Co-cultures were treated with either mock, poly I:C (10µg/ml), LPS (10µg/ml), or heat inactivated LACV (1 MOI) and at 48 HPI assessed for changes in gene expression for selected cytokines/chemokines via qRT-PCR. Values are reported as fold change relative to mock treatment normalized to 18S RNA. (**b**) Supernatant was collected and assayed for changes in selected cytokine/chemokine secretion via BioPlex assay. Values are reported as raw measurements, as mock values were often below detection or at zero, making fold change calculations impossible. * P<0.5, **P<0.01, ***P<0.001, ****P<0.0001

hNSC DERIVED NEURON/ASTROCYTE CO-CULTURES RESPOND TO LACV INFECTION WITH PROINFLAMMATORY CHEMOKINE AND CYTOKINE RESPONSES

After demonstrating that hNSC derived neuron/astrocyte co-cultures are capable of responding to proinflammatory stimuli with the production of cytokines and chemokines, the co-cultures' responses to LACV infection were determined. To accomplish this, co-cultures were infected with 0.1, 1, or 10 MOI of LACV and responses measured over time. RNA was collected and analyzed via qRT-PCR. IFN-α responses were detected as early as 6 HPI and continued until 48 HPI before decreasing to near baseline levels at 72 HPI (Fig. 3.7a). IFN-β responses were detected later (24 HPI through 48 HPI) but were much stronger (Fig. 3.7a). The other cytokines and chemokines measured (IL-6, TNF-α, IL-8, CCL2, CCL4, CCL5, and CXCL10) displayed significant increases with peak mRNA induction at 48 HPI (Fig. 3.7a). In general, these responses were stronger in the 10 MOI group than in the 0.1 and 1 MOI groups. Additionally, responses in the 10 MOI group had a tendency to show significant upregulation earlier (24 HPI), which correlated with the viral growth kinetics (Fig. 3.1b and c).

Protein secretion patterns closely mirrored mRNA responses (Fig. 3.7b). Most measured analytes displayed significant upregulation at 48 and 72 HPI, with some analytes such as IFN-γ, CXCL10, and CCL5 responding at 24 HPI (Fig. 3.7b). In general, the responses were stronger in the 10 MOI group. Interestingly, no significant differences in CCL2 secretion was noted, despite large mRNA increases. Platelet-derived growth factor (PDGF), IL-1Rα, IL-4, IL-7, IL-9, Eotaxin, FGF, granulocyte colony stimulating factor (G-CSF), vascular endothelial growth factor (VEGF), macrophage inflammatory protein (MIP-1α), and granulocyte-macrophage colony stimulating factor (GM-CSF) also displayed upregulation at 48 and 72 HPI, IL-12, IL-10, and IL-13 displayed mild increases over mock, and IL-1β, IL-2, IL-5, IL-15, and IL-17 did not display significant increases (Appendix A, Fig. 2). These data demonstrate that neuron/astrocyte co-culture responded to LACV infection with a strong pro-inflammatory cytokine profile, with particularly large increases in monocytic and lymphocytic chemokines.

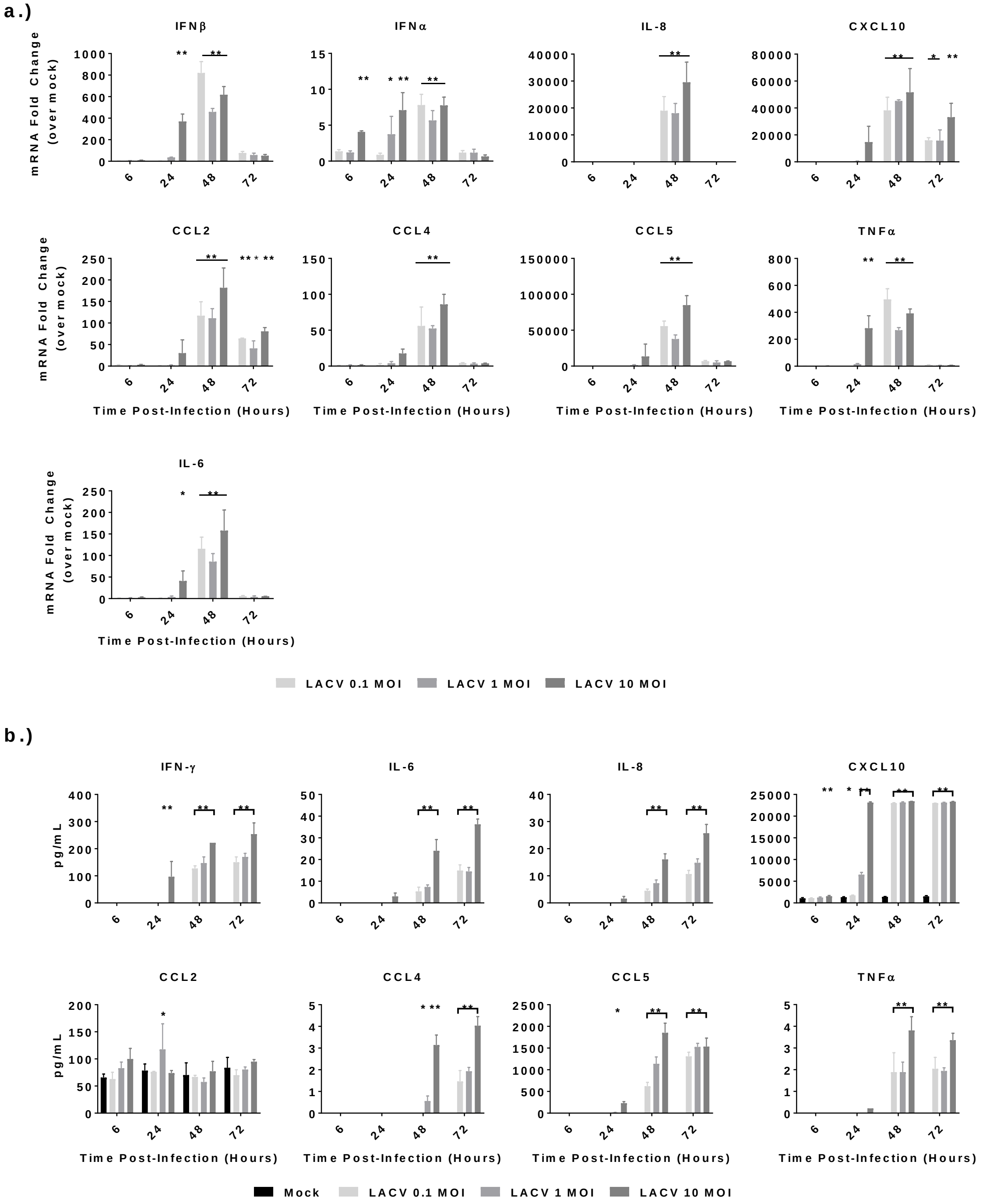

Figure 3.7: Cytokine and chemokine responses of neuron/astrocyte co-cultures to LACV infection.

Cells were either infected with 0.1, 1, or 10 MOI of LACV. **(a)** Cells were lysed and RNA was collected and assessed for changes in selected cytokine/chemokine expression via qRT-PCR. Values are reported as fold change relative to mock treatment normalized to 18S RNA. **(b)** Supernatant was collected and assayed for changes in selected cytokine/chemokine secretion via BioPlex assay. Values are reported as raw measurements, as mock values were often below detection or at zero, making fold change calculations impossible. *P<0.5, **P<0.01

HNSC DERIVED NEURON/ASTROCYTE CO-CULTURES ALTER MMP AND TIMP EXPRESSION IN RESPONSE TO LACV INFECTION

In addition to cytokine and chemokine responses, the levels of MMPs and TIMPs, which can influence the permeability of the blood-brain barrier, were also measured [235–237]. To determine the changes in MMP and TIMP expression in the neuron/astrocyte co-culture system, cells were treated as in previous experiments and RNA analyzed by qRT-PCR. MMP2, MMP7, MMP9, TIMP1, and TIMP2 were assayed. These have previously been described to be differentially expressed after infection of the CNS [54,238–240]. Low but significant increases were detected for MMP2 after LACV infection at higher MOI's, although interestingly, poly I:C failed to induce a significant change (Fig. 3.8a). MMP7 had the largest induction with significant upregulation for all three MOIs at 48 and 72 HPI (Fig. 3.8a). TIMP-1 was also significantly upregulated in response to viral infection and poly I:C at 48 and 72 HPI. Lastly, upregulation was not noted for TIMP2. In fact, there was significant downregulation of TIMP2 mRNA for co-cultures infected with 10 MOI at 72 HPI (Fig. 3.8a). Additionally, while not significant, poly I:C treatment trended to similar levels of downregulation. To confirm changes in MMP/TIMP expression, protein levels were measured via BioPlex (Fig. 3.8b). No increases in MMP2 were noted following LACV infection, suggesting that the small observed increase in RNA was not biologically significant. However, MMP7 and TIMP1 were upregulated in response to LACV infection. No changes were measured for MMP9.

Taken together, these data suggest that later responses in neurons and/or astrocytes significantly upregulate MMP7 and TIMP1 while potentially downregulating TIMP2.

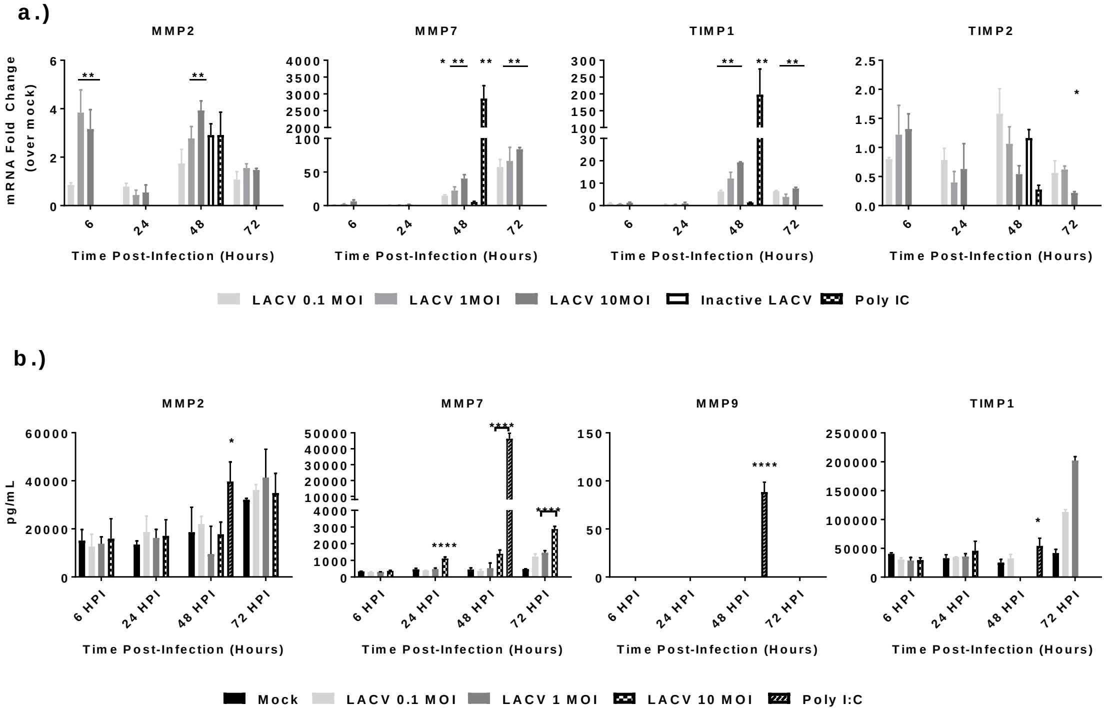

Figure 3.8: MMP and TIMP responses of LACV infected neuron/astrocyte co-cultures.

Neuron/astrocyte co-cultures were either mock infected, treated with inactivated LACV, treated with poly I:C, or infected with 0.1, 1, 10 MOI of LACV. **(a)** RNA was collected and analyzed via qRT-PCR against selected MMPs and TIMPs. Values are reported as fold change relative to mock treatment normalized to 18S RNA. **(b)** Protein levels were measured via BioPlex assays of supernatant. *P<0.5, **P<0.01

MICROGLIA DO NOT APPEAR SUSCEPTIBLE TO LACV INFECTION.

Microglia are not present in the co-culture system but are important producers of cytokines during viral encephalitis. In order to assess the roles of microglial cells during LACV infection, primary human microglial cells were infected with 1 MOI LACV. Of note, microglia were not from the isolated same donor as the hNSCs, but commercially acquired. Supernatant was collected over the course of 96 hours of infection, but no infectious virus was detected via plaque assays. Supernatant was also assayed for cytokine/chemokine responses via BioPlex assay to determine if microglia could respond to LACV in the absence of productive infection (Fig. 3.9). While microglia treated with poly I:C responded with upregulation of G-CSF, TNF-α, IL-6, IL-8, and CCL5, infection with LACV did not induce changes in any of these cytokines. LACV induced a slight increase in CXCL10 at 96 HPI, but appeared to decrease the same chemokine at 72 HPI. This decrease corresponded to an abnormal increase in mock, and is likely an artifact. In conclusion, human microglia do not seem susceptible to LACV infection and, furthermore, do not appear to induce a significant pro-inflammatory response.

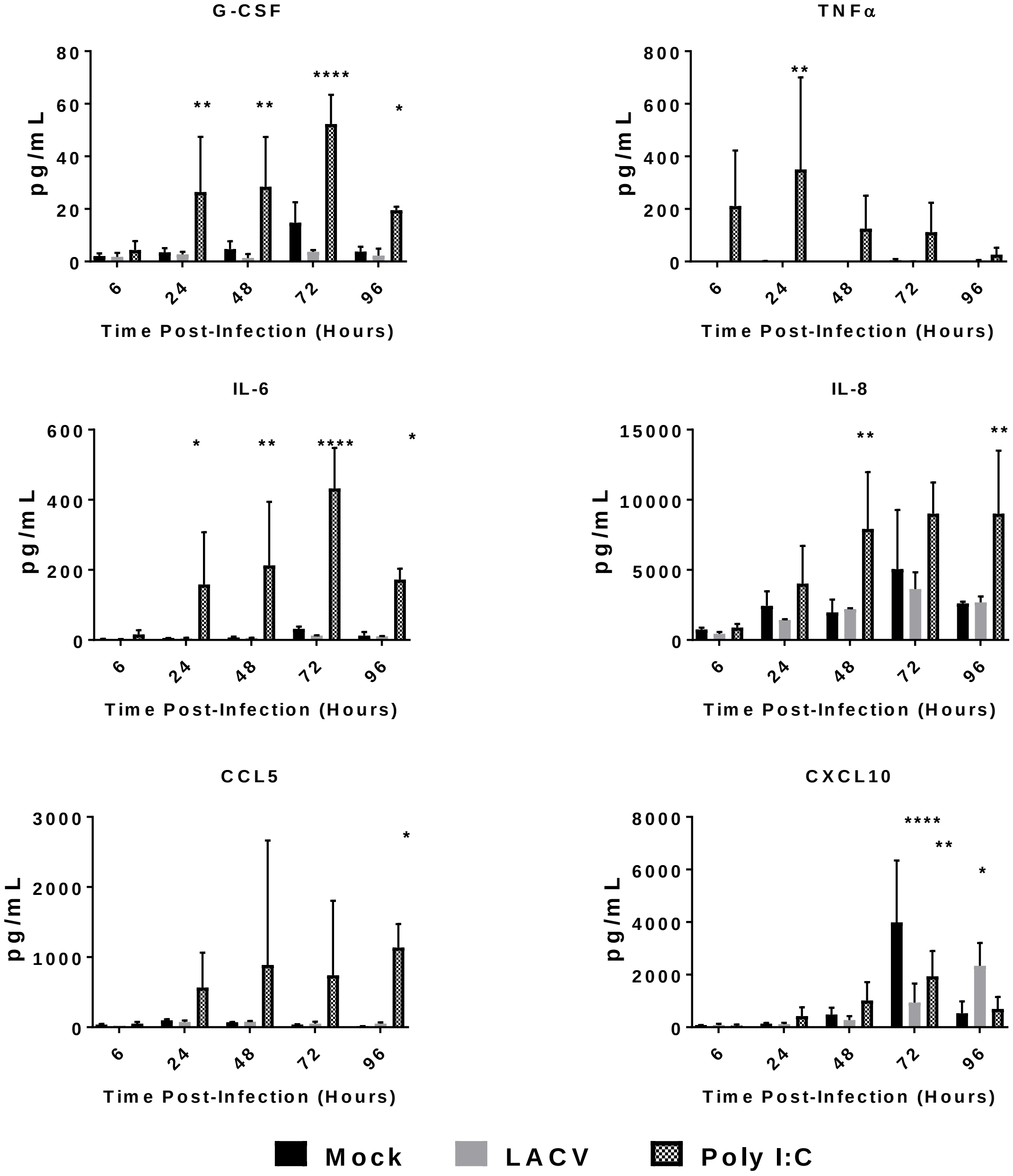

Figure 3.9: Microglial responses to LACV infection

Human microglia were infected with 1 MOI of LACV or treated with 1μg/ml poly I:C. Supernatant was collected and assayed for changes in selected cytokine/chemokine secretion via BioPlex assay. * P<0.5, **P<0.01, ***P<0.001, ****P<0.0001

DISCUSSION

Emerging encephalitic viruses continue to pose a significant public health threat. Despite this threat, *in vitro* models of CNS infection remain limited. Clinical samples are rarely obtained outside of autopsy due to the challenging nature of CNS biopsy. Animal models, both *in vivo* and *ex vivo* studies with primary cells, have been the primary models utilized and provided many important insights [241,242]. However, animal models often do not accurately model all aspects of clinical disease described in patients. Many studies have now demonstrated profound differences between murine and human cellular responses [209,210]. Differences also exist in the structure and function of human and murine parenchymal cells. For example, astrocytes are much larger and perform more complex signaling in humans than in mice [211]. Human primary CNS cells are relevant models, but they are difficult to obtain and introduce donor variability. Immortalized cell lines offer a useful alternative for *in vitro* studies, but the interpretation of results is limited by alterations in specific pathways and differences among different cell lines. This dissertation reports the use of a primary hNSC derived neuron/astrocyte cell co-culture system as powerful new *in vitro* model to study encephalitic viruses. In addition to allowing for the repeated study of human primary cells without donor variability, co-culturing neurons and astrocytes allows for a more physiologically relevant model than neuronal monoculture. While the lack of donor variability is useful for the identification of pathogenic mechanisms, it may also obscure different aspects of disease as seen in other studies where different hNSC strains responded differently to ZIKV infection [220]. Astrocytes play a key role in the physiologic support of neuronal health and function such as synaptic development, protection from glutamate toxicity and oxidative stress, and metabolic support [214]. Astrocytes also are increasingly recognized as major contributors to inflammatory responses during CNS infection. In addition to pathogenesis studies, neuron/astrocyte co-cultures may provide a relevant *in vitro* system for the evaluation of antiviral therapies against neurotropic viruses.

Neuron/astrocyte co-cultures were susceptible to LACV infection (Fig. 3.1) and high viral titers were reached regardless of initial viral inoculum (Fig. 3.1b). However, there was a drop in viral RNA measured at 48 HPI (Fig. 3.1c), for which the reasons are unknown, but the timing coincides with the peak IFN-β response suggesting that cells may become less susceptible to infection during this period (Fig. 3.7a). Future studies should evaluate the role of IFNs and the viral IFN antagonist NSs during LACV neuron/astrocyte infection using recombinant LACV lacking NSs expression. CPE was also observed at later time points consisting of cell rounding in detachment (Fig. 3.1a). Indeed, cytotoxicity and apoptosis assays indicate increased numbers of apoptotic cells beginning at 48 HPI (Fig. 3.5). These data mirror those seen in previous work using murine models and the human NT2N cell line [32,34,41,42]. Of note, while cytotoxicity and apoptosis were noted, large amounts of viable cells remain as late as 96 HPI. This contrasts reports of LACV as a highly cytopathic virus in mouse primary neurons and human NT2N cells, and are likely due to intact IFN responses and the protective effects of astrocytic co-culture resulting in a more physiologic response and greater resilience to infection [41,42]. To determine the contributions of IFN to this reduction in CPE, future studies should be performed by either adding exogenous IFN and to disrupt signaling by blocking IFNAR.

The overall percentage of cells infected during this study was lower than expected, reaching maximums of 50% infection even with an MOI of 10 (Fig. 3.2b). It should be noted that MOI estimates were derived from plaque assays using Vero cells lacking functional IFN responses, and therefore may overestimate the amount of fully infectious virus added to the co-cultures. Therefore, it is likely that this lowered level of infection is due to intact antiviral sensing pathways and IFN responses. Again, IFN addition and blockade experiments will be necessary to determine if this is the case.

Multiple studies have indicated that both neurons and astrocytes are important producers of type I IFN during LACV infection, but astrocytes appear to be responsible for greater responses [40,48]. Therefore, astrocytic IFN production may be responsible for limiting the magnitude of infection. The current study also demonstrates neurons and astrocytes are both highly susceptible to LACV infection.

Neurons have long been recognized as a target of infection, but astrocytic infection has been largely ignored [21,34,40,48]. One study demonstrated that in the weanling mouse model of LACV encephalitis less than 1% of infected cells were astrocytes [40]. However, in the same study deletion of the LACV NSs gene resulted in large increases of astrocytic IFN-β production suggesting nonproductive infections or infections below the detection limit of the utilized assays may be higher than previously thought [40]. Another group has proposed in a review that astrocytic infections are common, and that rapid death of infected astrocytes leads to a lack of detection *in vivo* [1]. The current study demonstrates that human astrocytes are indeed highly susceptible to LACV infection *in vitro* (Fig. 3.2). At early time points neurons and astrocytes are infected at a nearly 1:1 ratio, and at an initial MOI of 10, infection in astrocytes is significantly higher than in neurons at 12 HPI (Fig. 3.4). However, by 48 HPI neurons became the predominant cell type infected. Despite the shifting tropism of viral infection, no changes were detected in the overall ratio of neurons to astrocytes (Fig. 3.3). Therefore, it is unlikely that the observed shift in tropism is due to the initial target cells (astrocytes) dying at a faster rate than neurons, as was previously proposed [1]. The tropism shift may be due to the type I IFN response, which begins at 48 HPI. Astrocytes may be more sensitive to type I IFN signaling and induce strong antiviral states, protecting this cell type while weaker responses in neurons leave them more vulnerable. Indeed, this has been shown to be the case for several viral infections [175,176]. Initial characterizations of the co-cultures' responses to IFN in NiV infection (discussed in chapter 4) also suggest that this may be the case. Future studies will attempt to determine the relative roles of IFN on neurons and astrocytes during viral infection.

Neurons and astrocytes are increasingly recognized as important components of CNS innate immune responses. The responsiveness of hNSC derived neuron/astrocyte co-cultures was measured by stimulating with heat inactivated virus and a dsRNA analogue, poly I:C (Fig. 3.6 and Appendix A Fig. 1). The co-cultures were highly responsive to poly I:C, responding with large increases in IFNs and proinflammatory cytokines and chemokines at both the RNA and protein level. It is reasonable to conclude that these cells have intact antiviral sensing pathways and are capable of initiating inflammatory responses. No responses to inactivated LACV were detected, suggesting that viral replication is necessary for such cellular responses. Alternatively, this result may indicate that viral entry is necessary as heat inactivation may denature glycoproteins, therefore impairing clathrin-mediated endocytosis. Another interesting finding was that while CCL2 mRNA is induced following poly I:C treatment, the levels of CCL2 secretion remain unchanged. This suggests additional levels of regulation of CCL2 at the translational or secretory level.

LACV infection generated similar, but more limited, proinflammatory responses in neuron/astrocyte co-cultures with mRNA levels peaking around 48 HPI and protein levels closely mirroring these results (Fig. 3.7 and Appendix A Fig. 2). Interestingly, LACV, but not poly I:C induced an increase in IFN-α mRNA similar to previous studies [233,234]. At the same time, unlike poly I:C, LACV failed to induce IL-1β, IL-2, IL-5, IL-15, and IL-17. Additionally, LACV only resulted in modest increases in IL-10, IL-12, IL-9, and IL-13 and only at late time points with high MOIs. This may be explained as either viral inhibition of select responses, lower levels of stimulation relative to poly I:C, or differences in signaling pathways used to detect poly I:C versus LACV. Indeed, poly I:C was added to the supernatant without transfection, which typically stimulates TLR3 while LACV infection largely is sensed by RIG-I [44,243]. These results demonstrate that neurons and astrocytes are likely important factors in shaping the initial immune responses to LACV in the CNS. This has previously been demonstrated for the type I IFN responses, but not yet for proinflammatory chemokines [40,48].

Human pathology reports and animal models of LACV infection note inflammation primarily composed of macrophages and lymphocytes [21,34,50]. A recent study by Winkler *et al*. revealed that lymphocytes do not appear to be important in the development of neuropathology [49]. The same group has also shown inflammatory monocytes to be the primary infiltrating cell type within the CNS in the mouse model, although their role in immune mediated neuropathology was not addressed [50]. In the same study, it was noted that C-C chemokine receptor 2 (CCR2) was necessary for monocytes to migrate to lesions within the CNS, but not for recruitment to the CNS. Interestingly, while changes in mRNA expression for CCL2 (the CCR2 ligand) were noted, protein expression in the cell culture supernatant was unchanged. Neurons and astrocytes constitutively express low levels of CCL2 in the healthy brain, as seen in the current results and previous studies, but some studies have noted a microglial requirement for upregulation after infection [52,244]. Neurons in the co-culture system may require the addition of microglia to the system in order to produce robust CCL2 responses. Their response is likely via bystander effects as preliminary experiments infecting primary human microglia did not yield productive infection or chemokine responses on their own (Fig. 3.9). More complex CNS models continue to be developed such as tricultured microfluidic neuron/astrocyte/microglial cultures which may be of use to further understand the role of various cell types during infection [245]. Additionally, future studies should address the role of inflammatory monocytes during LACV encephalitis.

The strongest responses measured in this study were the monocytic and lymphocytic chemokines, CCL5 and CXCL10. These chemokines have been associated with a wide range of viral CNS infections and are particularly important for lymphocyte recruitment [246]. As previously mentioned, lymphocytes do not appear to play a role in immunopathology, but it is likely that during human infection their role is critical in the recovery from LACV encephalitis [49]. The receptors for these CCL5 and CXCL10 (CCR5 and CXCR3, respectively) have been shown to be critical for T-cell recruitment for several encephalitic viruses such as West Nile virus (WNV), murine hepatitis virus (MHV), and herpes simplex virus (HSV) [247–249]. CCR5 has also been shown to be important for the control of WNV [250]. The current data therefore suggest that neurons and/or astrocytes are important for the recruitment of T-cells to the CNS during LACV encephalitis, although *in vivo* studies will be required to confirm this hypothesis. Additionally, the co-cultures produce strong IFN-γ responses which have been shown to be critical for the control of several viral CNS infections such as HSV, SinV, MeV, and TMEV [191,204,206,251]. One limitation of the current study is the difficulty in determining which cell types are responsible for signaling. As cells behave differently in co-culture, simple assessment of primary astrocytes and neurons may not be accurate. Immunofluorescent or immunohistochemical staining for cytokines and chemokines is often problematic due to low intercellular levels of protein, and separation via FACS is difficult due to the fragility of the cells. Future effort needs to focus on better understanding cell-specific responses.

The neuron/astrocyte co-culture system also demonstrated a potential to disrupt the BBB. While initial LACV neuroinvasion is thought to occur via hematogenous spread through capillaries in the olfactory bulb, further disruption of the BBB after neuroinvasion may contribute to greater viral neuroinvasion or increased inflammatory responses leading to greater damage [39]. Rift Valley fever virus, a related bunyavirus, is likely to also use the olfactory bulb for CNS entry, but generally maintains BBB integrity during infection in contrast to LACV [252,253]. TNF-α, IL-6, and VEGF had modest upregulation in this study and have long been associated with increased BBB permeability (Fig. 3.7 and Appendix A Fig. 2) [53,54]. Additionally, MMPs and TIMPs were assessed (Fig. 3.8 and 3.9). MMPs are proteases, which degrade the extracellular matrix. TIMPs are inhibitors of MMPs. Within the CNS, MMP9 and MMP2 are associated with BBB disruption [54]. Initial BioPlex screens and RT-PCR did not detect MMP9 after virus infection (Fig. 3.9). However, there were modest increases in MMP2 and large increases in MMP7. MMP7 has not been commonly studied in the context of viral encephalitis and its relevance is unknown. However, MMP7 is important for leukocyte infiltration during experimental autoimmune encephalomyelitis and is found in the CSF during AIDS dementia [238,239]. TIMP-2 is constitutively expressed in the brain while TIMP-1 is inducible [240]. The current study demonstrates that TIMP-1 is induced following LACV infection and that TIMP-2 appears to be downregulated (Fig. 3.8). The overall BBB status requires future study as both MMPs and TIMPs are upregulated, but overall, it is likely that neurons and astrocytes contribute to continued BBB compromise.

These results demonstrate the feasibility, accuracy, and usefulness of hNSC derived neuron/astrocyte co-cultures to study encephalitic viruses. In the current study many aspects of LACV encephalitis such as neurotropism and apoptosis were replicated. In addition, this study demonstrated the susceptibility of astrocytes early in infection with a shifting tropism later during the course of infection. This may explain why while low levels of astrocyte infection have been noted in experimental models, they do not appear to be prevalent *in vivo*. The results also demonstrate intact viral sensing pathways and proinflammatory cytokine and chemokine responses. These neuron/astrocyte responses may drive the observed monocytic and lymphocytic infiltration observed during LACV encephalitis as well as prolonged disruption of the BBB. Together, these results highlight the role of neurons and astrocytes to the innate immune responses to LACV infection and suggest that these cells may play a large role in either immunopathogenicity or recruitment of an effective immune response.

Chapter 4: NiV Infection of hNSC-Derived Neuron/Astrocyte Co-Cultures

ABSTRACT

This chapter describes the experimental infection of hNSC-derived neuron/astrocyte co-cultures with NiV (and to a lesser extend HeV). After establishing this model using LACV in chapter 3, the next study focused on assessing NiV infection of these cells. Neurons are a primary target cell of NiV infection, but to date all experimental infections of neurons have used transformed neuroblastoma cell lines. This work provides the first detailed description of NiV infection of primary human neurons and astrocytes. It was hypothesized that neurons and astrocytes would both be susceptible to NiV and display extensive syncytia formation along with cytotoxicity. Additionally, the down regulation of host cell cytokine and chemokine responses was expected. Lastly, after initial characterizations, the goal became to conduct a mechanistic study to determine effects of IFN treatments on NiV replication within CNS cells. Due to the ability of IFN-γ to control MeV infection in neurons, it was hypothesized that IFN-γ would restrict NiV infection and replication and effectively clear virus from infected neurons. When it became apparent that this hypothesis was false, IFN-β was assessed because of its generally stronger antiviral effects. Together, these results demonstrate the susceptibility of neurons and astrocytes to NiV infection with nearly total shutdown of host responses. Furthermore, this study demonstrates that IFN-β protects neurons/astrocytes from NiV infection and apoptosis, but these effects may be greater in astrocytes than in neurons.

HNSC DERIVED NEURON/ASTROCYTE CO-CULTURES ARE SUSCEPTIBLE TO HNV INFECTION

hNSCs differentiated neuron/astrocyte co-cultures were infected with 0.01 MOI of NiV-M, NiV-B, and HeV, respectively. Replication of all three HNVs was supported and resulted in increases in viral titer by 2-3 logs over 48 HPI. (Fig. 4.1a). Similar to previously reported results with this system, HeV replicated to approximately 10-fold higher titers than NiV-M at 24 and 48 HPI [231]. Interestingly, at 48 HPI, NiV-B also reached higher titers than NiV-M. HeV titers were significantly higher than both NiV strains at both time points. All three HNVs demonstrated CPE in the form of extensive syncytia formation (Fig. 4.1c). Syncytia were first noted at 24 HPI for all viruses and became more frequent and larger at 48 HPI. In addition, extended time course experiments for NiV-M demonstrated peak titers were reached around 48 HPI, and were maintained through at least 96 HPI (Fig. 4.1b). During these extended time courses NiV-M induced extensive syncytia formation at later time points with almost no cells escaping. Together, these results reaffirm previous observations that human neuron/astrocyte co-cultures are highly susceptible to NiV and HeV infection with NiV-B and HeV replicating to higher titers than NiV-M.

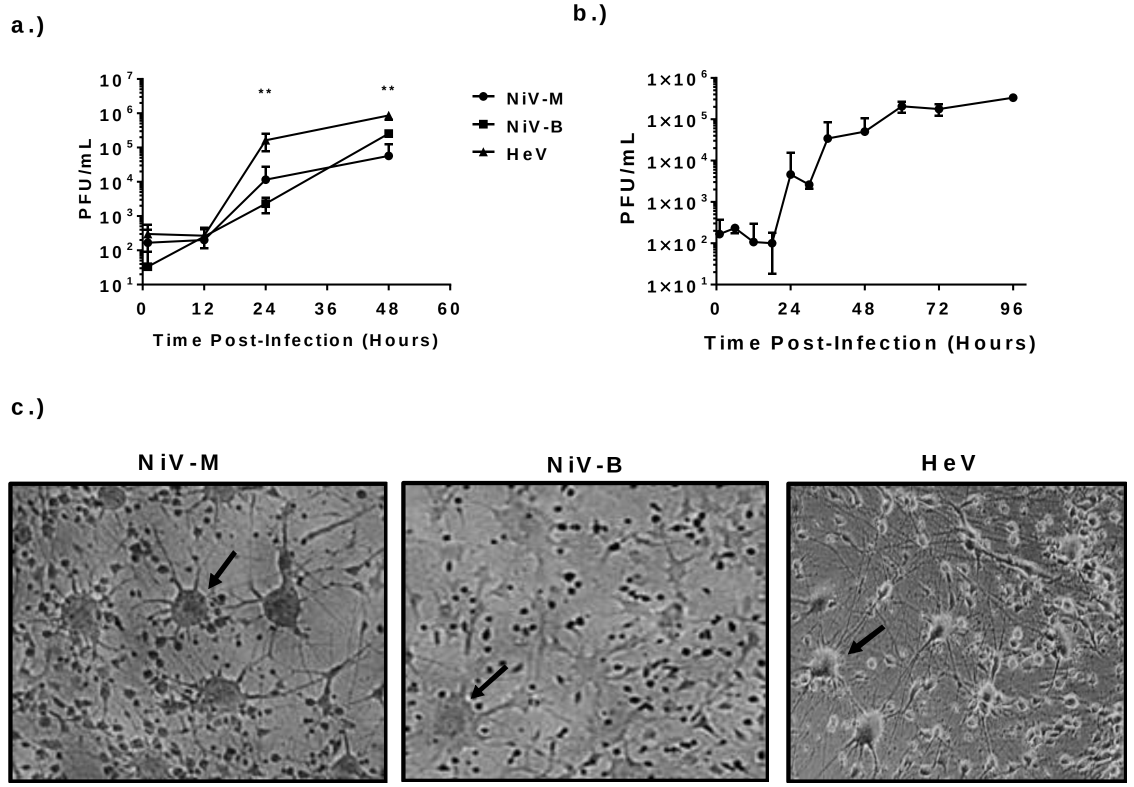

Figure 4.1: Susceptibility and multiplication kinetics of HNVs in human neuron/astrocyte co-cultures.

hNSCs were differentiated into neuron/astrocyte co-cultures. **(a)** On day 10 post-differentiation cells were infected with 0.01 MOI of NiV-M, NiV-B, or HeV. Supernatant was collected and titrated via plaque assay all infections were performed in triplicate, and presented data is an average of multiple experiments. **(b)** Additional infections with NiV-M were conducted to determine the multiplication kinetics over extended time courses. The presented data is an average of multiple experiments performed in triplicate. **(c)** Co-cultures were imaged at 48 HPI via phase contrast microscopy to visualize syncytia formation for NiV-M, NiV-B, and HeV. Arrows indicate syncytia formation **P<0.01

NIV-M INDUCES CYTOTOXICITY AND APOPTOSIS IN NEURON/ASTROCYTE CO-CULTURES

Previous studies reported NiV-induced apoptosis in human neuroblastoma cells, but the infected cell line did not appear productively infected when viral titers were measured [140]. To determine the effects of NiV-M infection on cell viability and apoptosis induction in primary neuron/astrocyte co-cultures, were infected with 0.01 MOI of NiV-M along with mock infections and staurosporine treatment. Cell viability was assessed via intracellular live-cell protease activity, cytotoxicity was determined via extracellular dead-cell protease activity, and apoptosis was measured via caspase 3/7 activity. Values were reported as ratios of viability:cytoxicity and apoptosis:viability to account for any differences in cell density between wells. Staurosporine induced cytotoxicity starting as early as 4 HPI, and viability was significantly decreased relative to mock treated cells throughout the course of the time course (Fig. 4.2a). Reductions in NiV-M infected cell viability were first noted at 48 HPI and decreased further at 72 and 96 HPI. As expected, staurosporine treatment resulted in an increase in apoptosis at 4 HPI, but caspase 3/7 activity quickly decreased to levels similar to mock by 24 HPI (Fig. 4.2b). NiV-M did not induce apoptosis until 72 HPI, but the increase was much greater than that seen in staurosporine. Apoptotic activity remained detectable at 96 HPI. These results indicate that NiV-M induces significant cytotoxicity in neuron/astrocyte co-cultures 2-3 days post-infection. Additionally, apoptosis accounts for some of the cytotoxicity at later time points.

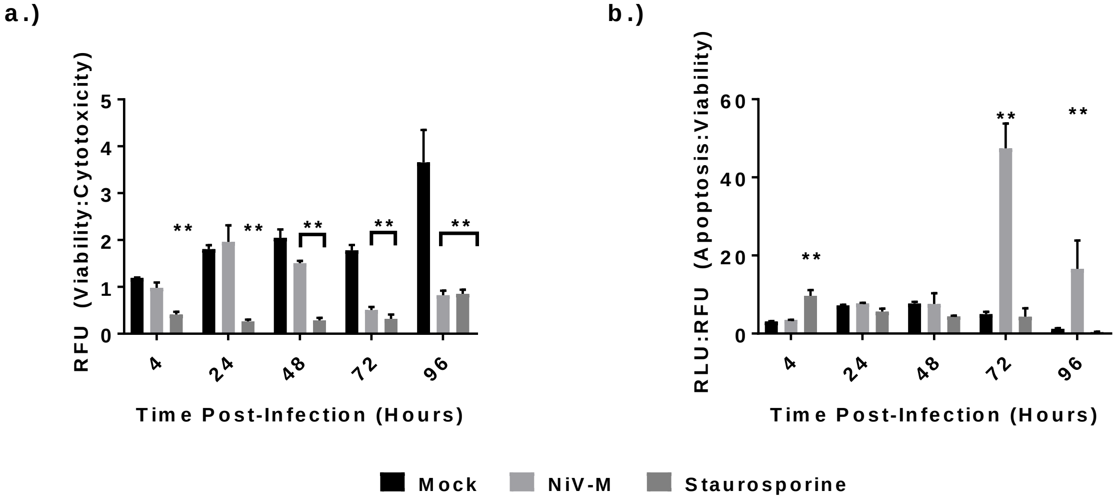

Figure 4.2: Cytotoxicity and apoptosis of NiV-M infected neuron/astrocyte co-cultures.

Differentiated neuron/astrocyte co-cultures were infected with 0.01 MOI of NiV and assayed for cell viability and cytotoxicity (via fluorescence of cell impermeable protease substrates) and apoptosis (via luminescence from a caspase 3/7 substrate). **(a)** Cytotoxicity is represented as the ratio of signals from viability and cytotoxicity assays (viability:cytotoxicity). **(b)** Apoptosis is represented as a ratio of signals for viability and apoptosis assays (apoptosis:viability) Significance values shown are compared to mock treated cells. $^{**}P<0.01$

NIV-M FAILS TO INDUCE A STRONG INFLAMMATORY CYTOKINE/CHEMOKINE RESPONSE

Next, the ability of NiV-M to induce IFN and proinflammatory cytokine/chemokine responses in neuron/astrocyte co-cultures was assessed. Chapter 3 demonstrated that this co-culture system responds to poly I:C stimulation and LACV infection with the production of IFN and proinflammatory cytokines and chemokines. Initially, transcriptional changes in response to infection were assessed between 6 and 60 HPI using qRTPCR (Fig. 4.3). All analyzed cytokines and chemokines were upregulated in response to poly I:C stimulation. In contrast, NiV-M infection only significantly upregulated IFN-β at 60 HPI. Increased transcripts were also detected for CCL5 and CXCL10, but those increases were not significant. CCL5 was not analyzed at 60 HPI; mock samples at this time point did not reach the detection threshold. While no significant differences compared to mock were measured for heat-inactivated NiV-M, there were small trends to increases for IL-8, CCL2, and CCL4 transcripts, suggesting that neurons and/or astrocytes may possess some limited ability to recognize viral particles in the absence of active replication. However, any such responses appear to be minimal.

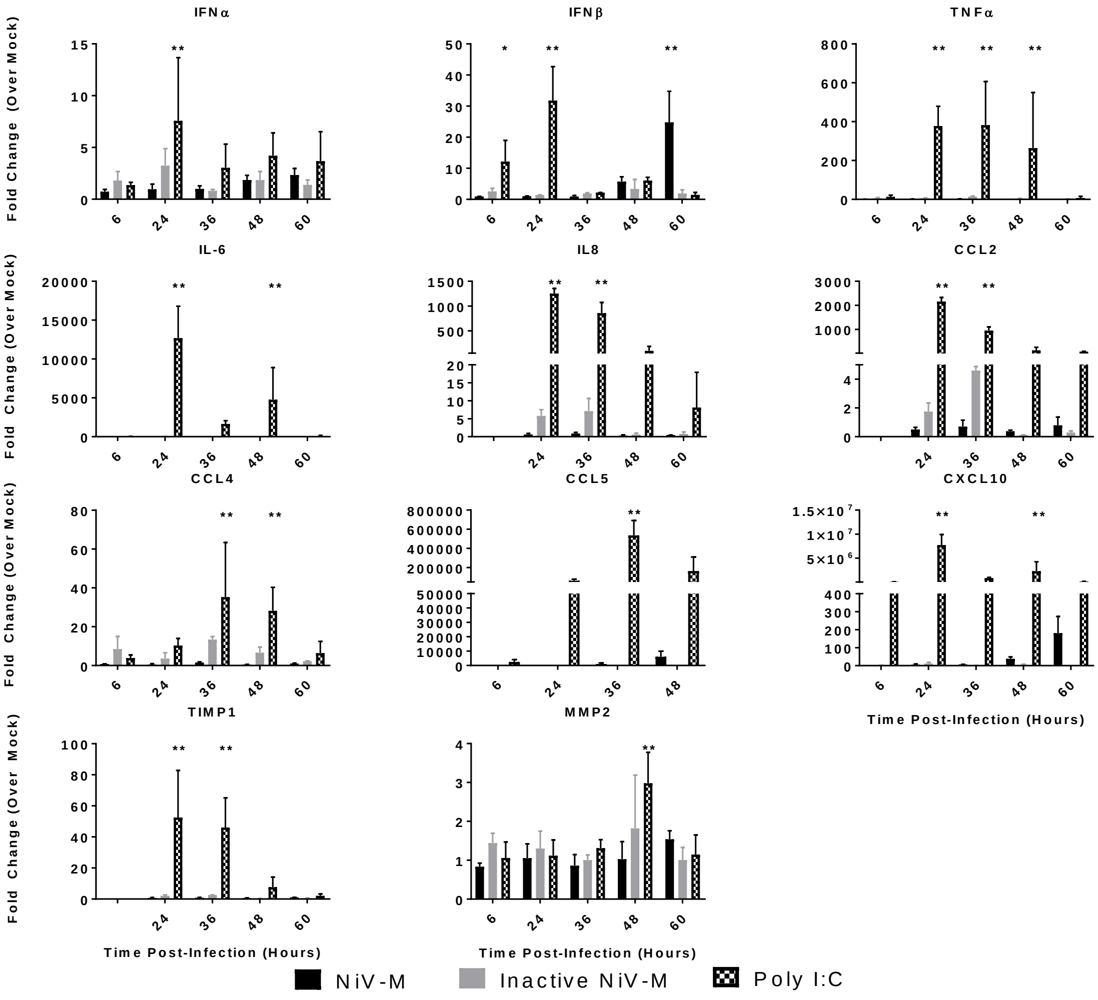

Figure 4.3: Transcription of cytokines and chemokines in response to NiV-M infection.

RT-PCR was performed to measure the cytokine and chemokine responses to NiV infection of neuron/astrocyte co-cultures. Co-cultures were either mock infected, infected with 0.01 MOI NiV-M, 0.01 MOI heat inactivated NiV-M, or treated with 1µg poly I:C. Changes in gene expression were quantified via qRT-PCR. Values are presented as fold change relative to mock treatment normalized to 18S RNA. $^*P<0.05$, $^{**}P<0.01$

Next, cytokine/chemokine responses at the protein level were measured using BioPlex assays. IL-1β, IL-6, IL-8, TNF-α, IFN-γ, CCL2, CCL4, CCL5, and CXCL10 levels are shown in Fig. 4.4. As expected based on qRT-PCR data, poly I:C induced significant increases in all shown cytokines and chemokines (Fig. 4.4). Again, infection with NiV-M did not result in any significant upregulated cytokines or chemokines (Fig.

4.4). Heat-inactivated NiV-M induced no responses for any measured cytokines. The remaining assayed cytokines/chemokines (Appendix A Fig. 3) also displayed poly I:C mediated increases and no responses to NiV-M. Together, these results demonstrate that NiV-M infected neuron/astrocyte co-cultures fail to produce a proinflammatory cytokine or chemokine response. Furthermore, co-cultures do not begin to upregulate IFN-β until 60 HPI.

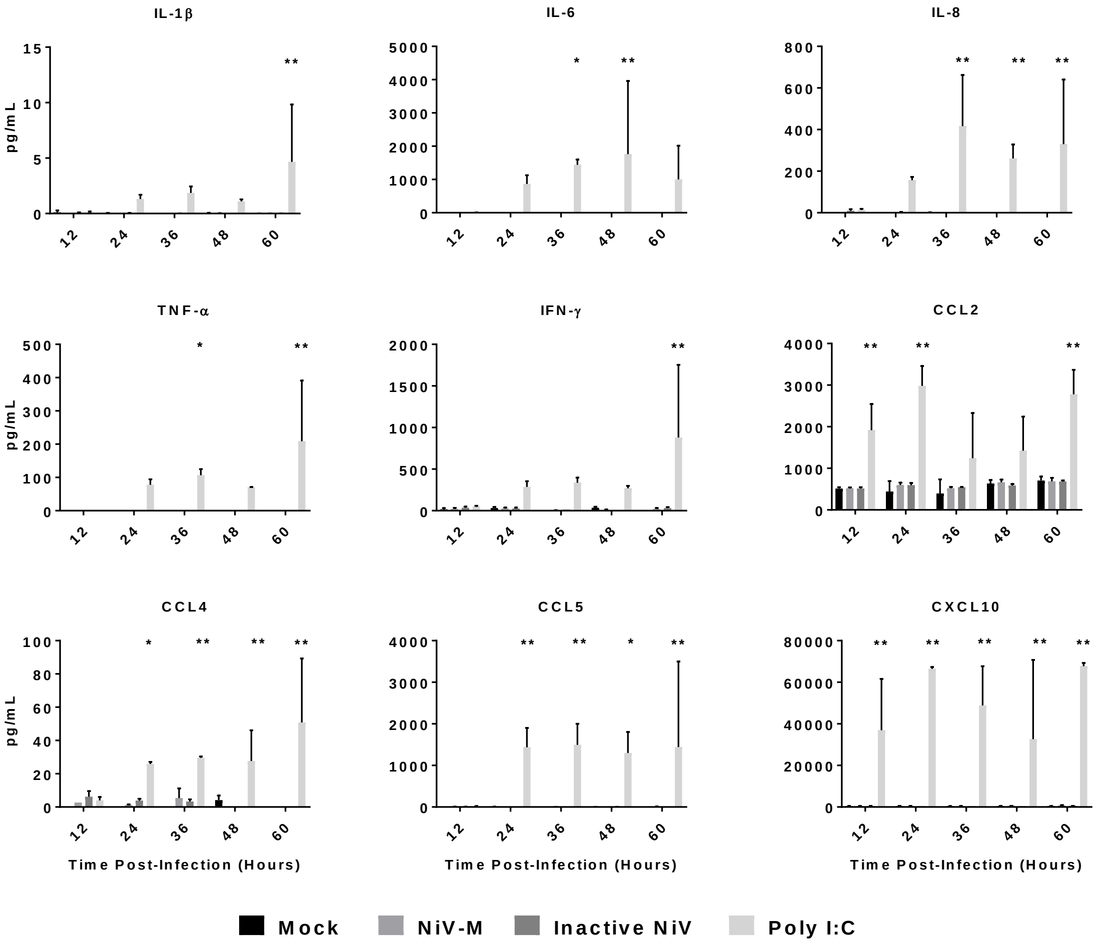

Figure 4.4: Neuron/Astrocyte cytokine and chemokine production in response to NiV-M infection.

BioPlex assays were performed to measure cytokine and chemokine production by neuron/astrocyte co-cultures in response to NiV infection. Cells were either mock infected, infected with 0.01 MOI NiV-M, infected with 0.01 MOI heat inactivated NiV-M, or 1μg poly I:C. Selected cytokines often upregulated during viral encephalitis are shown here, the full panel assessed are available in Appendix A Figure 3. $^*P<0.05$, $^{**}P<0.01$

Translational changes of neuron/astrocyte co-cultures after infection with HeV and NiV-B were then measured to evaluate if a similar lack of cellular responses can be detected for these two closely related HNVs (Fig. 4.5). Surprisingly, HeV induced significant increases in CXCL10 and CCL5 relative to mock and NiV-M at 48 HPI (Fig. 4.5a). NiV-B also induced a much stronger CXCL10 and CCL5 response compared to NiV-M, but at 72 and 96 HPI (Fig. 4.5b). In addition, to assess if replication differences or levels of viral infection were responsible for differential cytokine/chemokine responses co-cultures were infected with 0.1 MOI of NiV-M (Fig. 4.5b). Despite a 10-fold higher initial viral dose NiV-M still did not induce CCL5 or CXCL10 responses. This experiment measured later time points than the previous experiment, and NiV-M still failed to induce significant responses. Overall, these experiments indicate that neuron/astrocyte co-cultures respond to HNV infection in a virus and strain dependent manner.

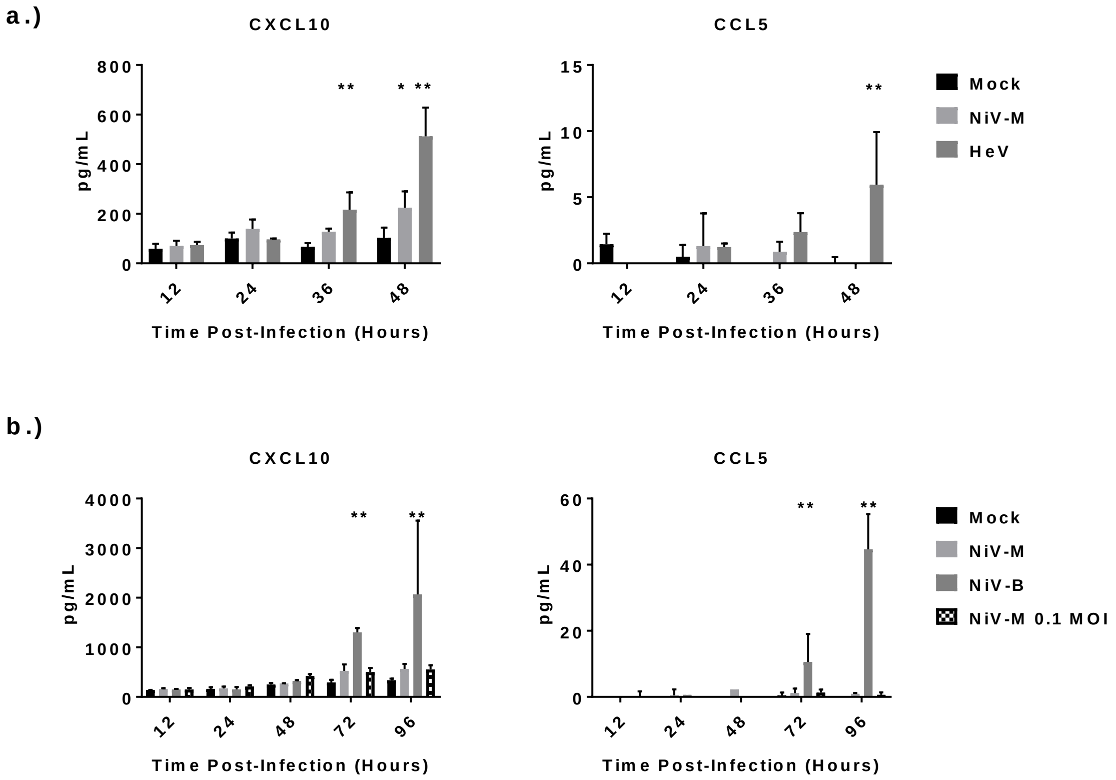

Figure 4.5: Differences in cytokine and chemokine expression among HNVs.

BioPlex assays were performed to determine the cytokine and chemokine production by neuron/astrocyte co-cultures in response to HeV and NiV-B infection. Cells were either infected with (a) mock, NiV-M (0.01 MOI) and HeV (0.01 MOI), or (b) mock, NiV-M (0.01 and 0.1 MOI), or NiV-B (0.01 MOI). **P<0.01

IFN-β AND POLY I:C REDUCED VIRAL TITERS IN NEURON/ASTROCYTE CO-CULTURES MORE THAN IFN-γ

Given that IFN-γ is sufficient for clearance of MeV infection from neurons, the effects of IFN-γ on NiV infected neuron/astrocyte co-cultures were assessed [191,192]. Recombinant NiV-M expressing eGFP (rNiV-eGFP) was used in the following experiments to be able to microscopically track viral infection in real time. rNiV-eGFP was shown to replicate to similar, but slightly higher, titers compared to NiV-M (Fig. 4.6).

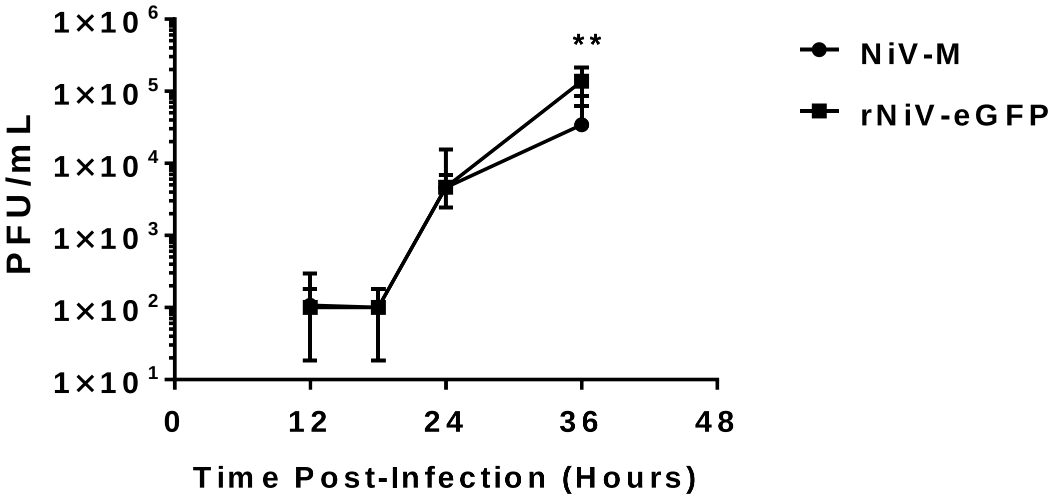

Figure 4.6: Comparison of NiV-M with rNiV-eGFP.

Viral titers were measured via plaque assay. Co-cultures were infected with 0.01 MOI of either NiV-M or rNiV-eGFP. ** P<0.01

Neuron/astrocyte co-cultures were infected with 0.01 MOI of rNiV-eGFP and treated with 100U of IFN-γ 24 hours before infection or 1 HPI. IFN-γ treatment, both before and after, infection resulted in significant decreases in viral titers after 48 HPI, with a stronger inhibition in cells treated pre-infection (Fig. 4.7a). At termination of the experiment at 96 HPI, an approximately 10-fold decrease in titers was measured in the IFN-γ pretreated co-cultures relative to untreated cells. Therefore, all future experiments were conducted with 24 hour pretreatments to observe maximum effects. Increasing the dose of IFN-γ to 1,000U did not result in further inhibition of virus replication compared to 100U (Fig. 4.8a). These experiments indicate that IFN-γ exerts antiviral effects on NiV infected neurons and/or astrocytes, but the protection is limited and not fully protective.

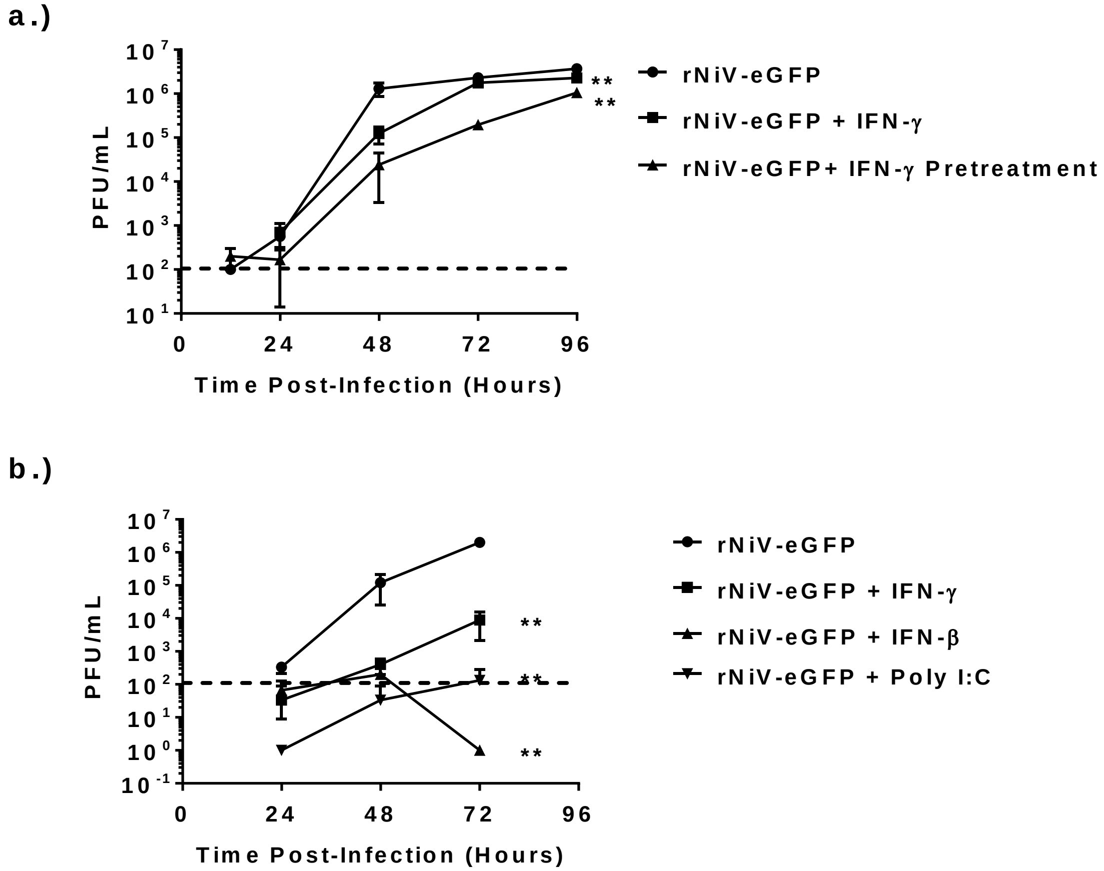

Figure 4.7: Viral multiplication in response to type I and II interferon and poly I:C treatment.

Viral titers from neuron/astrocyte co-cultures infected with 0.01 MOI NiV-M were determined via plaque assay. **(a)** Co-cultures treated with 100U IFN-γ either 24 hours before infection, 1 HPI, or left untreated. **(b)** Co-cultures were pretreated 24 hours before infection with 100U IFN-γ, 100U IFNβ, or 1μg poly I:C. Dashed lines indicate the limit of detection for the plaque assay. ** $P<0.01$

Type I IFNs typically exert much stronger antiviral effects than IFN-γ [202]. Activation of intracellular viral sensors can induce IFN and an antiviral state. In fact, poly I:C has been shown to protect 80% of hamsters from lethal NiV infection [254]. After initial characterizations of NiV infection of the neuron/astrocyte co-culture system, the next goal was to conduct a mechanistic study to evaluate the effects of IFN-β and poly I:C on NiV replication of neuron/astrocyte co-cultures. Cells were pretreated with either IFN-γ, IFN-β, or poly I:C and infected with rNiV-eGFP (Fig. 4.7b). Both IFN-β and poly I:C treatment resulted in significantly lower viral titers than untreated cells. Additionally, IFN-β and poly I:C treated co-cultures maintained titers at or below the detection limit of the plaque assay, an approximate decrease of 4 logs compared to untreated virus infected cells. IFN-β and poly I:C treatments also significantly decreased viral titers compared to IFN-γ treatments. It should be noted that variations in experiments existed; IFN-γ treatments showed variable reductions of 1-2 log differences. This is likely due to variations in cell density due to the nature of plating neurospheres for differentiation. Daily treatments of IFNs or poly I:C were also conducted to determine if multiple treatments could further reduce titers (Fig. 4.8b). Surprisingly, additional treatments with IFN-γ resulted in no further decreases in viral titers compared to single dosing 24 hours prior to infection. Repeated daily dosing of infected cells with IFN-β and poly I:C, respectively resulted in non-significant decreases, but all values were below the limit of detection and therefore could not be reliably compared. For this reason, all subsequent experiments received only one treatment 24 hours before infection. Overall, these data demonstrate that the type I IFN response provides significant protection against NiV infection of neuron/astrocyte co-cultures.

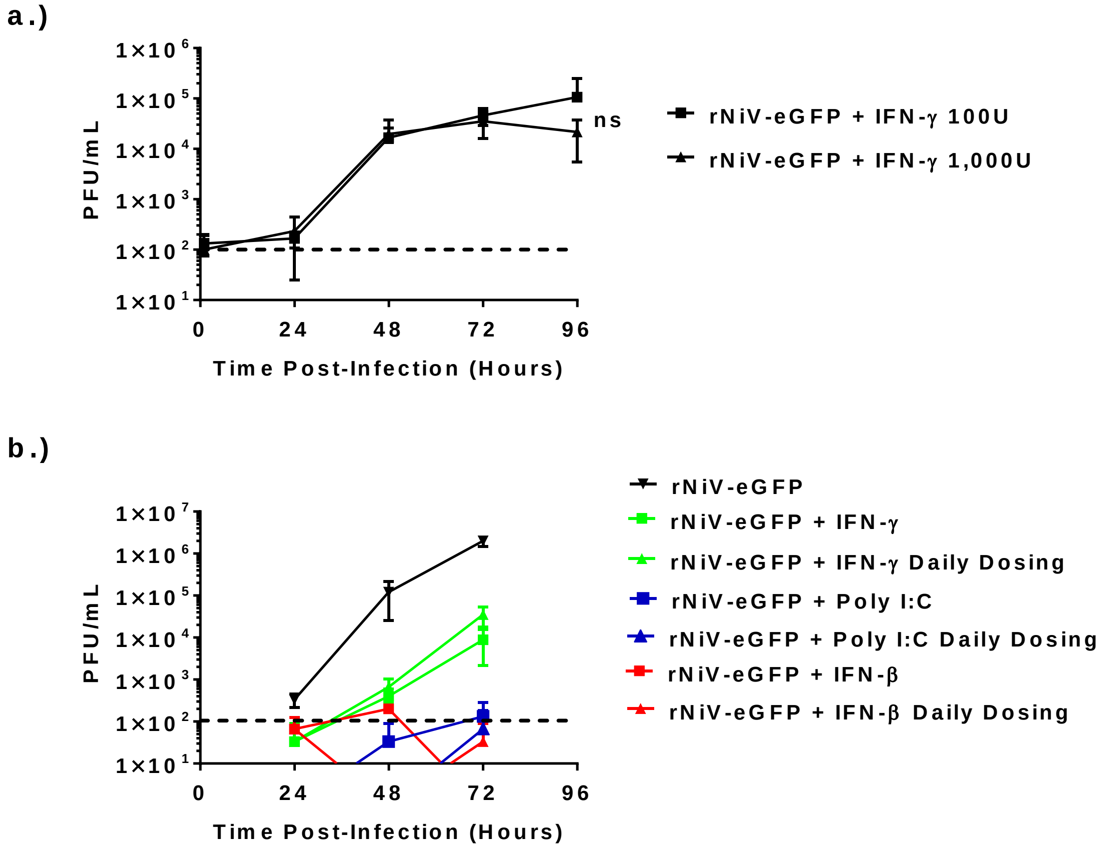

Figure 4.8: Effects of increased IFN-γ dose and multiple doses of interferon or poly I:C on viral titers.

Co-cultures were infected with 0.01 MOI of rNiV-eGFP and pretreated 24 hours prior to infection. **(a)** Cells were treated with either 100U or 1,000 U of IFN-γ prior to infection. **(b)** Cells were pretreated with 100U IFN-γ, 100U IFNβ, or 1μg poly I:C prior to infection with 0.01 MOI rNiV-eGFP. Cells were then treated daily with an equivalent dose of IFN or poly I:C, or with media only controls.

IFN AND POLY I:C TREATMENTS REDUCE CYTOTOXICITY AND APOPTOSIS OF NIV INFECTED NEURON/ASTROCYTE CO-CULTURES

Next, the effects of IFNs and poly I:C treatments on the viability of neuron/astrocyte co-cultures was measured. In the absence of NiV infection, no significant differences in apoptotic activity could be measured between IFN-γ, IFN-β, and poly I:C treated cells compared to mock treated cells (Fig. 4.9a). The only difference noted in viability was a slight decrease at 48 hours post treatment with poly I:C, although this was not observed at any other time point and is likely an artifact. This demonstrates that Type I and II IFN and poly I:C are not toxic to primary human neuron/astrocyte co-cultures at the doses used in these experiments.

Next, IFN-γ, IFN-β, and poly I:C treatments on rNiV-eGFP infected neuron/astrocyte co-cultures were assessed (Fig. 4.9b). No differences in viability were noted until 72 HPI at which point IFN-γ, IFN-β, and poly I:C treated cells had significantly higher viability than untreated rNiV-eGFP infected cells. There was no significant difference between IFN or poly I:C treated cells compared to untreated cells at 72 HPI, but viability was significantly higher in IFN-β treated cells compared to IFN-γ treated cells. By 96 HPI all infected cells, treated and untreated, had significantly lower viability compared to mock infected cells, but viability in IFN-γ and IFN-β treated groups remained significantly higher than in untreated infected cells. Interestingly, despite decreases in viral titers, poly I:C treatment did not reduce cytotoxicity at 96 HPI compared to rNiV-eGFP alone. Similarly, untreated rNiV-eGFP infected cells had higher apoptotic activity at 72 HPI than all other groups with no increases noted for IFN-γ, IFN-β, or poly I:C treated groups. At 96 HPI IFN-γ and IFN-β infected cells still did not display apoptotic activity. Poly I:C treated cells displayed a small but significant increase in apoptotic activity compared to mock infected cells, but this was still significantly reduced compared to rNiV-eGFP infection alone. These results indicate that type I and II IFN decrease cytotoxicity and protect against apoptosis during NiV infection of neurons/astrocytes. Despite the greater reduction in titers, poly I:C offered less protection from cytotoxicity and apoptosis than IFN-γ or IFN-β.

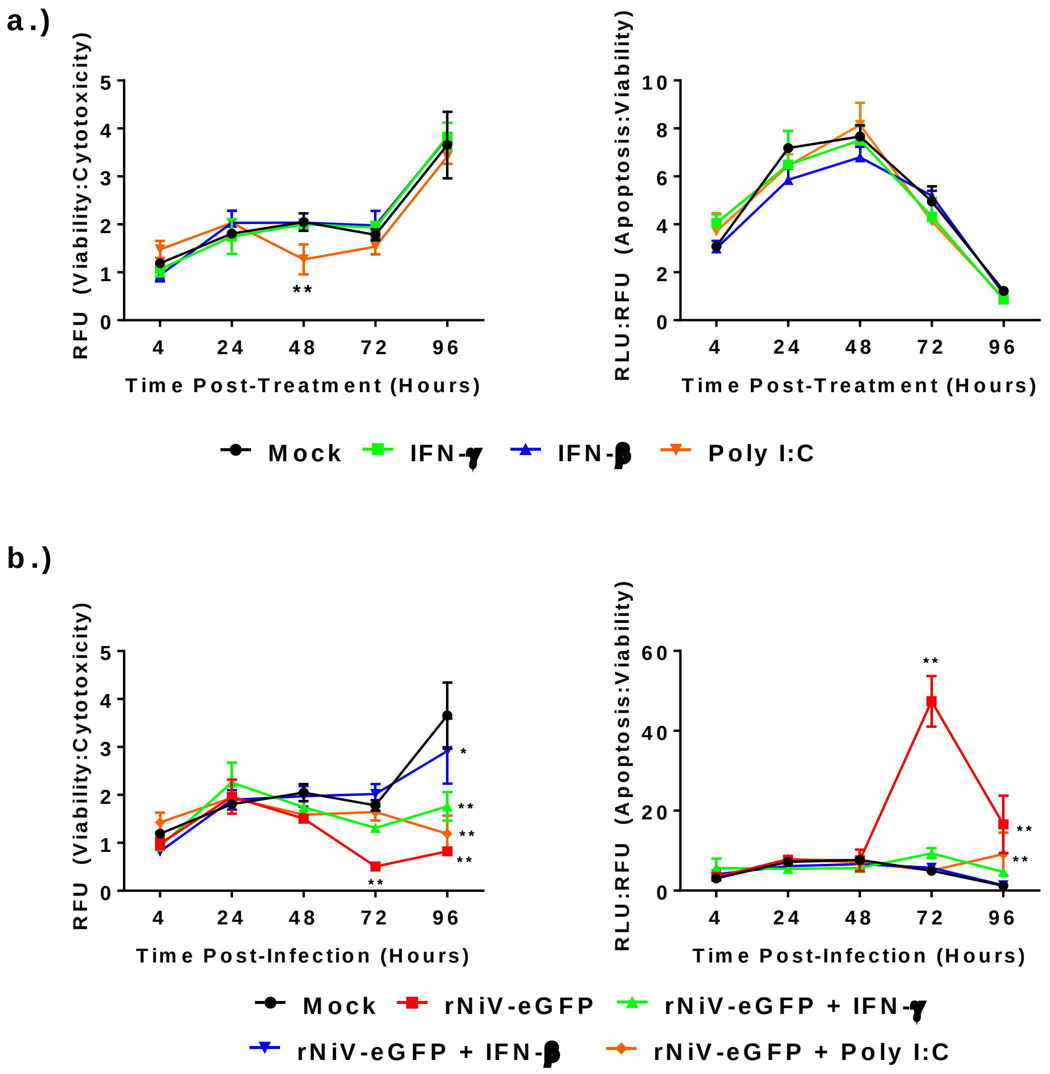

Figure 4.9: Cytotoxicity and apoptosis after interferon or poly I:C treatment

Cytotoxicity, viability, and apoptosis assays were then performed at various time points. **(a)** Cells were mock infected and treated with 100U IFN-γ, 100U IFNβ, or 1μg poly I:C. **(b)** Neuron/astrocyte co-cultures were pretreated with 100U IFN-γ, 100U IFNβ, or 1μg poly I:C prior to infection with 0.01 MOI rNiV-eGFP. Cytotoxicity is represented as the ratio of signals from viability and cytotoxicity assays (viability:cytotoxicity) (left panels). Apoptosis is represented as a ratio of signals for viability and apoptosis assays (apoptosis:viability) (right panels) *P <0.05, **P<0.01

IFN TREATED NEURON/ASTROCYTE CO-CULTURES PRODUCE MORE CHEMOKINES DURING NIV INFECTION

Cytokine and chemokine responses of rNiV-eGFP infected neuron/astrocyte co-cultures treated with IFN-γ and IFN-β were measured (Fig. 4.10). As noted before (Fig. 5), untreated rNiV-eGFP infected cells failed to respond to infection. However, this experiment resulted in very small increases in CCL5 production, which reached significance at 48 and 72 HPI (Fig. 4.10). IFN-γ treatment in the absence of infection induced a proinflammatory response inducing IL-6, IL-8, CXCL10, and CCL5. Of note, IL-6 and CCL5 expression were approximately 100-fold lower than noted with poly I:C and Il-8 was 10-fold lower, while the IFN-γ stimulated chemokine CXCL10 was very strongly upregulated (Fig. 4.10). IFN-β treatment did not affect cytokine production except for increases in CXCL10 and CCL5. However, rNiV-eGFP infected co-cultures treated with IFN-γ or IFN-β did not produce significant upregulations of IL-6 or IL-8. IFN-γ and IFN-β treatments of infected cells upregulated CCL5 expression. IFN-γ and IFN-β both significantly upregulated CXCL10 expression in infected cells. IFN-γ treatment of infected cells did not induce as large of CXCL10 responses as uninfected cells, while CXCL10 was increased after IFN-β treatment of infected cells at levels comparable to uninfected treated cells. These results suggest that neuron/astrocyte co-cultures respond to IFN-γ and IFN-β with proinflammatory cytokine and chemokine responses, but this response is decreased during NiV infection. However, IFN treatments can still induce CXCL10 and CCL5 responses during NiV infection, which may be important for recruiting lymphocytes to areas of infection.

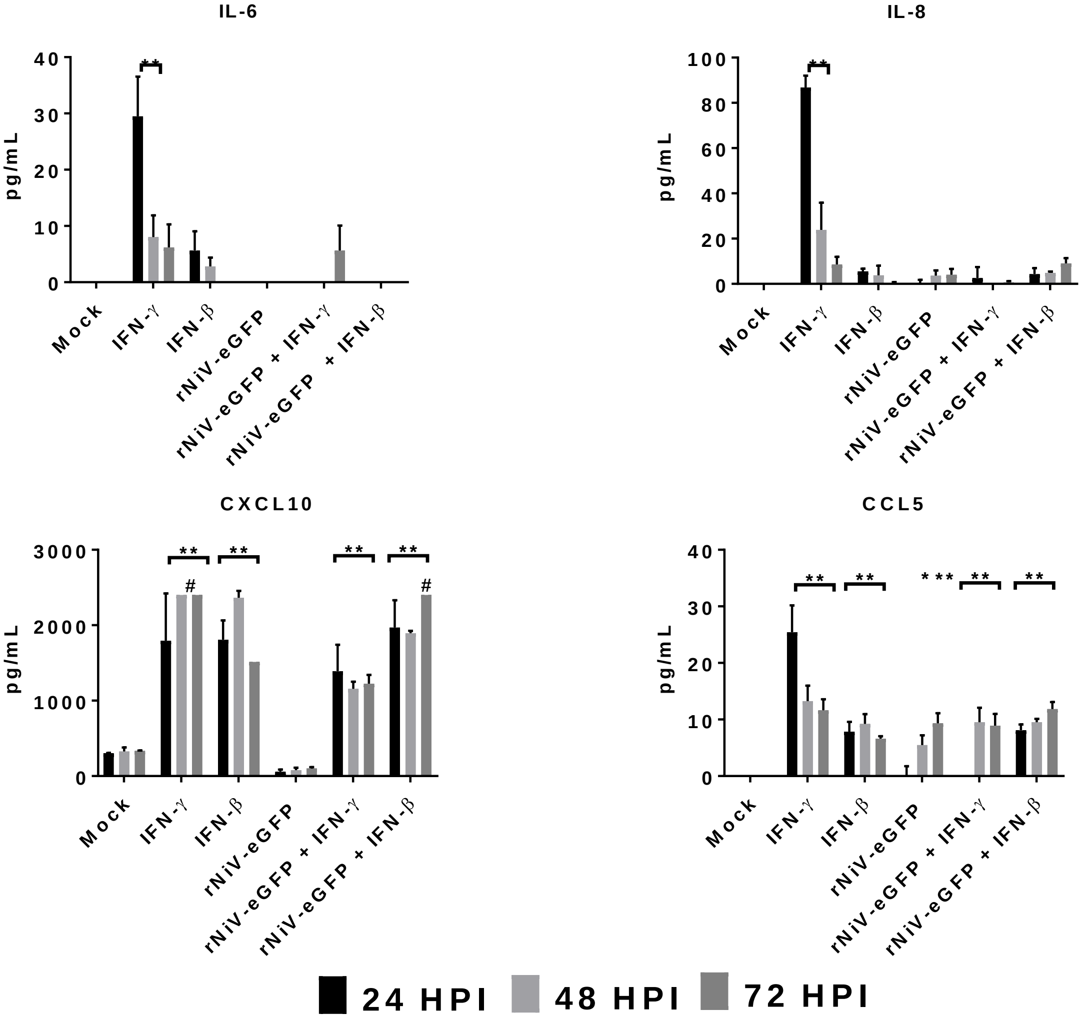

Figure 4.10: Cytokine and chemokine responses to interferon treatment during NiV-M infection.

Bioplex assays were performed on the supernatant of neuron/astrocyte co-cultures which were mock infected, infected with 0.01 MOI rNiV-eGFP, treated with 100U IFN-γ or 100U IFNβ alone, or IFN-γ/IFNβ treatment with infection with 0.01 MOI NiV-M. # samples assayed are above the observable limit based on the generated standard curve. * P<0.01 ** P<0.01

IFN-β AND POLY I:C DECREASE INITIAL INFECTION OF ASTROCYTES BUT FAIL TO PROTECT NEURONS

Lastly, experiments were conducted to determine the cell types infected during NiV infection and evaluate if IFN treatments affect shifts of tropism. To accomplish this, neuron/astrocyte co-cultures were infected with 0.01 MOI of rNiV-eGFP and fixed cells were stained for GFAP and MAP2, astrocyte and neuron markers, respectively (Fig. 4.11a). Initially, differences in the percentages of neurons and astrocytes present in culture in response to rNiV-eGFP infection in the presence or absence of IFN-γ, IFN-β, or poly I:C treatment were measured. Since syncytia were positive for both GFAP and MAP2, they were from any analysis requiring cell type identification (Fig. 4.11b). No differences in the percentages of cells expressing GFAP were observed for any condition throughout the entirety of the experiment (Fig. 4.12a). rNiV-eGFP in the presence or absence of poly I:C treatment resulted in a significant decrease in MAP2 positive cells at 48 HPI. At 72 HPI, rNiV-eGFP infected co-cultures treated with IFN-γ, IFN-β, or poly I:C had significant reductions in MAP2 positive cells (Fig. 4.12a). Importantly, IFN-γ, IFN-β, or poly I:C treatment in the absence of rNiV-eGFP infection had no effect on GFAP or MAP2 positive cell populations. These data suggest that IFN-γ, IFN-β, or poly I:C treatments provide more protection to astrocyte populations than to neurons at later stages of infection.

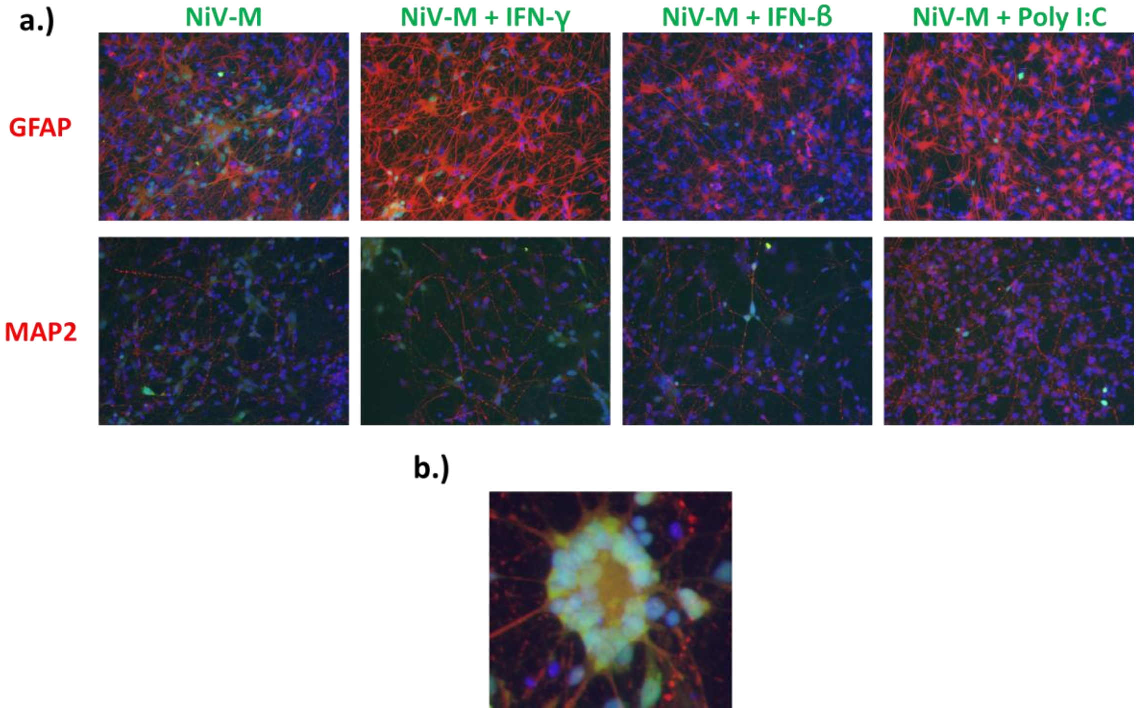

Figure 4.11: Imaging of NiV infected cells after IFN treatments.

(a) Fluorescent microscopy was performed on cells which were either mock infected, infected with 0.01 MOI rNiV-eGFP, treated with 100U IFN-γ, 100U IFNβ, or poly I:C with and without virus infection. Cells were stained with anti-MAP2 or GFAP antibodies (red staining) and nuclei with DAPI counterstain (blue staining). Images were obtained at 24 HPI before significant syncytia formation. **(b)** An example of syncytia formation in untreated cells, stained with anti-MAP2 antibody at 48 HPI.

Next, the effects of IFN-γ, IFN-β, or poly I:C treatments syncytia formation and overall percentages of infected cells were measured. These analyses included syncytial nuclei. Interestingly, nuclei within syncytia tended to have a peripheral distribution. This pattern is more characteristic of HeV infection, while NiV syncytia have been reported to mainly contain centralized nuclei [255] (Fig. 4.11b). IFN-γ treatment trended to decreased amounts of infected cells, but failed to reach significance (Fig. 4.12b). However, IFN-β and poly I:C treatments significantly reduced the percentage of infected cells at every time point. It should be noted that despite the large decrease, nearly half of all cells were infected by the end of the experiment even with IFN-β or poly I:C treatments despite the low titers measured in earlier experiments (Fig. 4.7b).

Additionally, IFN-γ, IFN-β, and poly I:C all significantly reduced the percentage of nuclei contained within syncytia (Fig. 4.12b). By 72 HPI over half of all nuclei in rNiV-eGFP infected co-cultures were contained in syncytia. IFN-γ reduced syncytial nuclei to approximately 40%, poly I:C to 30%, and IFN-β to 20%. These results indicate that IFN-γ, IFN-β, or poly I:C can reduce syncytia formation, but only IFN-β and poly I:C treatments can reduce overall levels of infection in NiV infected neuron/astrocyte co-cultures.

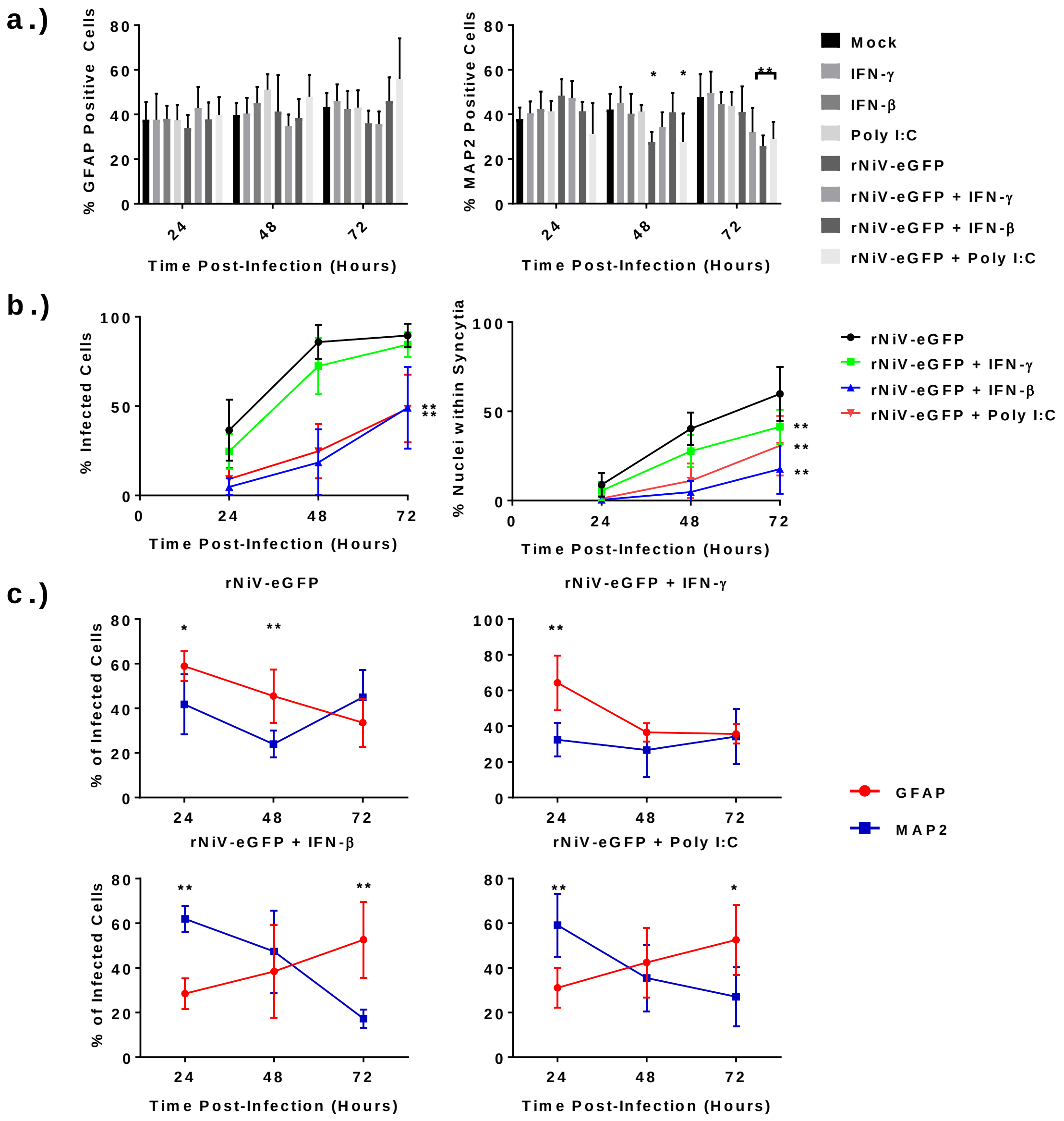

Figure 4.12: Determination of NiV-M tropism in neuron/astrocyte co-cultures treated with interferon.

Cells were either mock infected or infected with 0.01 MOI rNiV-eGFP in the presence or absence of 100U IFN-γ, 100U IFNβ, or poly I:C. Cells were stained with anti-MAP2 or GFAP antibodies with DAPI counterstain. **(a)** Cells were counted to determine the overall percentages of cells expressing GFAP or MAP2. **(b)** Cells and nuclei were also counted to determine the percentage of infected cells and the percentage of nuclei contained in syncytia. **(c)** Cells were counted to determine the percentage of infected cells that were GFAP or MAP2 positive. Each condition and staining was completed in duplicate and three random fields were quantified for each duplicate for a total of six fields. Data presented are averaged from all fields from all experiments. * $P<0.01$ ** $P<0.01$

Lastly, the effects of IFN-γ, IFN-β, or poly I:C treatments on the cell types infected by rNiV-eGFP were determined. For this analysis, syncytial cells/nuclei were excluded, as they cannot be accurately identified as neuronal or astrocytic in origin. As syncytia expressed both GFAP and MAP 2 they were likely comprised of both neurons and astrocytes (Fig. 4.11a). Astrocytes and neurons were infected in all tested conditions (Fig. 4.12c). rNiV-eGFP infection alone resulted in astrocytes being infected at greater rates than neurons for the first 2 days of infection (Fig. 4.12c). By 72 HPI there was no difference in levels of infection between neurons and astrocytes. Therefore, in this *in vitro* system astrocytes are more susceptible than neurons to NiV infection. IFN-γ showed similar trends (Fig. 4.12c). However, the difference in astrocytic vs. neuronal infection at 24 HPI was greater than in untreated cells. This suggests that IFN-γ does not change the tropism of NiV infection in CNS cells. Surprisingly, IFN-β and poly I:C treatments resulted in neurons being the predominant cell type infected at 24 HPI. At 48 HPI there was no difference in astrocytic vs. neuronal infection, and by 72 HPI astrocytes became the predominant cell type infected. These results indicate that the type I IFN response provides greater protection to astrocytes relative to neurons early during NiV infection and may explain the tropism seen during acute NiV infection *in vivo*.

DISCUSSION

Despite growing global concern for the potential for large NiV outbreaks, gaps exist in addressing the basic molecular mechanisms of NiV neuropathobiology [82]. There are several vaccine candidates against NiV, and therapeutic options including monoclonal antibodies and antiviral compounds such as favipiravir have been developed [84–87]. An example of NiV counter measure development is provided in appendix B, but the possibility of persistent infection and relapse after NiV and HeV infection is an important consideration for the ongoing development of HNV countermeasures. The development of a model system to study NiV CNS infection that can accurately reproduce persistent infection will be critical for the development of such antiviral compounds. To date very few studies have assessed NiV infection of CNS cells, and adequate models of persistent infection are lacking [92]. Studies of NiV neuronal infection have been limited to the use of neuroblastoma cell lines [140,141,143]. Only limited observations about NiV encephalitis have been made in animal models such as the upregulation of CXCL10 in animal and human brains during NiV infection by neurons and epithelial cells [139].

While work with immortalized cells allows for characterizing cellular responses to viral infections, there are often restrictions to the interpretations of data from those cell lines due to alterations in specific pathways and differences among cell lines. Animal models are critical for pathogenesis studies, but results should be verified in human tissue as differences between species can be profound [209,210]. In particular relevance to this study it has been reported that neuronal IFN responses are species specific [173]. This study used the hNSC derived neuron/astrocyte co-cultures to study NiV infection. The previous chapter discussed the initial characterization of this system using LACV. In addition, this system has also previously been used to study the effects of Zika virus infection on the differentiation of hNSCs [220]. hNSC derived neuron/astrocyte co-cultures offer many advantages such as the repeated study of primary human neurons without donor variability and the maintenance of neuron-astrocyte interactions *in vitro*.

A previous report indicated that this system can be productively infected with NiV and HeV, but further characterization was necessary [231]. This study reports the cellular responses to infection, the responsiveness of the system to IFN, and the tropism of NiV infection in the presence or absence of exogenous IFN.

Similar to previous reports, neuron/astrocyte co-cultures were also susceptible to infection with NiV-B in addition to NiV-M and HeV infection (Fig. 4.1a). These results suggest that these cultures express the ephrin-B2/B3 receptors. Interestingly, NiV-B replicated to higher titers than NiV-M, as already demonstrated for HeV. NiV-B has previously been reported to replicate more efficiently than NiV-M in respiratory epithelial cells[144]. In another recent report, NiV-B and NiV-M replicated to similar titers in human olfactory sensory epithelial cultures containing sensory neurons indicating that there may be region specific differences in viral replication kinetics [256]. The increased replication of NiV-B relative to NiV-M provides further evidence that strain differences may account for differences in disease presentation between cases of NiV infection in Malaysia and Bangladesh. However, it is important to note that the disease course in Malaysia tended to be more neurological than in Bangladesh [67]. The most recent NiV outbreak in Kerala, India, again highlights the uncertainty of these trends, as initial reports described high rates of neurologic disease and identification of NiV-B. Therefore, the strain dependent differences on disease progression remain unclear, but it seems unlikely that lower rates of neurologic disease in Bangladesh are due to decreased neurovirulence. One possibility is that NiV-B is more virulent, but as the initial sites of infection appear to be the respiratory tract this virulence causes severe respiratory disease and death before neuroinvasion or neurological symptoms become apparent [138].

NiV-M infection failed to induce inflammatory cytokines or chemokines except for non-significant increases in lymphocytic chemokines CCL5 and CXCL10 (Figs. 4.3 and 4.4). These results suggest that NiV-M effectively suppresses transcription and translation of proinflammatory cytokines and chemokines. This is not surprising as

HNVs encode several IFN and RLR antagonists [160]. Additionally, several NiV genes have also been shown to inhibit inflammatory responses. Deletion of W results in increased chemokine production [108]. Recently, V was also shown to inhibit IL-1β production through inhibition of NLRP3 [106]. In neuroblastoma cell lines NiV-M inhibits IFN and cytokine production, but much greater responses are observed in endothelial cells [143]. Importantly, the hNSC derived neuron/astrocyte co-cultures used in this study are able to mount inflammatory cytokine and chemokine responses as shown by stimulation with poly I:C (Fig. 4.3 and 4.4) and infection with LACV (chapter 3). The lack of responses may be due to lower viral multiplication kinetics compared to LACV, but increasing the infectious dose of NiV did not lead to any observable increases in cytokine/chemokine responses (Fig. 4.5c). Therefore, the lack of cytokine and chemokine production is likely not due to an inability of neuron/astrocyte co-cultures to sense and respond to NiV infection, but rather a consequence of NiV inhibition of viral sensing, IFN, and inflammatory pathways. NiV-B and HeV induced greater CXCL10 and CCL5 responses later in infection compared to NiV-M (Fig. 4.5). Differences in cytokine and chemokine expression between NiV strains and HeV have also been observed in several studies using respiratory epithelial cells, but the patterns observed vary based on the system used. NiV-B induced higher levels of CXCL10 compared to NiV-M in bronchial and small airway epithelial cells in air-liquid interfaces cultures [144]. HeV induced much stronger CXCL10 responses than either NiV-M or NiV-B in monolayers of bronchial and small airway epithelial cells, but CCL5 transcription was reduced in NiV-B compared to NiV-M or HeV [159]. One study using the hamster model demonstrated increased CXCL10, IL-6, and IFN-γ production in HeV infected brains compared to NiV-M suggesting that these differences exist *in vivo* as well [126]. Together, these studies suggest that differences between strains differentially affect inflammatory responses in a cell type dependent fashion. Whether these differences affect clinical disease is unknown. It is possible that increased lymphocytic recruitment to the CNS during NiV-B infection could result in more effective clearance of the virus. This could explain why relapsed encephalitis has not been observed to the same degree as during NiV-M infection. Alternatively, increased inflammation could play a pathogenic role and contribute to the increased virulence seen during NiV-B cases.

Interestingly, NiV-M induced an IFN-β response at late time points post-infection. This contradicts previous reports that neuroblastoma cell lines could not produce IFN in response to NiV infection [143]. As this system is composed of primary cells, their IFN and viral sensing responses should be more robust than those described for cell lines. These responses were likely too late to have any protective effects in an *in vitro* system. However, it is possible that *in vivo* limited IFN production may be important for control of viral spread within the CNS. This study did not assess which cells were producing IFN-β. Astrocytes and neurons can both produce IFN-β in response to viral infection, but astrocytes seem to be more important IFN producers [40,48]. In fact, astrocytic IFN-β appears critical for restricting the spread of VSV in the brain and protecting distant regions form infection [168]. It is possible that late IFN production in the CNS during NiV infection is insufficient to protect infected lesions, but can prevent viral spread to surrounding regions. Future studies should determine the cell-specific responses to NiV infection.

IFN-γ has been shown to be necessary and sufficient for control of neuronal MeV infection in the brain [192]. Given that HNV relapsed encephalitis is due to long term paramyxovirus CNS infection with certain similarities to MeV SSPE, it was hypothesized that IFN-γ would likewise be sufficient for control of NiV neuronal infection. However, while IFN-γ pretreatment reduced viral titers, it was not sufficient to control NiV infection (Fig. 4.7a). NiV has an increased virulence compared to MeV, and it is likely that treatment after infection is insufficient to control rapid spread and NiV IFN antagonism. However, it is interesting to note that even pretreatment was insufficient to fully protect co-cultures from widespread infection. Type I IFN responses typically establish stronger antiviral states than type II IFN and have been shown to be critical for the control of viral encephalitis in most viral encephalitis models [202,257]. In the context of MeV encephalitis the type I IFN response appears to be important for early viral control in mice [174]. IFN-β and poly I:C pretreatment significantly reduced viral titers in neuron/astrocyte co-cultures. Poly I:C was used as an agonist for IFN induction, demonstrating the ability of innate viral sensing pathways to protect neuron/astrocyte co-cultures from NiV infection. Poly I:C treatment induces IFN-β and IFN-γ production (Figs. 4.3 and 4.4) with the type I IFN responses likely responsible for the observed protection due to similar titers. These results suggest that initial control of NiV infection is due to type I IFNs.

IFN and poly I:C treatments also reduced cytotoxicity and apoptosis in NiV infected neuron/astrocyte co-cultures (Fig. 4.9). NiV induced cytotoxicity and apoptosis were not noted until 72 HPI, and peaked at 96 HPI. IFN-β maintained viability at levels comparable to uninfected cells while IFN-γ and poly I:C were less protective (Fig. 4.9b). Much of the IFN-β and poly I:C mediated protection is likely a direct consequence of reduced levels of infection (Fig. 4.7b). The reduction due to IFN-γ is more interesting as it only mildly reduced overall infection levels, but nearly completely protected against apoptosis, which suggest a neuroprotective role during infection. IFN-γ has been shown to reduce viral mediated apoptosis in neurons via BCL-2 activation [200]. Another study in mouse hippocampal neurons demonstrated that IFN-γ induced ERK1/2 signaling protected against apoptosis as well [194]. While IFN-γ may not protect neurons or astrocytes from NiV infection, protection against apoptosis may delay neuronal damage until later immune responses mediated by antibodies or CD8+ T-cells can mediate viral clearance.

In addition, IFN-γ and IFN-β treatment of NiV-infected co-cultures resulted in significant upregulation of CXCL10 and CCL5, but not other cytokines or chemokines. This suggests that NiV can effectively suppress the majority of cytokine responses even in the presence of IFN signaling. CCL5 and CXCL10 are important lymphocytic chemoattractants, and CXCL10 has been shown to be strongly produced in neurons and endothelial cells with in the brains of NiV patients [139]. These results suggest that IFN signaling may be required for the efficient production of CXCL10 in observed in neurons during human infection. The role of these chemokines during NiV infection remains to be seen. They may be protective and necessary for lymphocytic viral clearance in the CNS, or they may lead to damaging immunopathology.

This study further found that IFN-β changes NiV tropism in neuron/astrocyte co-cultures. Neurons are the primary target cell during human infection, and glial infection appears rare during acute infection [80]. Determining the cell types infected during *in vitro* NiV infection is difficult to accurately determine due to the development of syncytia. Therefore, the results from 24 HPI are likely the most accurate due to limited syncytia formation at this time. NiV was able to infect both neurons and astrocytes (Fig. 4.12c). During early time points after infection, it appeared that astrocytes are more commonly infected than neurons (Fig. 4.12c). This interesting observation differs from observed *in vivo* tropism [80]. The development of syncytia is also not commonly observed *in vivo* involving neuronal cells, although this may be due simply to the increased area of contact between cells in culture. By 72 HPI, approximately 80% of cells are infected and there were no visual differences in neuronal vs. astrocytic infection. IFN-γ treatment did not reduce the percentage of infected cells, and the percentages of syncytia were only mildly reduced. The tropism following IFN-γ treatment 24 HPI was similar to that observed in untreated NiV infection. These results are consistent with the incomplete protection provided by IFN-γ observed throughout this study. Interestingly, there were decreases in MAP2 positive cell populations at 72 HPI relative to mock infected cells following IFN-γ treatment. This suggests that neurons may be more susceptible to cell death than astrocytes, potentially due to stronger antiviral responses in astrocytes vs. neurons. IFN-β and poly I:C treatments resulted in a shifted tropism at 24

HPI with neurons becoming the predominate cell type infected (Fig. 4.12c). In addition, both IFN-β and poly I:C treatment significantly reduced levels of infection, syncytia formation, and MAP2 positive cell populations. It should be noted that protection appears to weaken by 72 HPI with nearly 40% of cells becoming infected. It is unknown if this is due to viral IFN antagonism or weakened IFN signaling/responses late in infection. Regardless, it appears that while IFN-β protects both cell types overall, protection is stronger in astrocytes. This is likely due to stronger IFN-induced antiviral state in astrocytes relative to neurons.

Exposure to IFNs *in vivo* may explain differences in tropism observed *in vitro*. Additionally, these results suggest that there are heterogenous responses to IFN between neurons and astrocytes. Heterogenous IFN responses between these cell types has been commonly observed, with astrocytes typically having stronger induction of interferon stimulated genes (ISGs) and consequently stronger antiviral activity than neurons [175–178]. Differences in IFN responses have also been noted for different neuronal populations in a region specific manner, with cerebellar neurons being more responsive than cortical neurons [179,180]. These results correlate with these studies in terms of astrocytic responses, and because neurons in this co-culture system are most similar to cortical neurons and therefore may not be as sensitive to IFN activity. An additional explanation could be neuronal maturity. While in the present co-culture system neurons are differentiated, they are still young and derived from fetal stem cells. Age dependent differences in neuron IFN-γ and IFN-β responses have been noted with increasing responsiveness in more differentiated states [51,258]. Specifically, a recent study demonstrated that IFN-γ did not protect recently differentiated neurons from MeV infection [259]. One could also envision a similar phenomenon where recently differentiated astrocytes may be more susceptible to NiV infection than more mature astrocytes. An alternate explanation for the altered tropism observed in this system is that replication kinetics in neurons are slower than in astrocytes, and therefore virus is not as readily visualized at early timepoints. Regardless, in this system, astrocyte type I IFN signaling likely contributes to control of early NiV CNS infection similar to observations made for other viruses [185,186].

Based on the data presented, hNSC derived neuron/astrocyte co-cultures represent a valuable human primary cell system for the further understanding of CNS HNV infection and for the development of models to study persistent or relapsed infection. This co-culture is highly susceptible to infection with viral mediated inhibition of IFN and inflammatory responses. Furthermore, type I IFN responses are protective at least at early time points after infection. These results suggest that type I IFN responses, particularly in astrocytes, are necessary for early control of NiV infection of CNS cells. Future studies should address the role of IFN responses on viral persistence and relapse. IFN-β treatment reduced syncytia formation and produced a primarily neuronal infection similar to *in vivo* NiV infection. It also reduced production of viral particles and reduced spread of the virus. These are likely necessary factors for the development of persistent viral infection and suggest that the type I IFN response is a critical factor for the observed CNS phenotypes. Additionally, NiV infected co-cultures treated with IFNs produced CXCL10 similar to *in vivo* observations. Together, these results highlight the importance of IFN-β in shaping responses to NiV infection to more closely resemble *in vivo* phenotypes. Future models that recreate persistent or relapsed infection will likely require IFN-β to accurately reproduce a physiologic state and attenuate viral infection. Recent studies have suggested that the NiV encoded W and C proteins but not the V protein are dispensable for CNS infection, with deletions of W or W and C leading to protracted CNS involvement [108,158]. W was characterized as being more important for inhibition of inflammatory responses while V was a stronger IFN antagonist [108]. Future studies of NiV lacking these immunomodulatory proteins in this system will be useful to further elucidate both the host and viral factors involved in persistent NiV infection and potentially lead to the development of a suitable animal model for pathogenesis studies and the assessment of antiviral candidates.

Chapter 5: Discussion, Conclusions, and Future Directions

SUMMARY

This dissertation describes the evaluation of a hNSC derived neuron/astrocyte co-culture model for the study of viral encephalitis. Infections with LACV and NiV were studied in order to perform initial validations of the system due to their relevance to human health. LACV has been well characterized in other systems, which allows for comparisons of the co-culture system to other relevant LACV systems. In addition, gaps still exist in the knowledge of neuronal/astrocytic responses to LACV infection, and this system can provide a basis from which to begin mechanistic studies. NiV neuropathobiology has not been extensively studied, and models of neuronal infection are needed. In addition, models of CNS persistence do not exist. This system could provide a basis from which to conduct mechanistic NiV studies and potentially lead to a model of persistence. An overview and comparison of results for LACV and NiV studies in the neuron/astrocyte co-cultures is found in table 5.1. IFN-ß

Outcome	LACV	NiV
Replication	Robust Replication	Robust Replication
Apoptosis	Strong Apoptotic Response	Late Apoptotic Response
Cytokine/Chemokine Response	Strong Proinflammatory/IFN Response	Minimal CXCL10/IFN-β Reponse NiV-B/HeV Induce Stronger CCL5/CXCL10 Responses
Cell Types Infected	Early After Infection (24 HPI): Neuron=Astrocyte Late After Infection (96 HPI): Neuron>Astrocyte	Early After Infection (24 HPI): Astrocyte>Neuron Late After Infection (72 HPI): Neuron=Astrocyte
Effect of IFN	?	IFN-β Strongly Reduces Viral Replication
Effect of IFN on Tropism	? (Possible Reason for Tropism Shift)	Astrocytes become less susceptible

Table 5.1: Comparison of LACV and NiV infection of hNSC derived neuron/astrocyte co-cultures

The above table summarizes the characterizations of LACV and NiV infection in neuron/astrocyte co-cultures. Findings in green represent findings, which agree with other models. Findings in red are different than those found in other models. Findings in blue represent novel findings not assessed elsewhere.

The results of these studies indicate that this system replicates many aspects observed previous models for NiV and LACV infection. While the hNSC derived neuron/astrocyte co-culture system was susceptible to both viruses, the characterization of each virus revealed striking differences. While NiV infected nearly all cells in the co-culture, LACV only infected around half at maximum. This may indicate differences in susceptibility or differences in virulence. Additionally, syncytia formation during NiV infection and cell/cell fusion likely played a large role in the spread of infection. Despite this, LACV appears to induce cytotoxicity and apoptosis earlier (48 HPI) than NiV (72/96 HPI). Previous studies have shown both viruses induce apoptosis, and these results lend support to the validity of the co-culture system [41,42,140]. This time difference is an interesting observation as NiV is a more virulent virus and caused more extensive CPE, but actual cell death was delayed compared to the more moderate LACV infection. This result supports the hypothesis that direct infection of neurons (more than immunopathology) mediates the damage seen in LACV encephalitis. Furthermore, it suggests neurons and or astrocytes may be infected for long time periods during NiV infection, which may be a factor in the development of persistent infection.

The ability of the co-cultures to induce IFN and inflammatory responses was also studied. The LACV study confirmed that the co-cultures could sense viral replication, and mount responses. LACV infection induced very strong IFN and proinflammatory responses. This was particularly true of monocytic and lymphocytic chemoattractants. This was somewhat surprising, as viral NSs has been shown to reduce transcription of IFN and inflammatory cytokines [260,261]. In this system, NSs was unable to overcome host responses. In contrast, NiV shuts down almost all production of cytokines. IFN-β was induced, but only at very late time points, limiting its ability to protect uninfected cells. CCL5 and CXCL10 were the only proinflammatory cytokines to show any upregulation. Indeed, these are two of the most important chemokines with regards to CNS infection, and are generally necessary for the recruitment of T-cells which mediate viral clearance (or damage depending on the model). NiV encodes several immune antagonists and appears much more adapt at shutting down host responses. Almost all NiV proteins (N, P, V, W, C, and M) have been shown to disrupt IFN and/or proinflammatory responses [102,106,113,160]. These results generally match with clinical outcomes; LACV is generally cleared by the immune system within a few days during human infection, while NiV is commonly fatal and may persist within the CNS.

Each virus's induction of cytokines/chemokines lends itself to the suggestion that this plays a role in the outcomes of infection.

The tropism of each virus in the co-culture system was also evaluated. Both viruses infect primarily neurons *in vivo* with reports of rare glial infection [21,80]. The current results were unexpected, with astrocytes being a major target for both viruses. For LACV initially both cell types are infected equally, but as the infection progresses, neurons become the predominant target. NiV seemed to infect astrocytes in greater numbers early during infection, but near the end resulted in a nearly 1:1 ratio of neurons to astrocytes (mostly due to almost all cells being infected). LACV seemed to resemble its *in vivo* phenotype at the latest timepoint, while NiV never appeared to be a predominately neuronal infection. Importantly, for both viruses as the infection progressed, astrocytes became a smaller percentage of infected cells. This highlights a potential limitation of the current co-culture system, but also highlights an important question. If astrocytes are readily infected *in* vitro why are they resistant *in vivo*? The change in tropism correlated with the induction of IFN-β during LACV infection, and it was proposed that this may be a mediator of astrocytic protection.

Following the interesting tropism results and the initial characterizations of co-culture responses to viral infection, a mechanistic study evaluating the effects of IFN on NiV infected neuron/astrocyte co-cultures was conducted. The IFN responses were of particular interest during NiV infection, as they likely contribute to persistent infection. IFN-induced antiviral states may be necessary to suppress viral replication in a manner leading to persistence. Failures of the IFN response to clear viral infection are also likely necessary for the establishment of persistent infection. IFN-γ limited viral replication and protected from apoptosis, but it was unable to fully protect the co-cultures in a manner similar to that observed during MeV infection. The importance of IFN- γ during NiV infection is still unknown; while it does not appear important for the direct clearance of virus, it may still be necessary for the CD8 dependent clearance of virus, or failures of this response may be a reason for viral persistence. Type I IFN responses resulted greatly reduced viral replication, syncytia formation, and resulted in neurons being the predominant cell type infected. This study provides the foundation for a hypothesis that the type I IFN response may be responsible for the restriction of NiV infection to neurons via its effects on astrocytes. In fact, it is tempting to conclude that the observed *in vivo* tropism is dependent on type I IFNs. The true answer is likely more complicated, as in IFNAR$^{-/-}$ mice the infection still seems to be predominately neuronal, although species differences cannot be ruled out [132]. It is also possible that similar IFN-induced astrocytic protection is responsible for the *in vivo* tropism differences. Because IFN-β treatments result in a phenotype more similar to *in vivo* infection this factor will likely be necessary for any future models of persistence. This would suggest that the murine (IFNAR$^{-/-}$) model would not be appropriate for studies of viral persistence. Therefore, this dissertation proposes that optimization of IFN-β treatments of the neuron/astrocyte co-culture system may eventually produce a viable model of persistent NiV infection.

FUTURE DIRECTIONS

These studies have demonstrated the value of the hNSC derived neuron/astrocyte co-culture system while providing novel insights to LACV and NiV infection. However, further study is required to determine the relevance of many of these results. To begin, future effort must be given to identifying the cell types responsible for each response. It is unknown which cells were responding to infection with IFN or cytokine production, which cells produced CCL5 or CXCL10, or which cells underwent apoptosis. Cytokine responses are likely predominately from astrocytes as they tend to be potent drivers of neuroinflammation and IFN [40]. Apoptotic responses are likely found in neurons as described in other studies, but may also be found in astrocytes [42,262]. Future studies can determine which cells are undergoing apoptosis via terminal deoxynucleotidyl transferase dUTP nick-end labeling (TUNEL) staining. Intracellular staining for cytokines is often difficult, as they are often quickly secreted. Identifying transcriptional changes is more traditional but requires the separation of cell types. Protocols to separate neurons and astrocytes in this system would be invaluable in the future study of this model. Currently, protocols exist for separating neurons and astrocytes, but these are generally following dissociation of full brain tissue or require specialized equipment. Cells in this *in vitro* system are difficult to detach intact and furthermore difficult to sort via fluorescence-activated cell sorting (FACS). New technologies such as RNAScope may prove to be useful in labeling specific transcripts without the need to dissociate cells.

The pathways via which signaling occurs are also of interest. IFN signaling may occur via canonical and non-canonical pathways [167]. It would be useful to determine which pathways are activated during viral infection and during stimulation with IFNs. Of particular interest is the neuroprotective effects of IFN-γ. Other studies have associated neuronal protection from apoptosis by IFN-γ to be STAT1 independent and mediated via ERK1/2 [194]. It would be interesting to see if a similar phenomenon is observed during NiV infection. Again, a way to analyze cell-type specific responses would be necessary for future studies of the effects of IFN and to determine why astrocytes become less susceptible during IFN treatment relative to neurons. Additionally, the role of IFN in restricting astrocyte LACV infection should be confirmed via IFN treatment and/or IFNAR blockade experiments.

Additional studies should be conducted to assess the role of other resident CNS cells (microglia, and endothelial cells) as well as inflammatory cells during viral infection. During NiV infection upregulation of IL-6, TNF-α, CXCL10, IFN-γ, and IL-1β are detectable within the brain [126,139]. This study failed to detect most of these cytokines. The likely reason is the presence of other cell types in the brain during infection. Endothelial cells appear to respond with stronger cytokine responses during NiV infection and likely play a role in the observed increases during *in vivo* infection [143]. However, the roles of microglia and inflammatory cells remain unassessed. In this work, preliminary studies with primary human microglia were conducted, but these cells were unable to be productively infected with LACV as demonstrated by lack of viral titers or cytokine responses. Addition of microglia and/or oligodendrocytes to the co-cultures could provide an even stronger model system.

An additional area of focus for future research is the use of reverse genetics systems to study the virus specific effects on co-cultures. Of particular interest would be LACV with NSs deletion, and NiV lacking the V, W, and C accessory proteins. These genes all antagonize the innate immune system, and it will be important to assess their specific effects in neuron/astrocyte co-cultures. LACV NSs should be inhibiting transcription of IFN, yet in the co-culture system there are measurable INF responses. Would the deletion of LACV NSs further increase IFN production, or does it play a different role within the CNS? Additionally, the NiV accessory proteins are likely to be very important in the development of relapse encephalitis. Deletions of W seem to increase neurologic disease in ferrets [108]. While much of this is likely achieved peripherally due to decreased mortality, it seems W is expendable for NiV neurological disease. It would be interesting to determine if an absence of W enhances neuronal infection. Additionally, W was shown to have the strongest anti-inflammatory effects of the accessory proteins, and it would be worthwhile to confirm this result in neuronal cell types. Furthermore, as V deletion mutants appeared to be controlled peripherally, V’s role in the CNS remains unknown [108]. *In vivo* V appears to be the primary IFN antagonist, but this also should be confirmed in CNS cells. Interestingly, one study did demonstrate differential localization of W between different cell types which correlated with IFN antagonism [143]. Therefore, the NiV accessory proteins seem to have cell specific effects, and it will be necessary to determine their roles during neuronal/astrocytic infection. It is likely that a better understanding of these proteins will be necessary to develop appropriate models of relapse and persistence.

CONCLUSION

In conclusion, this study has demonstrated the value, reproducibility, and physiologic strengths (and limitations) of hNSC derived neuron/astrocyte co-cultures as a model to study viral encephalitis. Neuron/astrocyte co-cultures accurately replicate key aspects of viral CNS infection such as IFN responses, cytokine/chemokine production, and cytotoxicity via apoptosis. This study represents the first study of LACV and NiV in primary human neuronal cells. This led to the novel finding that neurons/astrocytes actively respond to LACV, but not NiV, infection with the production of proinflammatory cytokines and chemokines. Furthermore, this study observed the novel finding that human astrocytes are highly susceptible to LACV and NiV infections but become less susceptible throughout the course of infection. Lastly, it was demonstrated that the type I IFN response could reduce viral replication, apoptosis, and astrocytic infection, making it likely that type I IFNs play an important role in the *in* vivo neuropathogenesis of NiV infection. These results demonstrate that host factors likely play a role in restricting astrocytic infection *in vivo*. Together, these results indicate the usefulness of this co-culture system as a model to conduct mechanistic studies of viral neuronal infections. Furthermore, they highlight the likely role of IFN-β in the development of persistent NiV infection and provide the first steps towards a model of NiV persistence *in vitro*.

Appendix A: Supplementary Cytokine and Chemokine Data

Chapter 3 Supplemental Data

The following section contains the qRT-PCR and BioPlex assay results not shown in the main chapter text. The main chapter figures show representative cytokines and chemokines. In the interest of displaying full data sets acquired, the remaining analytes are available in this appendix.

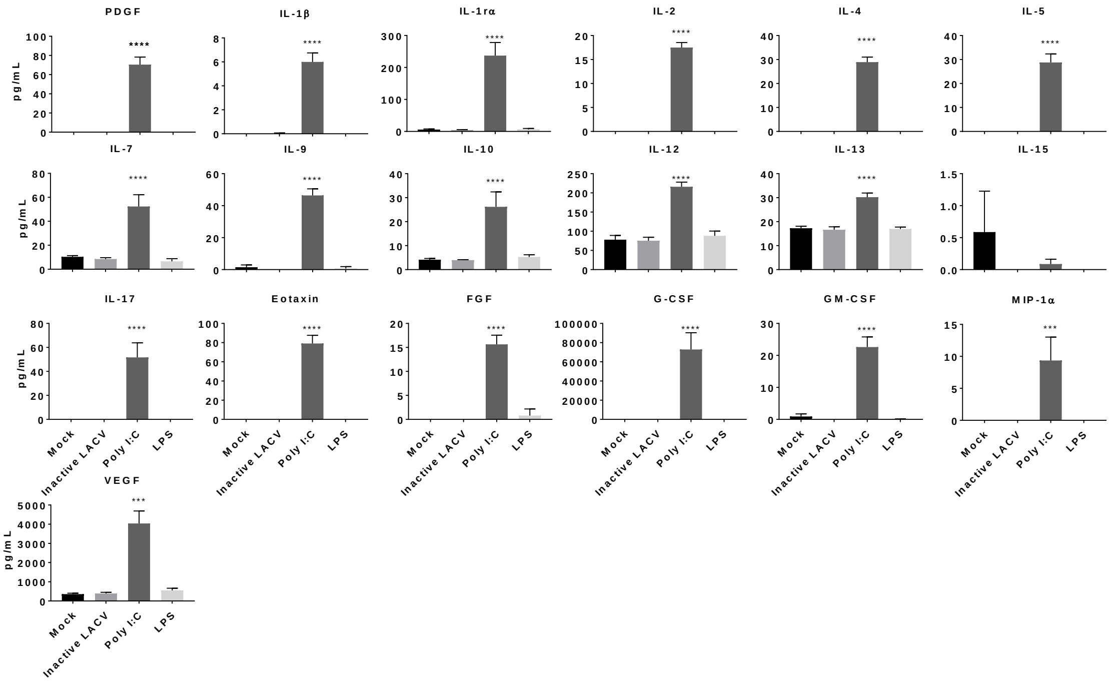

Appendix A Figure 1: Full neuron/astrocyte responses to inflammatory stimuli

Bioplex assays were performed to determine the cytokine and chemokine responses of neuron/astrocyte co-cultures. Co-cultures were treated with either mock, poly I:C, LPS, or heat inactivated LACV and supernatant was collected and assayed for changes in selected cytokine/chemokine secretion via BioPlex assay. * P<0.5, **P<0.01, ***P<0.001, ****P<0.0001

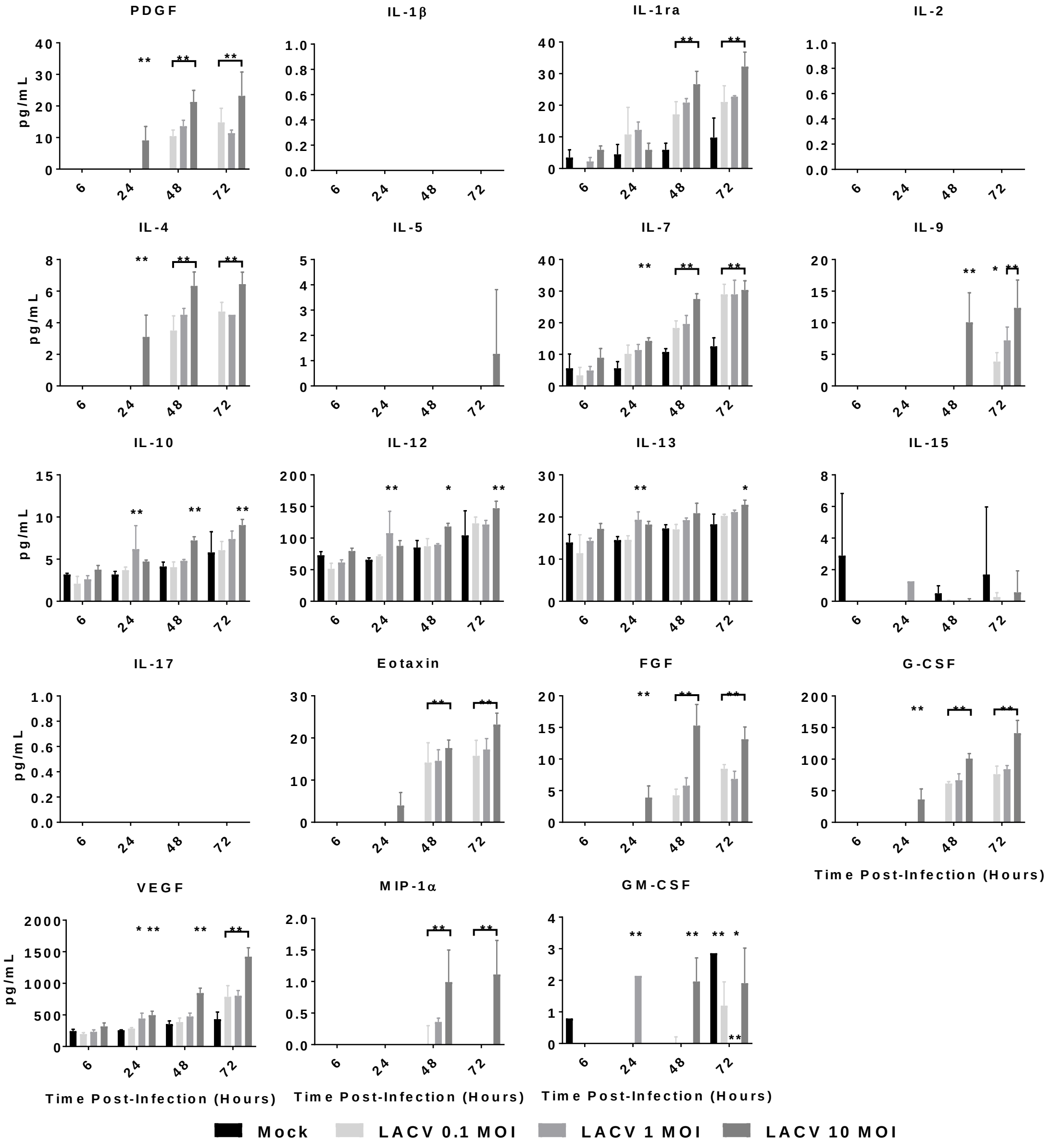

Appendix A Figure 2: Full cytokine and chemokine responses of neuron/astrocyte co-cultures to LACV infection

Cells were either infected with 0.1, 1, or 10 MOI of LACV. Supernatant was collected and assayed for changes in selected cytokine/chemokine secretion via BioPlex assay *P<0.5, **P<0.01

Chapter 4 Supplemental Data

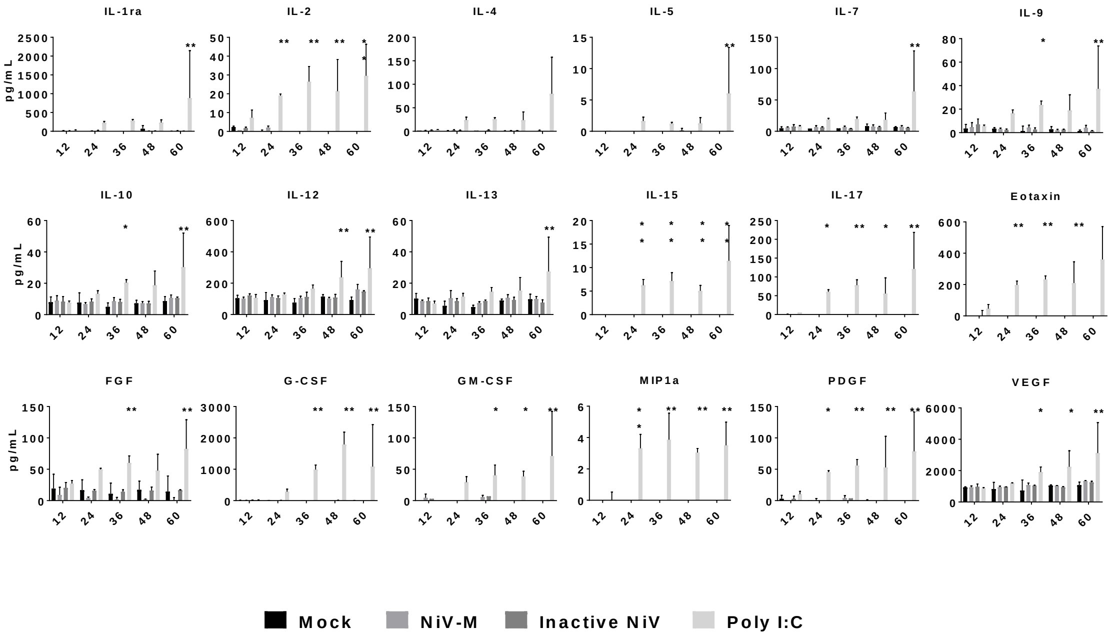

Appendix A Figure 3: Full cytokine and chemokine expression profile.

BioPlex assays were performed to determine the cytokine and chemokine production by neuron/astrocyte co-cultures in response to infection. Cells were either mock infected, infected with 0.01 MOI NiV-M, infected with 0.01 MOI heat inactivated NiV-M, or 1µg poly I:C. Selected cytokines are shown here, the full panel assessed are available in supplemental figure 3. *P<0.05, **P<0.01

Appendix B: Evaluation of Favipiravir for Use Against NiV

The following Appendix contains a separate study I conducted assessing the efficacy of the antiviral compound favipiravir against NiV infection in the hamster model. This work is separate from the development of the hNSC derived neuron/astrocyte co-cultures, and therefore not included in the main text. Nevertheless, it is an important advance in the field. The following section has been published in the online peer-reviewed journal *Scientific Reports* as:

Dawes, Brian E, Birte Kalveram, Tetsuro Ikegami, Terry Juelich, Jennifer K Smith, Lihong Zhang, Arnold Park, et al. 2018. "Favipiravir (T-705) Protects against Nipah Virus Infection in the Hamster Model." *Scientific Reports*, no. November 2017. Springer US: 1–11. https://doi.org/10.1038/s41598-018-25780-3.

INTRODUCTION

Nipah virus (NiV) and Hendra virus (HeV), prototypical species of the genus *Henipavirus*, are emerging highly pathogenic paramyxoviruses which cause severe encephalitic and respiratory disease in a wide range of mammalian species, including humans [55,56]. HeV causes sporadic outbreaks in horses with human spillover in Australia, while NiV was first isolated during a large human and porcine outbreak in Malaysia and Singapore [55,263]. Almost yearly NiV outbreaks in Bangladesh and India with mortality rates averaging 70%, and a small outbreak in the Philippines have since followed [56,64,70,264]. Furthermore, recently discovered genetic and serologic evidence points to the presence of henipa-like viruses in African bats and spillover into humans [116,117]. The natural reservoirs for henipaviruses have been identified as fruit bats from the *Pteropus* genus [62,265]. Due to their wide host range, evidence of human-to-human spread, and the highly pathogenic nature of illness, these viruses have been proposed to have pandemic potential [82].

Despite the pathogenicity of henipaviruses, no approved vaccines or therapeutics are available for use in humans. A subunit vaccine against HeV, which has been approved as a veterinary vaccine for use in horses in Australia, is effective in several animal models, and appears to be safe for use in humans [266–268]. Monoclonal antibodies targeting the viral envelope proteins have also shown efficacy in animal models for post-exposure prophylaxis, and have been used safely in humans under compassionate use, although their efficacy for the treatment of human disease is unknown [87,267]. The broad-spectrum antiviral ribavirin was initially used in the Malaysian outbreak in an open label trial with a reported 36% reduction in mortality [269]. However, several studies using disease-relevant animal models have repeatedly demonstrated ribavirin monotherapy as well as combination treatment with chloroquine to be ineffective at reducing the mortality of henipavirus infections [129,130,254,270]. Recently, the adenosine nucleoside analogue GS-441524, and its monophosphate prodrug GS-5734, were demonstrated to have *in vitro* antiviral activity against NiV and HeV with EC_{50} values between 0.49 to 1 μM and 0.032 to 0.055 μM, respectively [271]. Importantly, GS-5734 was protective in a non-human primate model for Ebola virus post exposure and is currently in phase 2 clinical development for the treatment of Ebola virus disease (www.clinicaltrials.gov) [272]. Additionally, another nucleoside analogue, R1479 (balapiravir), demonstrated *in vitro* antiviral efficacy against NiV and HeV with EC_{50} values of 4 μM and 2.25 μM, respectively [273].

The viral RNA-dependent RNA polymerase (RdRp) inhibitor favipiravir (T-705; 6-flouro-3-hydroxy-2-pyrazinecarboxamine; [Avigan]) was developed by Toyama Chemical Company as an antiviral for use against influenza [88,274]. It is currently licensed in Japan for the treatment of novel or re-emerging influenza and has also undergone several phase 3 clinical trials in the United States and Europe for use against influenza (www.clinicaltrials.gov) [275]. Favipiravir acts as a purine analogue, which selectively inhibits viral RdRps [276]. In addition to its potent anti-influenza activity, favipiravir has demonstrated efficacy against a wide variety of other RNA viruses including bunyaviruses, arenaviruses, filoviruses, norovirus, flaviviruses, alphaviruses, enteroviruses, and rhabdoviruses [88,277,278]. Of note, recently completed phase 2 clinical trials for use in Ebola virus infection suggest that favipiravir treatment may result in reduced mortality when given to patients with moderate viral loads [279]. Activity against paramyxoviruses has been demonstrated *in vitro* for respiratory syncytial virus, measles virus, human metapneumovirus (hMPV), human parainfluenza virus 3, Newcastle disease virus, and avian metapneumovirus and *in vivo* against hMPV in a hamster model [274,280]. In this study, we assessed the ability of favipiravir to inhibit NiV and HeV *in vitro* as well as its efficacy in a lethal NiV-infected Syrian hamster model.

RESULTS

Favipiravir inhibits henipavirus replication *in vitro*

To determine the inhibitory potential of favipiravir on NiV and HeV replication *in vitro*, we employed a virus yield reduction assay analysing virus titres at 48 hours post-infection (HPI). Treatment of henipavirus-infected Vero cells with favipiravir resulted in the reduction of viral titres in a dose-dependent manner for NiV-Malaysia (NiV-M), HeV, NiV-Bangladesh (NiV-B), and recombinant NiV expressing *Gaussia* luciferase and eGFP (rNiV-Gluc-eGFP) (Appendix B Fig. 1a, b, c, d). Cytotoxicity was only minimal at the highest concentration tested, with a CC_{50} value of >1,000 µM (Appendix B Fig. 2). Analysis of the dose-response curves demonstrated EC_{50} values of 44.24 µM for NiV-M, 11.71 µM for HeV, 14.82 µM for NiV-B, and 14.57 µM for rNiV-Gluc-eGFP. Selective index (SI) values were >22.60 for NiV, >85.39 for HeV, >67.47 for NiV-B, and >66.63 for rNiV-Gluc-eGFP. EC_{90} values were 123.8 µM for NiV-M,16.49 µM for HeV, 15.87 µM for NiV-B, and 16.25 µM for rNiV-Gluc-eGFP. Additionally, we assessed if the observed inhibition was due to favipiravir’s purine analogue activity by the addition of molar excess purine or pyrimidine nucleosides (Appendix B Fig. 1e). As expected, the addition of adenosine resulted in almost complete negation of favipiravir’s reduction in viral titres, while the addition of cytidine left the antiviral activity largely intact. These data demonstrate that henipaviruses are sensitive to treatment with favipiravir with EC_{90}s that are consistent with those described for other paramyxoviruses and that the antiviral activity is likely due to favipiravir's purine analogue activity [280].

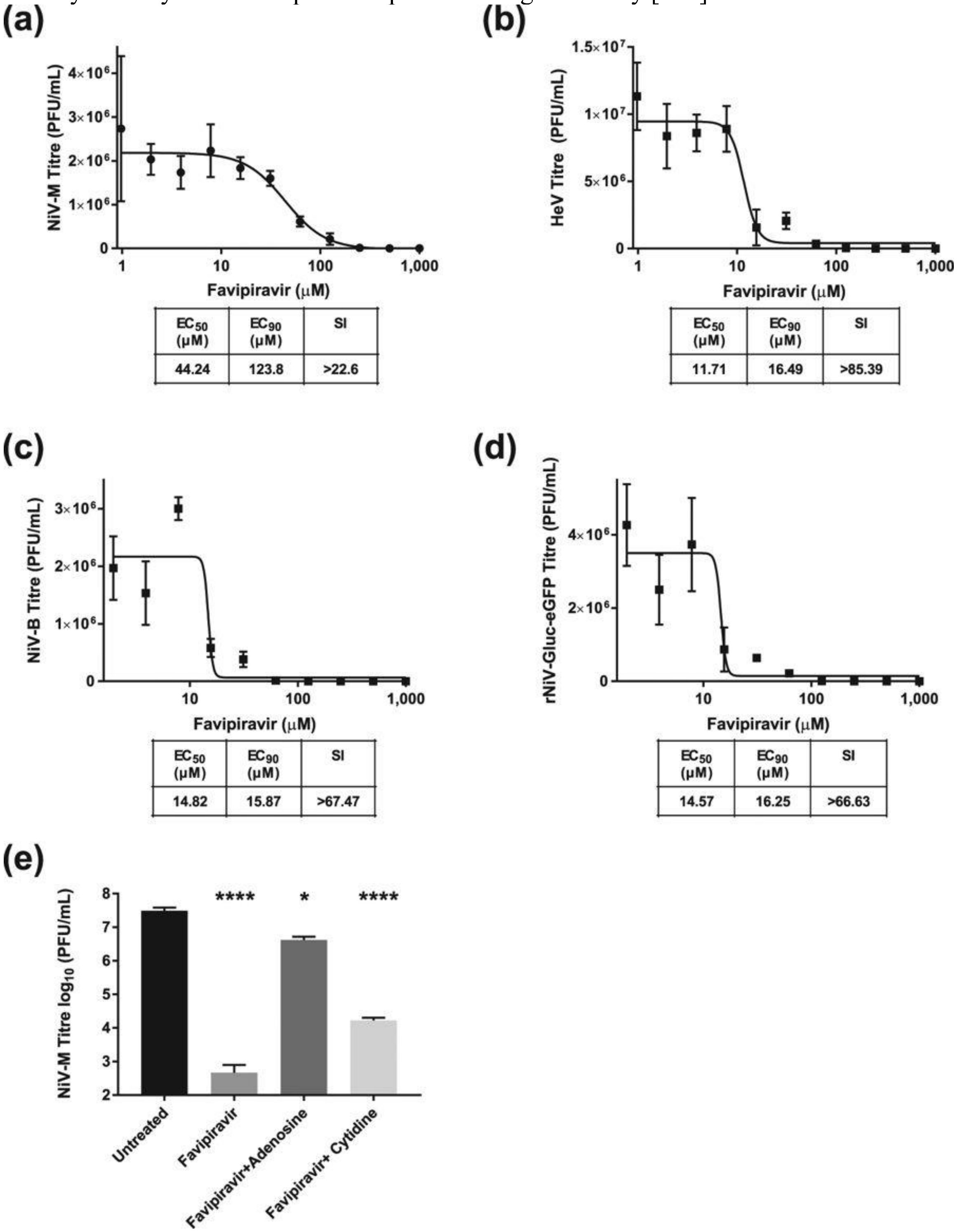

EC_{50} (μM)	EC_{90} (μM)	SI
44.24	123.8	>22.6

EC_{50} (μM)	EC_{90} (μM)	SI
11.71	16.49	>85.39

EC_{50} (μM)	EC_{90} (μM)	SI
14.82	15.87	>67.47

EC_{50} (μM)	EC_{90} (μM)	SI
14.57	16.25	>66.63

Appendix B Figure 1: *In vitro* dose response of favipiravir against henipaviruses.

Vero cells were infected with **(a)** NiV-M or **(b)** HeV, **(c)** NiV-B, **(d)** or rNiV-Gluc-eGFP at an MOI of 0.01. Cell culture media supplemented with serial 2-fold dilutions of favipiravir was added 1 hour post infection (HPI). Reduction in virus yield was determined at 48 HPI via plaque assay. **(e)** Vero cells were infected with NiV-M (MOI 0.01) and treated with 250 μM favipiravir alone or in combination with 400 μM adenosine or cytidine. Viral titres at 48HPI were then determined via plaque assay. Error bars are representing the S.D. from three individual experiments. Statistics are compared to untreated controls. *P<0.05 and ****P<0.0001

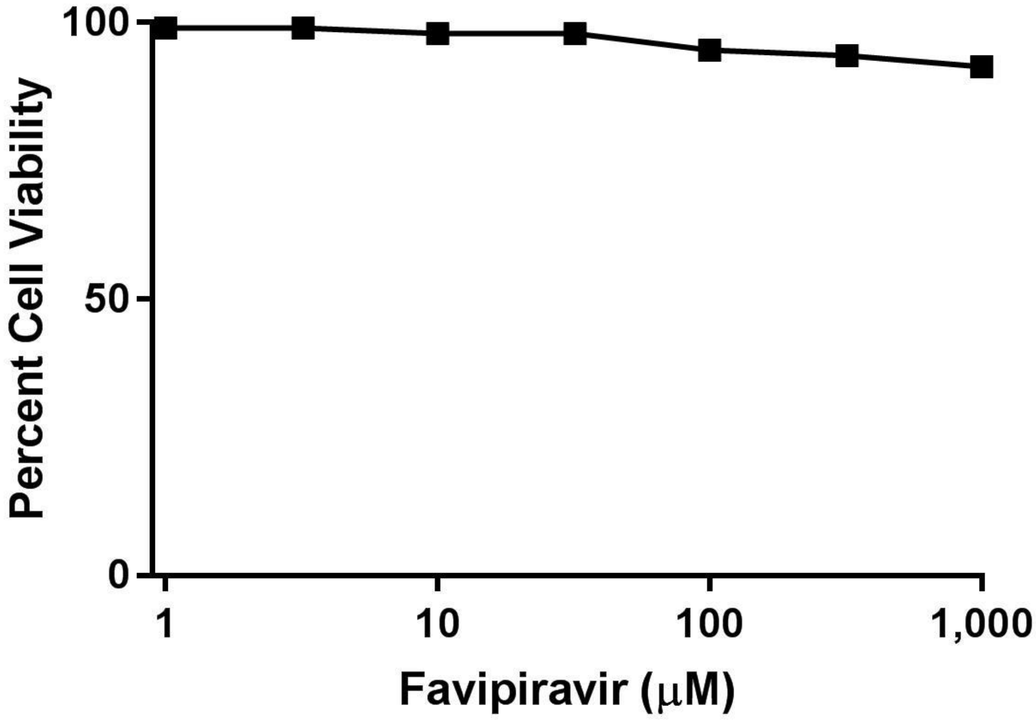

Appendix B Figure 2: Cytotoxicity of favipiravir

Vero cells were treated with two-fold dilutions of favipiravir and cell viability was assessed using a neutral red assay. CC_{50} was determined to be >1,000 μM.

Delayed treatment efficacy of favipiravir on Nipah virus infection *in vitro*

Next, we evaluated the inhibitory effect of favipiravir on henipavirus infection for post-exposure treatment *in vitro*. Vero cells were infected with rNiV-Gluc-eGFP, and favipiravir was added at 250 μM at 1, 12, and 24 HPI. This concentration almost completely inhibited NiV replication (>99% inhibition) in previous assays when added directly after infection at 1 HPI (Appendix B Fig. 1a). Previous studies have shown rNiV expressing reporter genes such as eGFP and/or Gluc to replicate equally well when compared to *wild type* virus [117,231]. Microscopic examination of untreated infected cells revealed NiV-induced cytopathic effect (CPE) with rapid syncytia formation (Appendix B Fig. 3). By 48 HPI virtually every cell was infected and involved in syncytia formation, with almost all cells detached by 72 HPI. Addition of favipiravir at 1 HPI yielded only a few infected cells with low levels of eGFP expression, which did not further progress to syncytial formation. Cells treated at 12 HPI formed smaller syncytia compared to untreated cells, and expansion of infection and syncytia halted between 24 and 48 HPI. No GFP-positive cells were observed at 72 HPI, but small plaques were visible with light microscopy, suggesting that the syncytia had detached without further spread of infection. Cells treated with favipiravir at 24 HPI demonstrated similar CPE progression up to 48 HPI. At this time point most cells were infected, but well-defined syncytia were still visible. At 72 HPI, more cells appeared to be attached and viable compared to untreated controls.

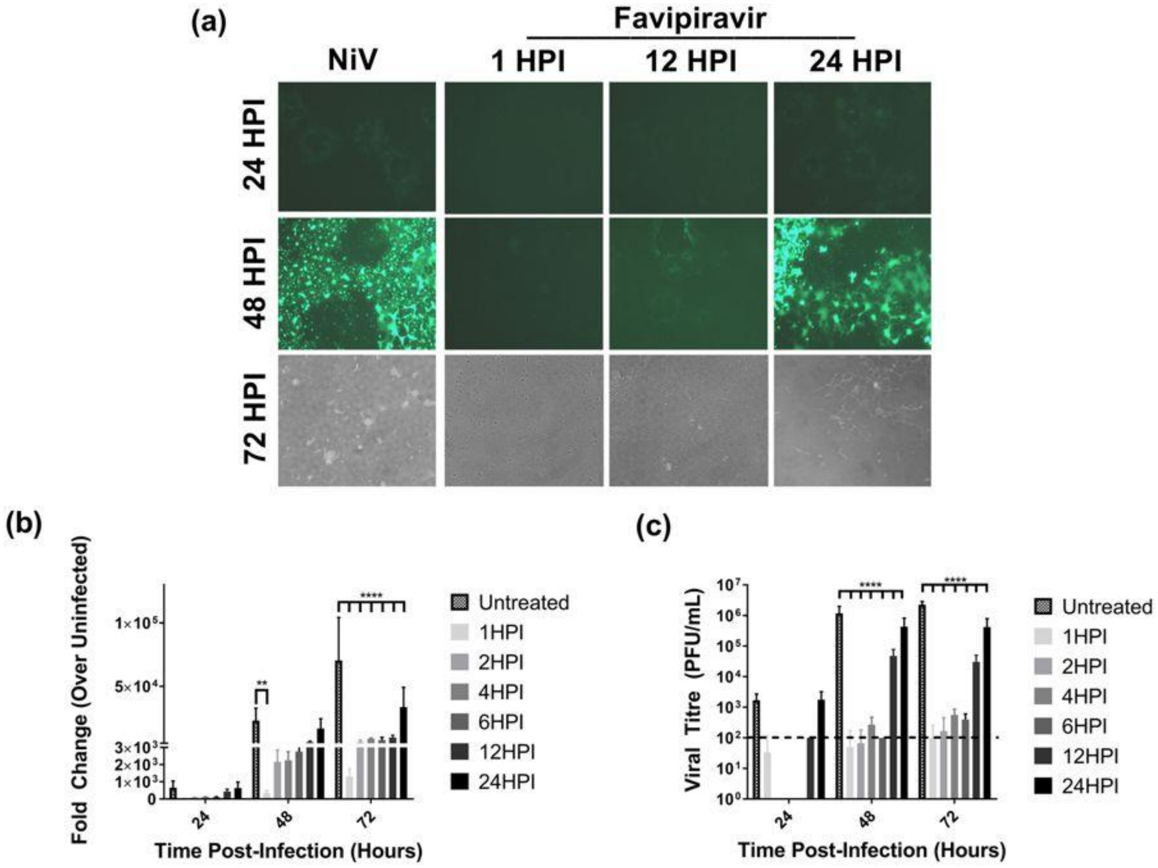

Appendix B Figure 3: Delayed treatment *in vitro* efficacy of favipiravir against NiV infection.

(a) Microscopic analysis of Vero cells infected with rNiV-Gluc-eGFP (MOI 0.01). Favipiravir (250 µM) was added at 1, 12, and 24 HPI; eGFP expression, development of syncytia, and cytopathic effect were monitored by microscopy at 24, 48 and 72 HPI. (b) and (c) Vero cells were infected with rNiV-Gluc-eGFP at an MOI of 0.01 and treated with 250 µM favipiravir at the indicated time points post infection. Cell culture supernatant samples were assayed for (b) Gaussia luciferase activity relative to uninfected cells and (c) for viral titre. Data shown in (b) and (c) represent results from two separate experiments and thus luciferase activity is normalized to uninfected cells. $^{**}P<0.01$ and $^{****}P<0.0001$.

To further refine the *in vitro* treatment window, favipiravir at 250 µM was added at six different time points between 1 and 24 HPI and every 24 hours luciferase activity was measured to determine the efficacy of favipiravir on viral gene expression (Appendix B Fig. 3b). Our previous studies have confirmed a linear relationship between luciferase activity and viral titres [117]. Luciferase activity at 24 HPI revealed no significant differences between the samples. By 48 HPI the luciferase activity in the untreated controls had increased over 22,000-fold compared to uninfected cells, while cells treated with favipiravir at 1 HPI showed a significant reduction compared to untreated controls (300-fold increase relative to uninfected) at this time point, and the cells treated at 2 to 6 HPI displayed an intermediate reduction (approximately 2,000-fold increase relative to uninfected cells). By 72 HPI the luciferase activity of all treated samples was significantly lower than in the untreated controls. Addition of favipiravir to infected cells between 1 and 12 HPI resulted in reduced viral titres compared to the untreated controls (Appendix B Fig. 3c). Although non-significant, titres for the treated cells at 24 HPI were below or close to the limit of detection of the plaque assay. By 48 HPI, the cells treated at 1 to 6 HPI yielded titres at or below the detection limit in contrast to untreated cells reaching titres around 10^6 plaque forming units (PFU)/ml. Cells treated at 12 or 24 HPI also showed significant reductions in viral titres, although to a lesser degree. By 72 HPI, titres in all groups remained similar to those determined at 48 HPI. These results demonstrate that while favipiravir is most effective at inhibiting NiV replication when added immediately after infection, delaying treatment *in vitro* for up to 24 HPI still leads to a significant reduction in viral load.

Oral administration of favipiravir fully protects from lethal Nipah virus infection in the hamster model

Favipiravir has been demonstrated to reduce mortality in various experimental models of viral haemorrhagic fever, encephalitic, or respiratory disease [280–287]. To evaluate the *in vivo* efficacy of favipiravir against NiV-M, we utilized the Syrian hamster model which closely mirrors most aspects of human disease, such as widespread vasculitis, pneumonia, and encephalitis and has been widely accepted for the evaluation of antiviral therapeutics and vaccine candidates [126,127,254,270,288–291]. Hamsters were infected with a lethal dose of 10^4 PFU NiV-M via the intraperitoneal (i.p.) route similar to previous studies and treatment was initiated immediately after infection

[270,292]. Favipiravir was administered twice daily via the perioral (p.o.) route for 14 days, again similar to previous studies evaluating the antiviral activity of favipiravir [284,286,293]. On challenge day, a loading dose of 600 mg/kg/d was administered immediately after infection, followed by 300 mg/kg/d on days 1-13. Control animals were dosed according to the same schedule with vehicle only. All vehicle-treated NiV-infected animals uniformly developed clinical signs of disease including hyperreflexia, ataxia, irregular breathing, and lethargy and succumbed to disease or were humanely euthanized on days 5 or 6 PI (Appendix B Fig. 4a). Animals treated with favipiravir did not develop clinical signs of disease during the course of the study through 42 days post infection (DPI; Appendix B Fig. 4a). Furthermore, weight data revealed steep weight loss prior to death or euthanasia in vehicle-treated animals, while favipiravir-treated animals steadily gained weight throughout the duration of the study (Appendix B Fig. 5a). Virus titrations from tissues were inconclusive as we were only able to recover viable virus in one of the four vehicle-treated animals, but no virus was detected in the favipiravir-treated group (data not shown). Real time RT-PCR for the viral P gene was conducted on brains, spleens, and lungs to compare viral load between moribund animals that were euthanized and survivors. As expected, high levels of viral P gene expression were detected in all three tissues in the vehicle-only controls compared to favipiravir-treated animals, where no viral RNA was detected (Appendix B Fig. 4b-d). Two of five survivors developed neutralizing antibody titres ($PRNT_{50}$s) of >80 and >1280, respectively, while the remaining three survivors had titres of <20 (Appendix B Table 1). These results demonstrate that favipiravir administered twice daily p.o. beginning immediately after infection is highly efficacious in preventing NiV-induced morbidity and mortality in the hamster model.

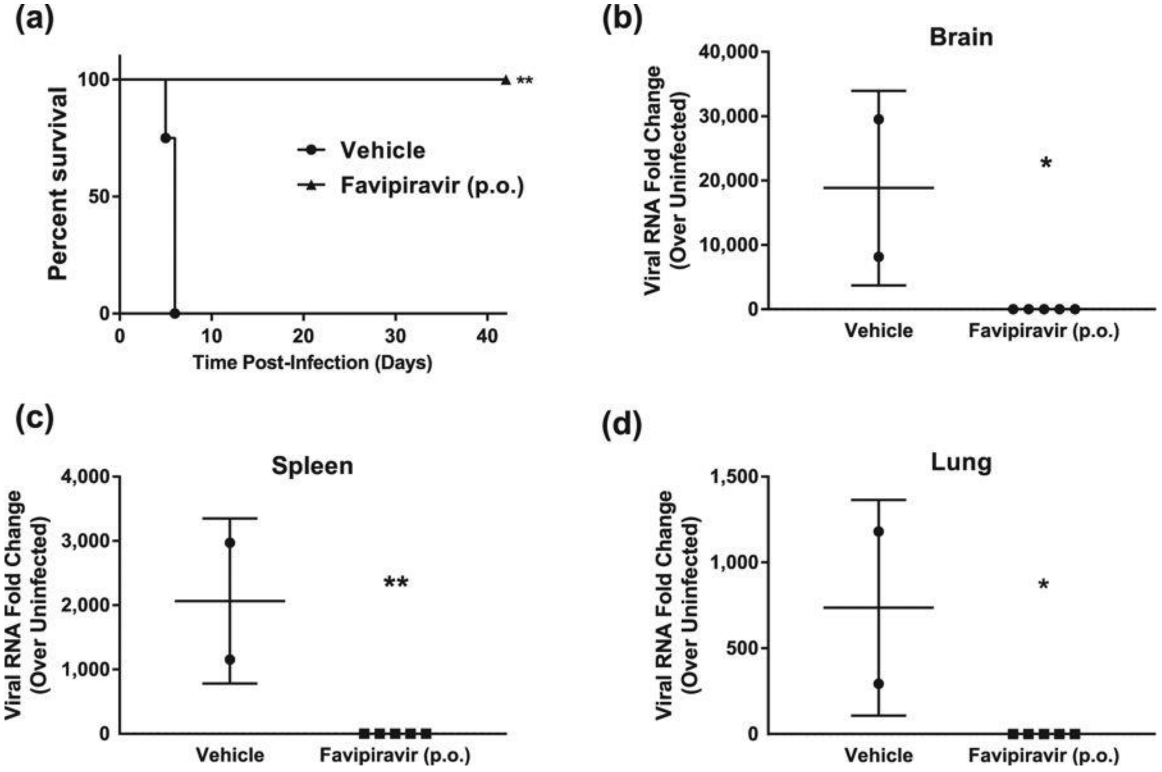

Appendix B Figure 4: ***In vivo* efficacy of orally administered favipiravir against NiV infection in Syrian hamsters.**

Hamsters were infected with 10^4 PFU NiV Malaysia strain via the intraperitoneal route. Treatment with favipiravir was initiated immediately after infection. Favipiravir (*n*=5) or vehicle (*n*=4) was administered twice daily via oral gavage (about 12 hours apart) for 14 days. A 600mg/kg loading dose was given on day 0, followed by 300mg/kg/day on days 1-13 post-infection. **(a)** Survival graph of animals receiving favipiravir (black triangles) or vehicle (black circles). Graphs **(b)** to **(d)** show results from qRT-PCR analysis of tissue samples. NiV-M phosphoprotein gene copy numbers were determined in **(b)** brains, **(c)** spleens, and **(d)** lungs from euthanized control hamsters (vehicle) and survivors after favipiravir treatment. Copy numbers were quantified via comparison to a standard curve of purified NiV-M genome and normalized relative to uninfected tissues due to background detected in uninfected tissue. *P<0.05 and **P<0.01.

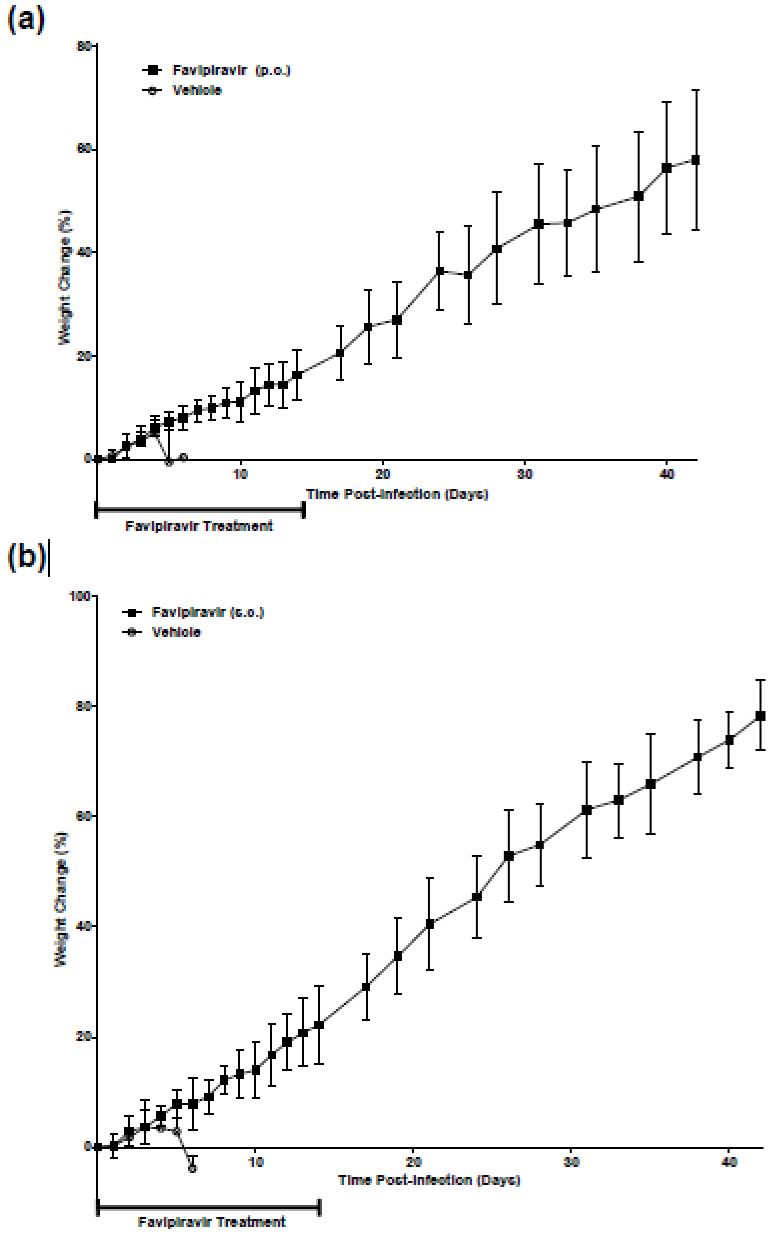

Appendix B Figure 5: Weights of infected hamsters during favipiravir treatment
Weights of infected hamsters undergoing **(a)** p.o. or **(b)** s.c. treatments. Weights were monitored daily for all infected animals through day 14 and every other day thereafter.

Group	PRNT₅₀	PRNT₉₀
Favipiravir p.o.	**<20**	**<20**
	80	**20**
	<20	**<20**
	1280	**320**
	<20	**<20**
Favipiravir s.c.	**<20**	**<20**
	80	**20**
	<20	**<20**
	80	**20**
	20	**<20**

Appendix B Table 1: Neutralizing antibody titers from *in vivo* efficacy studies

Serum collected from survivors was gamma irradiated and heat inactivated. Serum was then diluted and incubated with 50PFU NiV-M prior to infection of Vero CCL81 cells. Cells were incubated for 3 days and plaques were quantified for calculations of $PRNT_{50}$ and $PRNT_{90}$.

Administration of favipiravir subcutaneously protects hamsters from lethal Nipah virus infection

To determine the efficacy of once daily subcutaneous (s.c.) administration of favipiravir, such as recently used in a Lassa virus (LASV) guinea pig model [281], hamsters were infected with a lethal dose of 10^4 PFU NiV-M via the i.p. route and treatment was initiated immediately after infection. Similar to the oral administration study described above, a loading dose of 600 mg/kg/d was administered immediately after infection, followed by 300 mg/kg/d on days 1-13. All vehicle-treated animals became ill within 7 DPI and displayed signs of paralysis, ataxia, and irregular breathing (Appendix B Fig. 6a). Favipiravir-treated animals survived until the end of the study (42 DPI) with no development of clinical signs of disease and steadily gained weight throughout the course of the experiment (Appendix B Fig. 5b). As with the previous study, attempts at virus titration from tissue were inconclusive, and high loads of the viral P gene were detected by RT-PCR in all three tissues examined in non-treated animals (Appendix B Fig. 6b-d), while the viral load in all survivors was not detectable. Of the five surviving animals, three developed neutralizing antibody titres (two >80 and one >20), while the remaining two survivors had titres of <20 (Appendix B Table 1). These results demonstrate that administration of favipiravir s.c. once daily beginning immediately after infection is also highly efficacious in preventing NiV-induced morbidity and mortality in the hamster model.

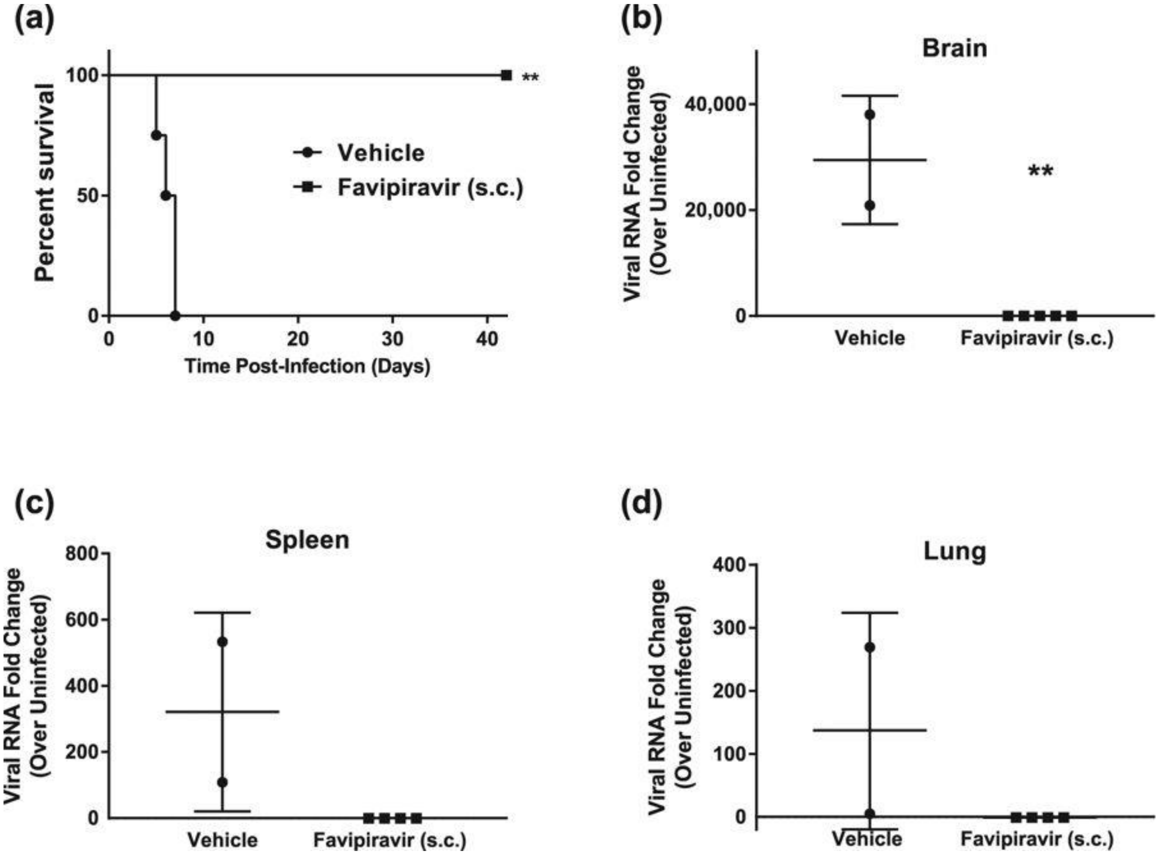

Appendix B Figure 6: ***In vivo* efficacy of subcutaneously administered favipiravir against NiV infection in Syrian hamsters.**

Hamsters were infected with 10^4 PFU NiV Malaysia strain via the intraperitoneal route. Treatment with favipiravir was initiated immediately after infection. Favipiravir (*n=5)* or vehicle (*n*=4) was administered once daily via the subcutaneous route for 14 days. A 600mg/kg loading dose was given on day 0, followed by 300mg/kg/day on days 1-13 post-infection. **(a)** Survival graph of animals receiving favipiravir (black squares) or vehicle (black circles). Graphs **(b)** to **(d)** show results from qRT-PCR analysis of tissue samples. NiV-M phosphoprotein gene copy numbers were determined in **(b)** brains, **(c)** spleens, and **(d)** lungs from euthanized control hamsters (vehicle) and survivors after favipiravir treatment. Copy numbers were quantified via comparison to a standard curve of purified NiV-M genome and normalized relative to uninfected tissues due to background detected in uninfected tissue. **P<0.01.

Favipiravir treatment results in decreased viral antigen and histopathological changes

In order to determine the pathological changes present in favipiravir-treated NiV-M-infected hamsters we examined brain, spleen, and lung collected from euthanized animals during the study and survivors at 42 DPI via H&E stains (Appendix B Fig. 7a) and IHC (Appendix B Fig. 7b) against NiV nucleoprotein. Vehicle-treated animals displayed characteristic pathological lesions of NiV infection (Appendix B Fig. 7) [87,267]: Lungs displayed perivascular infiltration of inflammatory cells, and NiV antigens were detected in endothelial cells, which occasionally formed syncytia, as well as in smooth muscle cells of pulmonary vessels. Mild to moderate interstitial pneumonia with alveolar edema or haemorrhage and occasional increase in type II pneumocytes were also seen. In the spleen, follicles were less visible, and the red pulp cord displayed necrotic areas scattered with mononuclear or reticular cells with NiV antigens. In brains, meningitis with an infiltration of neutrophils and mononuclear cells was found, and viral antigens were detected in mononuclear cells with elongated cytoplasm in meninges and occasionally in neurons in parenchyma. Tissues of animals which were treated with favipiravir, either p.o. or s.c., were similar: no prominent findings of diseases were detected in brains, lungs, and spleens in the H&E sections (Appendix B Fig. 7a). None of the treated hamsters displayed detectable NiV antigens in brains, lungs, or spleen spleens (Appendix B Fig. 7b). Lungs of treated hamsters did not show cellular infiltration in pulmonary blood vessels, although mild consolidation of lung parenchyma was observed (Appendix B Fig. 7a).

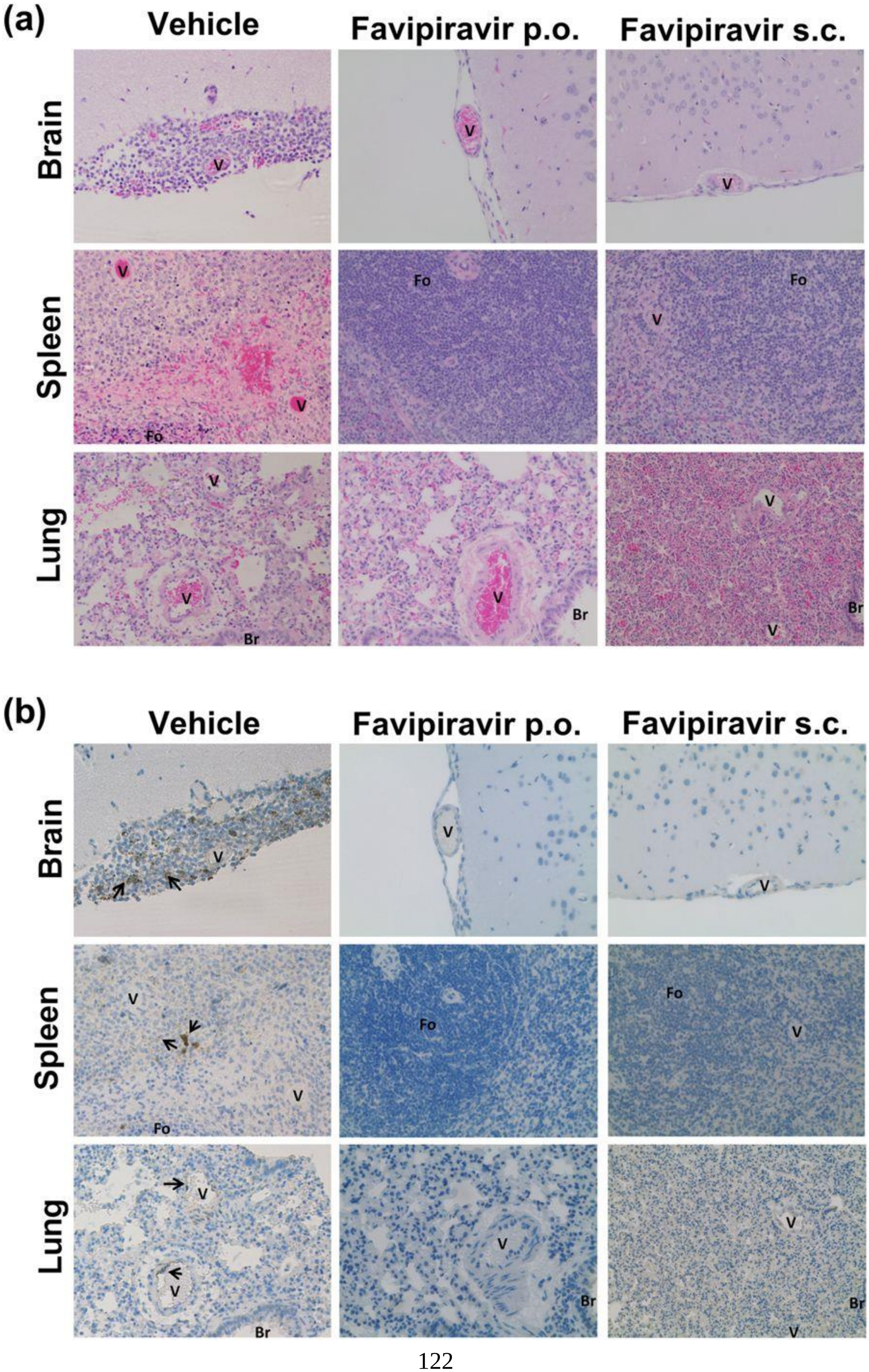
(a)
Vehicle
Favipiravir p.o.
Favipiravir s.c.
Brain
Spleen
Lung
V
Fo
Br
(b)
Vehicle
Favipiravir p.o.
Favipiravir s.c.
Brain
Spleen
Lung
V
Fo
Br

Appendix B Figure 7: Histopathology and immunohistochemistry.

(a) Formalin fixed tissues were embedded in paraffin and H&E stained. Images represent brains, lungs, and spleens of vehicle control animals, favipiravir p.o. and favipiravir s.c. **(b)** Formalin fixed tissues were embedded in paraffin and stained with anti-NiV nucleoprotein antibodies. Images represent brains, lungs, and spleens of vehicle control animals, favipiravir p.o. and favipiravir s.c. V, blood vessels; Br, bronchioles; Fo, follicles; Arrows, NiV nucleoprotein antigens.

DISCUSSION

Despite the high virulence of henipaviruses, no therapeutics are approved for human use. Several approaches have shown efficacy in animal models: monoclonal antibodies against the envelope F and G proteins appear to be effective post-exposure treatments in various animal models [87,128,290,294], and peptides derived from the C-terminal heptad repeat of the F protein inhibit fusion and viral entry *in vitro* and reduce mortality *in vivo* [291,295]. However, none of these have been moved forward into human clinical trials. Furthermore, the unpredictable and rare nature of human henipavirus infection requires quick deployment of antiviral compounds for use in rural areas in developing countries, where monoclonal antibody and peptide therapies may not be feasible. A small molecule antiviral, on the other hand, could be more easily stockpiled and would not rely on a cold-chain for rapid deployment. In Malaysia, ribavirin was evaluated in an open label trial reporting a 36% reduction in mortality [269]. However, this study used historical controls, was small in nature, and was not blinded or randomized, clouding the true efficacy. Several *in vivo* studies have failed to demonstrate efficacy of ribavirin and or chloroquine against henipavirus infection across various animal models [129,130,254,270]. We hypothesized that favipiravir, due to its ability to inhibit a wide range of RNA viruses – including several highly pathogenic RNA viruses – and demonstrated safety in humans, may be an effective therapy against henipaviruses, which could be applied during outbreaks.

In the present proof-of-concept study we demonstrate data establishing *in vitro* and *in vivo* efficacy of favipiravir against henipaviruses. *In vitro* studies showed similar efficacies to those seen in other paramyxoviruses [280]. Additionally, *in vivo* studies using the well-characterized Syrian hamster model of NiV-M infection demonstrate for the first time the ability of a small molecule, favipiravir, to prevent NiV-induced morbidity and mortality when administered directly after infection. These promising results warrant further evaluation of favipiravir for the treatment of henipavirus infection.

In vitro, favipiravir displayed EC_{50}s of 44.24 µM, 11.71 µM, 14.82 µM, and 14.57 µM and EC_{90}s of 123.8 µM, 16.49 µM, 15.87 µM, and 16.25 µM against NiV-M, HeV, NiV-B, and rNiV-Gluc-eGFP respectively (Appendix B Fig. 1). The EC_{90} against HeV and NiV-B is comparable to those recently determined for other paramyxoviruses (2-55 µM), while the EC_{90} against NiV-M is higher [280]. The L genes of the two viruses share only 87% amino acid homology, suggesting that potential structural differences in the polymerase may make HeV more susceptible to favipiravir. Interestingly, the EC_{90} of rNiV-Gluc-eGFP is lower than NiV-M despite the backbone of this strain being derived from NiV-M. It is possible that the addition of reporter genes slightly attenuates the recombinant strain with regards to its susceptibility to antivirals, although the difference remains small. Additionally, we affirmed via nucleoside supplementation assays that favipiravir's mechanism of action is likely as a purine analogue.

In time of addition experiments *in vitro* we demonstrated that delay of treatment for up to 6 hours after NiV infection resulted in essentially complete inhibition of viral replication as measured by viral titre and viral transcription of the reporter gene luciferase. Treatment delays of 12 and 24 hours still resulted in significantly reduced luciferase activity and virus titres compared to untreated controls (Appendix B Fig. 3b-c). Viral titres and luciferase activity were closely correlated throughout the experiment.

Previous *in vivo* studies have established a standard dosing route and dose for hamsters of 300 mg/kg/d favipiravir p.o. [296,297]. In the current study, dosing NiV-M-infected hamsters with 300 mg/kg/d twice daily p.o. resulted in complete survival and no obvious signs of morbidity, such as weight loss, clinical disease or behavioural changes (Appendix B Fig. 4a). While virus titrations were inconclusive, qRT-PCR demonstrated the lack of detectable viral RNA in all tissues tested in favipiravir-treated animals compared to untreated controls (Appendix B Fig. 4b-d).

Favipiravir has been designed as a drug for oral delivery [88], and twice daily oral administration most closely resembles the treatment regiments currently approved for human use. However, under biosafety level (BSL)-4 conditions animals must be anesthetized for every dosing, and twice daily dosing may thus place added stress on infected animals. Therefore, we also evaluated a once daily s.c. dosing regimen similar to one which has recently been shown to be highly efficacious in a lethal LASV guinea pig model [281]. As in our oral dosing study, hamsters that were dosed once daily with 300 mg/kg/d of favipiravir s.c. displayed 100% survival and no obvious morbidity after lethal NiV-M challenge (Appendix B Fig. 6a). Similarly, all tissues in favipiravir-treated animals appeared negative for viral RNA (Appendix B Fig. 6b-d).

Either favipiravir treatment regimen greatly reduced histopathological changes in brains, lungs, and spleens (Appendix B Fig. 7a). Moreover, viral antigens were not detectable in those treated animals (Appendix B Fig. 7b). The only changes noted were mild consolidation in the lungs. Previous studies have not looked at the long term pathological outcomes of favipiravir treatment of acute viral diseases, although several have shown that acute pathological injuries can still occur during viral infection with favipiravir treatment [281,282,284,298]. While both NiV and HeV have been shown to persist in the CNS and to cause neurologic relapse in a low percentage of recovered patients [58,92] we observed no changes in brain histology and noted the absence of viral antigen in brains of treated animals.

Together, the results presented in this study clearly demonstrate the *in vitro* and *in vivo* efficacy of favipiravir against highly pathogenic henipaviruses, and provide a foundation for further studies regarding the optimization of doses, routes, and timing of treatment after infection. Additionally, while *in vivo* efficacy was demonstrated for NiV-M, efficacy must be confirmed against HeV and NiV-B. Further studies are also required to assess the post-exposure efficacy of favipiravir when added at delayed treatment times after infection. Our data indicate that favipiravir is a small molecule antiviral candidate for potential post-exposure prophylaxis for lab workers, healthcare providers, or patient contacts potentially exposed to Nipah virus.

METHODS

Cells and viruses

Vero CCL81 cells were purchased from the American Type Culture Collection (ATCC, Manassas, VA). Cells were grown and maintained in minimal essential media (MEM) supplemented with 10% fetal bovine serum (FBS) at 37°C under 5% CO_2. FBS was lowered to 2% during viral infections.

NiV (Malaysia and Bangladesh (NiV-M and NiV-B, respectively) strain) was provided by the Special Pathogens Branch (Centers for Disease Control and Prevention, Atlanta, GA, USA) and HeV (prototype strain) was provided by the Special Pathogens Program (National Microbiology Laboratory, Canadian Science Centre for Human and Animal Health, Winnipeg, Canada). rNiV-Gaussia luciferase and green fluorescent protein (rNiV-Rbz-NP-Gluc-p2A-eGFP; here abbreviated as rNiV-Gluc-eGFP) was rescued as described previously [231]. Virus titres were determined by plaque assay on Vero cells and indicated as PFU/ml. All work with infectious virus was conducted in the Robert E. Shope BSL-4 or Galveston National Laboratory BSL-4 laboratories at the University of Texas Medical Branch (UTMB).

Compounds

Favipiravir was provided by Toyama Chemical Company, Ltd. (Toyama, Japan). For *in vitro* studies, favipiravir was dissolved in MEM. For *in vivo* studies, favipiravir was dissolved in 0.5% carboxymethylcellulose (Sigma Aldrich) for dosing via oral gavage (p.o.) and in 74.6 mg/ml meglumine solution (Sigma Aldrich) at pH 8.5 for dosing via the subcutaneous (s.c.) route.

In vitro virus yield reduction assay

Vero cells were infected with each virus at a multiplicity of infection (MOI) of 0.01 for one hour. Virus was removed; cells washed with DPBS, and overlaid with fresh MEM supplemented with 2% FBS and 2-fold dilutions of favipiravir (1,000 to 0.98 µM). Supernatant samples were collected at 48 hours post-infection (HPI) and titrated. Virus yield reduction was calculated as percent reduction of viral titres compared to untreated controls. Cellular cytotoxicity of favipiravir was determined in the absence of viral infection using a neutral red based *in vitro* toxicology assay kit (Sigma-Aldrich) The 50% effective concentration (EC_{50}) and 50% cell cytotoxic dose (CC_{50}) were determined as the favipiravir concentration at which viral titres were 50% of the untreated controls at the respective time point and the favipiravir concentration leading to 50% cytotoxicity and were calculated using regression analysis. The selectivity index (SI) was calculated using the formula $SI = CC_{50}/EC_{50}$.

In vitro time of addition experiments

Vero cells were infected with rNiV-Gluc-eGFP (MOI of 0.01). At one HPI, inoculum was removed, cells washed with DPBS, and fresh media added. Favipiravir was added at 250 µM at 1, 2, 4, 6, 12, and 24 HPI and supernatant was sampled at 24, 48, and 72 HPI. Cells were imaged by fluorescence microscopy at the indicated time points. Viral titres were determined via plaque assay, and *Gaussia* luciferase activity was measured using the Biolux® Gaussia luciferase assay kit (New England Biolabs, Ipswich, MA) following the manufacturer's protocol. Luciferase readings were recorded using a Modulus™ luminometer (Turner Biosystems, Sunnyvale, CA). All experiments were performed in biological triplicates and figures are reported in fold change to compare two separate experiments.

Nucleoside supplementation assay

Vero cells were infected with NiV-M (MOI of 0.01). At 1 HPI, cells were treated with either mock treatment, 250 μM favipiravir, 250 μM favipiravir with 400 μM adenosine (Sigma-Aldrich), or 250 μM favipiravir with 400 μM cytidine (Sigma-Aldrich). At 48 HPI supernatant was collected and titrated via plaque assay.

Animals and ethics statements

Female Syrian hamsters (4-5 weeks old, 70-100 g) were purchased from Harlan Laboratories. All procedures were conducted under animal protocols approved by the UTMB Institutional Animal Care and Use Committee and complied with USDA guidelines in an AAALAC-accredited lab. Animals were housed in microisolator caging equipped with HEPA filters in the BSL-4 laboratories.

Hamster efficacy studies

Hamsters were challenged with 10^4 PFU of NiV-M by intraperitoneal (i.p.) injection. Animals (n=5) received 300 mg/kg/d favipiravir p.o. every 12 hrs, initiated immediately after infection and continued twice daily until 13 days post-infection (DPI). Animals received a loading dose of 600 mg/kg/d on the challenge day, and a 300 mg/kg/d maintenance dose thereafter.

In a second experiment, animals (n=5) received 300 mg/kg/d favipiravir once daily s.c.. Dosing was initiated immediately after infection with a 600 mg/kg/d loading dose and a 300 mg/kg/d maintenance dose thereafter until 13 DPI. In each experiment, a virus-only control group (n=4) received the relevant vehicle solution only.

Animals determined to be moribund via daily clinical scoring or displaying greater than 20% weight loss were euthanized. Blood was collected via terminal cardiac puncture, and tissues were formalin fixed for immunohistochemical (IHC) studies or homogenized in PBS for viral titre measurements, or homogenized in TRIzol reagent (Life Technologies, Carlsbad, CA) for qRT-PCR. Survivors were monitored up to day 42 at which point they were euthanized and serum and tissues were collected. For each manipulation (viral infection or drug administration), animals were anesthetized with isoflurane (Piramal, Bethlehem, PA).

Histopathology

Formalin fixed tissues were embedded in paraffin at the UTMB Research Histopathology Core. Embedded tissues were sectioned and stained with haematoxylin and eosin (H&E). Additional sections underwent IHC staining with rabbit anti-NiV N antibody (Dr. Basler, Georgia State University) at a dilution of (1:1,000), an HRP-conjugated anti-rabbit antibody and counterstained with haematoxylin. Images were obtained using an Evos XL Core microscope (Life Technologies).

qRT-PCR

qRT-PCR was used to quantitate viral loads in tissues. RNA was extracted from tissues homogenized in TRIzol reagent using Direct-zol RNA Miniprep kits (Zymo Research, Irvine, CA). qRT-PCR assays were then run using QuantiFast RT-PCR mix (Qiagen, Hilden, Germany), probes targeting NiV-M P gene (5'-ACATACAACTGGACCCARTGGTT-3' and 5'-CACCCTCTCTCAGGGCTTGA-3') (IDT, Coralville, IA), and fluorescent probe (5'-6FAM-ACAGACGTTGTATA+C+CAT+G-TMR) (TIB MOLBIOL, Adelphia, NJ). qRT-PCR was performed using the following cycle: 10 minutes at 50°C, 5 minutes at 95°C, and 40 cycles of 10 seconds at 95°C and 30 seconds at 60°C using a BioRad CFX96 real time system. Assays were run in parallel with uninfected hamster tissues and a NiV-M stock standard curve. Gene copies were quantified based on a standard curve and fold changes compared to uninfected tissue were reported due to background detected in uninfected tissues.

Neutralizing antibody titres

Neutralizing antibodies from moribund animals or survivors were measured using a plaque reduction neutralization test (PRNT). Serum was gamma-irradiated (5 Mrad), followed by heat inactivation at 56°C for 30 minutes, then diluted in series in MEM with 2%FBS, and incubated with a dose of 50 PFU NiV-M for one hour. Vero cells were infected with the virus:serum mix and a standard plaque assay was conducted. $PRNT_{50}$ was defined as the antibody dilution yielding 50% reduction in plaques (±10%) and $PRNT_{90}$ was defined as the titre at which there was a 90% (±10%) reduction in plaques.

Statistical analysis

All statistical analysis was completed using Prism (GraphPad Software, La Jolla, CA). Comparisons of viral titres and luminescence were subjected to a two-way repeated measure analysis of variance (ANOVA) with a Tukey post-test. Dose response curves were developed using nonlinear regression. Survival curves were compared using the Mantel-Cox log-rank test. Fold changes in viral gene copies were compared using an unpaired t-test.

References

1. Soldan SS, González-Scarano F. The Bunyaviridae. Handb Clin Neurol. 2014;123:449–63.
2. THOMPSON WH, KALFAYAN B, ANSLOW RO. ISOLATION OF CALIFORNIA ENCEPHALITIS GROUP VIRUS FROM A FATAL HUMAN ILLNESS. Am J Epidemiol. United States; 1965;81:245–53.
3. Balfour HH, Siem A, Quie G, Ph D. CALIFORNIA I . Clinical ARBOVIRUS (LA CROSSE) Findings With Meningoencephalitis. 1973;52.
4. Johnson KP, Lepow ML, Johnson RT. California encephalitis. I. Clinical and epidemiological studies. Neurology. United States; 1968;18:250–4.
5. La Crosse encephalitis in West Virginia. MMWR Morb Mortal Wkly Rep. United States; 1988;37:79–82.
6. Jones TF, Craig a S, Nasci RS, Patterson LE, Erwin PC, Gerhardt RR, et al. Newly recognized focus of La Crosse encephalitis in Tennessee. Clin Infect Dis. 1999;28:93–7.
7. Gaensbauer JT, Lindsey NP, Messacar K, Staples JE, Fischer M. Neuroinvasive Arboviral Disease in the United States: 2003 to 2012. Pediatrics [Internet]. 2014; Available from: http://pediatrics.aappublications.org/content/early/2014/08/06/peds.2014-0498.abstract
8. Haddow AD, Odoi A. The incidence risk, clustering, and clinical presentation of La Crosse virus infections in the Eastern United States, 2003-2007. PLoS One. 2009;4:2003–7.
9. Baldridge GD, Beaty BJ, Hewlett MJ. Genomic stability of La Crosse virus during vertical and horizontal transmission. Arch Virol. Austria; 1989;108:89–99.
10. Moulton DW, Thompson WH. California group virus infections in small, forest-dwelling mammals of Wisconsin. Some ecological considerations. Am J Trop Med Hyg. United States; 1971;20:474–82.
11. Gauld LW, Yuill TM, Hanson RP, Sinha SK. Isolation of La Crosse virus (California encephalitis group) from the chipmunk (Tamias striatus), an amplifier host. Am J Trop Med Hyg. United States; 1975;24:999–1005.
12. Grimstad PR, Kobayashi JF, Zhang MB, Craig GBJ. Recently introduced Aedes albopictus in the United States: potential vector of La Crosse virus (Bunyaviridae: California serogroup). J Am Mosq Control Assoc. United States; 1989;5:422–7.
13. Gerhardt RR, Gottfried KL, Apperson CS, Davis BS, Erwin PC, Smith AB, et al. First isolation of La Crosse virus from naturally infected Aedes albopictus. Emerg Infect Dis. United States; 2001;7:807–11.

14. Sardelis MR, Turell MJ, Andre RG. Laboratory transmission of La Crosse virus by Ochlerotatus j. japonicus (Diptera: Culicidae). J Med Entomol. England; 2002;39:635–9.

15. Harris MC, Dotseth EJ, Jackson BT, Zink SD, Marek PE, Kramer LD, et al. La Crosse Virus in Aedes japonicus japonicus Mosquitoes in the Appalachian Region, United States. Emerg. Infect. Dis. 2015. p. 646–9.

16. McJunkin JE, de los Reyes EC, Irazuzta JE, Caceres MJ, Khan RR, Minnich LL, et al. La Crosse Encephalitis in Children. N Engl J Med [Internet]. 2001;344:801–7. Available from: http://www.nejm.org/doi/abs/10.1056/NEJM200103153441103

17. Teleron ALA, Rose BK, Williams DM, Kemper SE, McJunkin JE. La Crosse Encephalitis: An Adult Case Series. Am J Med [Internet]. Elsevier Inc; 2016;129:881–4. Available from: http://dx.doi.org/10.1016/j.amjmed.2016.03.021

18. Rust RS, Thompson WH, Matthews CG, Beaty BJ, Chun RWM. Topical review: La Crosse and other forms of California encephalitis. J Child Neurol [Internet]. 1999;14:1–14. Available from: http://jcn.sagepub.com/cgi/doi/10.1177/088307389901400101

19. Woodruff BA, Baron RC, Tsai TF. Symptomatic La Crosse virus infections of the central nervous system: a study of risk factors in an endemic area. Am J Epidemiol. United States; 1992;136:320–7.

20. Utz JT, Apperson CS, MacCormack JN, Salyers M, Dietz EJ, McPherson JT. Economic and social impacts of La Crosse encephalitis in western North Carolina. Am J Trop Med Hyg. United States; 2003;69:509–18.

21. Kalfayan B. Pathology of La Crosse virus infection in humans. Prog Clin Biol Res. United States; 1983;123:179–86.

22. Pekosz A, Griot C, Stillmock K, Nathanson N, Gonzalez-Scarano F. Protection from La Crosse virus encephalitis with recombinant glycoproteins: role of neutralizing anti-G1 antibodies. J Virol. United States; 1995;69:3475–81.

23. Cassidy LF, Patterson JL. Mechanism of La Crosse virus inhibition by ribavirin. Antimicrob Agents Chemother. 1989;33:2009–11.

24. McJunkin JE, Nahata MC, De Los Reyes EC, Hunt WG, Caceres M, Khan RR, et al. Safety and pharmacokinetics of ribavirin for the treatment of la crosse encephalitis. Pediatr Infect Dis J. United States; 2011;30:860–5.

25. Gowen BB, Wong MH, Jung KH, Sanders AB, Mendenhall M, Bailey KW, et al. In vitro and in vivo activities of T-705 against arenavirus and bunyavirus infections. Antimicrob Agents Chemother. 2007;51:3168–76.

26. Lednicky JA, White SK, Stephenson CJ, Cherabuddi K, Loeb JC, Moussatche N, et al. Keystone Virus Isolated from a Florida Teenager with Rash and Subjective Fever: Another Endemic Arbovirus in the Southeastern United States? Clin Infect Dis. United States; 2018;

27. Artsob H, Spence L, Surgeoner G, Helson B, Thorsen J, Grant L, et al. Snowshoe hare virus activity in Southern Ontario. Can J Public Health. Canada; 1982;73:345–9.

28. Elliott RM, Schmaljohn CS. Bunyaviradae. In: Knipe DM, Howley PM, editors. Fields Virol. 6th ed. Philadelphia: Wolters Kluwer; 2013. p. 1244–78.

29. Hofmann H, Li X, Zhang X, Liu W, Kuhl A, Kaup F, et al. Severe Fever with Thrombocytopenia Virus Glycoproteins Are Targeted by Neutralizing Antibodies and Can Use DC-SIGN as a Receptor for pH-Dependent Entry into Human and Animal Cell Lines. J Virol [Internet]. 2013;87:4384–94. Available from: http://jvi.asm.org/cgi/doi/10.1128/JVI.02628-12

30. Hollidge BS, Nedelsky NB, Salzano M-V, Fraser JW, Gonzalez-Scarano F, Soldan SS. Orthobunyavirus Entry into Neurons and Other Mammalian Cells Occurs via Clathrin-Mediated Endocytosis and Requires Trafficking into Early Endosomes. J Virol [Internet]. 2012;86:7988–8001. Available from: http://jvi.asm.org/cgi/doi/10.1128/JVI.00140-12

31. Griot C, Gonzalez-Scarano F, Nathanson N. Molecular determinants of the virulence and infectivity of California serogroup bunyaviruses. Annu Rev Microbiol. United States; 1993;47:117–38.

32. Soldan SS, Hollidge BS, Wagner V, Weber F, González-Scarano F. La Crosse virus (LACV) Gc fusion peptide mutants have impaired growth and fusion phenotypes, but remain neurotoxic. Virology [Internet]. Academic Press; 2010 [cited 2018 Feb 17];404:139–47. Available from: https://www.sciencedirect.com/science/article/pii/S0042682210002473?via%3Dihub

33. Tilston-Lunel NL, Acrani GO, Randall RE, Elliott RM. Generation of Recombinant Oropouche Viruses Lacking the Nonstructural Protein NSm or NSs. J Virol. United States; 2015;90:2616–27.

34. Bennett RS, Cress CM, Ward JM, Firestone CY, Murphy BR, Whitehead SS. La Crosse virus infectivity, pathogenesis, and immunogenicity in mice and monkeys. Virol J. 2008;5:1–15.

35. Johnson RT. Pathogenesis of La Crosse virus in mice. Prog Clin Biol Res. United States; 1983;123:139–44.

36. Endres MJ, Jacoby DR, Janssen RS, Gonzalez-Scarano F, Nathanson N. The Large Viral RNA Segment of California Serogroup Bunyaviruses Encodes the Large Viral Protein. J Gen Virol [Internet]. 1989;70:223–8. Available from: http://jgv.microbiologyresearch.org/content/journal/jgv/10.1099/0022-1317-70-1-223

37. Janssen R, Gonzalez-Scarano F, Nathanson N. Mechanisms of bunyavirus virulence. Comparative pathogenesis of a virulent strain of La Crosse and an avirulent strain of Tahyna virus. Lab Invest. United States; 1984;50:447–55.

38. Taylor KG, Woods TA, Winkler CW, Carmody AB, Peterson KE. Age-Dependent Myeloid Dendritic Cell Responses Mediate Resistance to La Crosse Virus-

Induced Neurological Disease. J Virol [Internet]. 2014;88:11070–9. Available from: http://jvi.asm.org/cgi/doi/10.1128/JVI.01866-14

39. Winkler CW, Race B, Phillips K, Peterson KE. Capillaries in the olfactory bulb but not the cortex are highly susceptible to virus-induced vascular leak and promote viral neuroinvasion. Acta Neuropathol. Springer Berlin Heidelberg; 2015;130:233–45.

40. Kallfass C, Ackerman A, Lienenklaus S, Weiss S, Heimrich B, Staeheli P. Visualizing Production of Beta Interferon by Astrocytes and Microglia in Brain of La Crosse Virus-Infected Mice. J Virol [Internet]. 2012;86:11223–30. Available from: http://jvi.asm.org/cgi/doi/10.1128/JVI.01093-12

41. Mukherjee P, Woods TA, Moore RA, Peterson KE. Activation of the innate signaling molecule mavs by bunyavirus infection upregulates the adaptor protein sarm1, leading to neuronal death. Immunity [Internet]. Elsevier Inc.; 2013;38:705–16. Available from: http://dx.doi.org/10.1016/j.immuni.2013.02.013

42. Pekosz a, Phillips J, Pleasure D, Merry D, Gonzalez-Scarano F. Induction of apoptosis by La Crosse virus infection and role of neuronal differentiation and human bcl-2 expression in its prevention. J Virol [Internet]. 1996;70:5329–35. Available from: http://www.pubmedcentral.nih.gov/articlerender.fcgi?artid=190490&tool=pmcentrez&rendertype=abstract

43. Colón-Ramos DA, Irusta PM, Gan EC, Olson MR, Song J, Morimoto RI, et al. Inhibition of Translation and Induction of Apoptosis by Bunyaviral Nonstructural Proteins Bearing Sequence Similarity to Reaper. Hunter T, editor. Mol. Biol. Cell. 2003. p. 4162–72.

44. Verbruggen P, Ruf M, Blakqori G, Överby AK, Heidemann M, Eick D, et al. Interferon antagonist NSs of la crosse virus triggers a DNA damage response-like degradation of transcribing RNA polymerase II. J Biol Chem. 2011;286:3681–92.

45. Proenca-Modena JL, Sesti-Costa R, Pinto AK, Richner JM, Lazear HM, Lucas T, et al. Oropouche Virus Infection and Pathogenesis Are Restricted by MAVS, IRF-3, IRF-7, and Type I Interferon Signaling Pathways in Nonmyeloid Cells. J Virol [Internet]. 2015;89:4720–37. Available from: http://jvi.asm.org/lookup/doi/10.1128/JVI.00077-15

46. Kochs G, Janzen C, Hohenberg H, Haller O. Antivirally active MxA protein sequesters La Crosse virus nucleocapsid protein into perinuclear complexes. Proc Natl Acad Sci [Internet]. 2002;99:3153–8. Available from: http://www.pnas.org/cgi/doi/10.1073/pnas.052430399

47. Blakqori G, Delhaye S, Habjan M, Blair CD, Sanchez-Vargas I, Olson KE, et al. La Crosse Bunyavirus Nonstructural Protein NSs Serves To Suppress the Type I Interferon System of Mammalian Hosts. J Virol [Internet]. 2007;81:4991–9. Available from: http://jvi.asm.org/cgi/doi/10.1128/JVI.01933-06

48. Delhaye S, Paul S, Blakqori G, Minet M, Weber F, Staeheli P, et al. Neurons produce type I interferon during viral encephalitis. Proc Natl Acad Sci [Internet].

2006;103:7835–40. Available from: http://www.pnas.org/cgi/doi/10.1073/pnas.0602460103

49. Winkler CW, Myers LM, Woods TA, Carmody AB, Taylor KG, Peterson KE. Lymphocytes have a role in protection, but not in pathogenesis, during La Crosse Virus infection in mice. J Neuroinflammation. Journal of Neuroinflammation; 2017;14:1–14.

50. Winkler CW, Woods TA, Robertson SJ, McNally KL, Carmody AB, Best SM, et al. Cutting Edge: CCR2 Is Not Required for Ly6C ^{hi} Monocyte Egress from the Bone Marrow but Is Necessary for Migration within the Brain in La Crosse Virus Encephalitis. J Immunol [Internet]. 2018;200:471–6. Available from: http://www.jimmunol.org/lookup/doi/10.4049/jimmunol.1701230

51. Schultz KLW, Vernon PS, Griffin DE. Differentiation of Neurons Restricts Arbovirus Replication and Increases Expression of the Alpha Isoform of IRF-7. J Virol [Internet]. 2015;89:48–60. Available from: http://jvi.asm.org/lookup/doi/10.1128/JVI.02394-14

52. Hou Y-J, Banerjee R, Thomas B, Nathan C, Garcia-Sastre A, Ding A, et al. SARM Is Required for Neuronal Injury and Cytokine Production in Response to Central Nervous System Viral Infection. J Immunol [Internet]. 2013;191:875–83. Available from: http://www.jimmunol.org/cgi/doi/10.4049/jimmunol.1300374

53. Daniels BP, Holman DW, Cruz-Orengo L, Jujjavarapu H, Durrant DM, Klein RS. Viral pathogen-associated molecular patterns regulate blood-brain barrier integrity via competing innate cytokine signals. MBio. 2014;5:1–13.

54. Chang C-Y, Li J-R, Chen W-Y, Ou Y-C, Lai C-Y, Hu Y-H, et al. Disruption of in vitro endothelial barrier integrity by Japanese encephalitis virus-Infected astrocytes. Glia. United States; 2015;

55. Selvey LA, Wells RM, McCormack JG, Ansford AJ, Murray K, Rogers RJ, et al. Infection of humans and horses by a newly described morbillivirus. Med J Aust. Australia; 1995;162:642–5.

56. Chua KB, Bellini WJ, Rota PA, Harcourt BH, Tamin A, Lam SK, et al. Nipah virus:a recently emergent deadly paramyxovirus. Science (80-). 2000;288:1432 –1435.

57. Murray K, Selleck P, Hooper P, Hyatt A, Gould A, Gleeson L, et al. A morbillivirus that caused fatal disease in horses and humans. Science. United States; 1995;268:94–7.

58. O’Sullivan JD, Allworth AM, Paterson DL, Snow TM, Boots R, Gleeson LJ, et al. Fatal encephalitis due to novel paramyxovirus transmitted from horses. Lancet. 1997;349:93–5.

59. Wong KT, Robertson T, Ong BB, Chong JW, Yaiw KC, Wang LF, et al. Human Hendra virus infection causes acute and relapsing encephalitis. Neuropathol Appl Neurobiol. 2009;35:296–305.

60. Field HE. Hendra virus ecology and transmission. Curr Opin Virol [Internet]. Elsevier B.V.; 2016;16:120–5. Available from: http://dx.doi.org/10.1016/j.coviro.2016.02.004

61. Field H, Crameri G, Kung NY-H, Wang L-F. Ecological aspects of hendra virus. Curr Top Microbiol Immunol. Germany; 2012;359:11–23.

62. Young PL, Halpin K, Selleck PW, Field H, Gravel JL, Kelly MA, et al. Serologic evidence for the presence in Pteropus bats of a paramyxovirus related to equine morbillivirus. Emerg Infect Dis. United States; 1996;2:239–40.

63. Halpin K, Young PL, Field HE, Mackenzie JS. Isolation of Hendra virus from pteropid bats: a natural reservoir of Hendra virus. J Gen Virol. England; 2000;81:1927–32.

64. Chua KB, Goh KJ, Wong KT, Kamarulzaman A, Tan PS, Ksiazek TG, et al. Fatal encephalitis due to Nipah virus among pig-farmers in Malaysia. Lancet (London, England). England; 1999;354:1257–9.

65. Goh KJ, Tan CT, Chew NK, Tan PSK, Kamarulzaman A, Sarji SA, et al. Clinical Features of Nipah Virus Encephalitis among Pig Farmers in Malaysia. N Engl J Med [Internet]. 2000;342:1229–35. Available from: http://www.nejm.org/doi/abs/10.1056/NEJM200004273421701

66. Paton NI, Leo YS, Zaki SR, Auchus AP, Lee KE, Ling AE, et al. Outbreak of Nipah-virus infection among abattoir workers in Singapore. Lancet. 1999;354:1253–6.

67. Ang BSP, Lim TCC, Wang L. Nipah Virus Infection. J Clin Microbiol. United States; 2018;56.

68. Hosono H, Kono H, Ito S, Shirai J. Economic Impact of Nipah Virus Infection Outbreak in Malaysia 1. SciQuest. 2006;1998–2000.

69. Chua KB, Koh CL, Hooi PS, Wee KF, Khong JH, Chua BH, et al. Isolation of Nipah virus from Malaysian Island flying-foxes. Microbes Infect. France; 2002;4:145–51.

70. Ching PKG, de los Reyes VC, Sucaldito MN, Tayag E, Columna-Vingno AB, Malbas FFJ, et al. Outbreak of henipavirus infection, Philippines, 2014. Emerg Infect Dis. United States; 2015;21:328–31.

71. Luby SP, Gurley ES, Hossain MJ. Transmission of human infection with Nipah virus. Clin Infect Dis. United States; 2009;49:1743–8.

72. Donaldson H, Lucey D. Enhancing Preparation for Large Nipah Outbreaks Beyond Bangladesh: Preventing a Tragedy like Ebola in West Africa. Int J Infect Dis. Canada; 2018;

73. Luby SP, Gurley ES. Epidemiology of henipavirus disease in humans. Curr Top Microbiol Immunol. Germany; 2012;359:25–40.

74. Luby SP, Rahman M, Hossain MJ, Blum LS, Husain MM, Gurley E, et al. Foodborne transmission of Nipah virus, Bangladesh. Emerg Infect Dis. United States; 2006;12:1888–94.

75. Hsu VP, Hossain MJ, Parashar UD, Ali MM, Ksiazek TG, Kuzmin I, et al. Nipah virus encephalitis reemergence, Bangladesh. Emerg Infect Dis. United States; 2004;10:2082–7.

76. Chadha MS, Comer JA, Lowe L, Rota PA, Rollin PE, Bellini WJ, et al. Nipah virus-associated encephalitis outbreak, Siliguri, India. Emerg Infect Dis. United States; 2006;12:235–40.

77. Montgomery JM, Hossain MJ, Gurley E, Carroll GDS, Croisier A, Bertherat E, et al. Risk factors for Nipah virus encephalitis in Bangladesh. Emerg Infect Dis. United States; 2008;14:1526–32.

78. Hossain MJ, Gurley ES, Montgomery JM, Bell M, Carroll DS, Hsu VP, et al. Clinical Presentation of Nipah Virus Infection in Bangladesh. Clin Infect Dis [Internet]. 2008;46:977–84. Available from: https://academic.oup.com/cid/article-lookup/doi/10.1086/529147

79. Harcourt BH, Lowe L, Tamin A, Liu X, Bankamp B, Bowden N, et al. Genetic characterization of Nipah virus, Bangladesh, 2004. Emerg Infect Dis. United States; 2005;11:1594–7.

80. Wong KT, Shieh W-J, Kumar S, Norain K, Abdullah W, Guarner J, et al. Nipah Virus Infection. Am J Pathol [Internet]. American Society for Investigative Pathology; 2002;161:2153–67. Available from: http://linkinghub.elsevier.com/retrieve/pii/S0002944010644938

81. Munster VJ, Prescott JB, Bushmaker T, Long D, Rosenke R, Thomas T, et al. Rapid Nipah virus entry into the central nervous system of hamsters via the olfactory route. Sci Rep. 2012;2:1–8.

82. Luby SP. The pandemic potential of Nipah virus. Antiviral Res [Internet]. Elsevier B.V.; 2013;100:38–43. Available from: http://dx.doi.org/10.1016/j.antiviral.2013.07.011

83. Rottingen J-A, Gouglas D, Feinberg M, Plotkin S, Raghavan K V, Witty A, et al. New Vaccines against Epidemic Infectious Diseases. N Engl J Med. United States; 2017;376:610–3.

84. Satterfield BA, Dawes BE, Milligan GN. Status of vaccine research and development of vaccines for Nipah virus. Vaccine [Internet]. Elsevier Ltd; 2016;34:2971–5. Available from: http://dx.doi.org/10.1016/j.vaccine.2015.12.075

85. Dawes BE, Kalveram B, Ikegami T, Juelich T, Smith JK, Zhang L, et al. Favipiravir (T-705) protects against Nipah virus infection in the hamster model. Sci Rep [Internet]. Springer US; 2018;1–11. Available from: http://dx.doi.org/10.1038/s41598-018-25780-3

86. Broder CC, Geisbert TW, Xu K, Nikolov DB, Wang LF, Middleton D, et al. Immunization strategies against henipaviruses. Curr. Top. Microbiol. Immunol. 2012.

87. Geisbert TW, Mire CE, Geisbert JB, Chan Y-P, Agans KN, Feldmann F, et al. Therapeutic treatment of Nipah virus infection in nonhuman primates with a

neutralizing human monoclonal antibody. Sci Transl Med. United States; 2014;6:242ra82.

88. Furuta Y, Gowen BB, Takahashi K, Shiraki K, Smee DF, Barnard DL. Favipiravir (T-705), a novel viral RNA polymerase inhibitor. Antiviral Res [Internet]. Elsevier B.V.; 2013;100:446–54. Available from: http://dx.doi.org/10.1016/j.antiviral.2013.09.015

89. Mathieu C, Porotto M, Figueira T, Horvat B, Moscona A. Fusion Inhibitory Lipopeptides Engineered for Prophylaxis of Nipah Virus in Primates. J Infect Dis [Internet]. 2018; Available from: http://www.ncbi.nlm.nih.gov/pubmed/29566184

90. Khan SU, Gurley ES, Hossain MJ, Nahar N, Sharker MAY, Luby SP. A randomized controlled trial of interventions to impede date palm sap contamination by bats to prevent nipah virus transmission in Bangladesh. PLoS One. United States; 2012;7:e42689.

91. Middleton D, Pallister J, Klein R, Feng Y-R, Haining J, Arkinstall R, et al. Hendra Virus Vaccine, a One Health Approach to Protecting Horse, Human, and Environmental Health. Emerg. Infect. Dis. 2014. p. 372–9.

92. Tan CT, Goh KJ, Wong KT, Sarji SA, Chua KB, Chew NK, et al. Relapsed and late-onset Nipah encephalitis. Ann Neurol. 2002;51:703–8.

93. Abdullah S, Tan CT. Henipavirus encephalitis [Internet]. 1st ed. Handb. Clin. Neurol. Elsevier B.V.; 2014. Available from: http://dx.doi.org/10.1016/B978-0-444-53488-0.00032-8

94. Sejvar JJ, Hossain J, Sana SK, Gurley ES, Banu S, Hamadani JD, et al. Long-term neurological and functional outcome in Nipah virus infection. Ann Neurol. 2007;62:235–42.

95. Abdullah S, Chang L-Y, Rahmat K, Goh KJ, Tan CT. Late-onset Nipah virus encephalitis 11 years after the initial outbreak: A case report. Neurol Asia. 2012;17.

96. Sarji SA, Abdullah BJJ, Goh KJ, Tan C tin, Wong K thong. MR imaging features of Nipah encephalitis. Am J Roentgenol. 2000;175:437–42.

97. Halpin K, Bankamp B, Harcourt BH, Bellini WJ, Rota PA. Nipah virus conforms to the rule of six in a minigenome replication assay. J Gen Virol. England; 2004;85:701–7.

98. Rota PA, Lo MK. Molecular virology of the henipaviruses. Curr Top Microbiol Immunol. Germany; 2012;359:41–58.

99. Bonaparte MI, Dimitrov AS, Bossart KN, Crameri G, Mungall BA, Bishop KA, et al. Ephrin-B2 ligand is a functional receptor for Hendra virus and Nipah virus. Proc Natl Acad Sci U S A. United States; 2005;102:10652–7.

100. Negrete OA, Levroney EL, Aguilar HC, Bertolotti-Ciarlet A, Nazarian R, Tajyar S, et al. EphrinB2 is the entry receptor for Nipah virus, an emergent deadly paramyxovirus. Nature. 2005;436:401–5.

101. Pernet O, Wang YE, Lee B. Henipavirus receptor usage and tropism. Curr Top Microbiol Immunol. Germany; 2012;359:59–78.

102. Sugai A, Sato H, Takayama I, Yoneda M, Kai C. Nipah and Hendra Virus Nucleoproteins Inhibit Nuclear Accumulation of Signal Transducer and Activator of Transcription 1 (STAT1) and STAT2 by Interfering with Their Complex Formation. J Virol. United States; 2017;91.

103. Shaw ML, García-Sastre A, Palese P, Basler CF. Nipah virus V and W proteins have a common STAT1-binding domain yet inhibit STAT1 activation from the cytoplasmic and nuclear compartments, respectively. J Virol. 2004;78:5633–41.

104. Andrejeva J, Childs KS, Young DF, Carlos TS, Stock N, Goodbourn S, et al. The V proteins of paramyxoviruses bind the IFN-inducible RNA helicase, mda-5, and inhibit its activation of the IFN-β promoter. Proc. Natl. Acad. Sci. U. S. A. 2004. p. 17264–9.

105. Sanchez-Aparicio MT, Feinman LJ, Garcia-Sastre A, Shaw ML. Paramyxovirus V Proteins Interact with the RIG-I/TRIM25 Regulatory Complex and Inhibit RIG-I Signaling. J Virol. United States; 2018;92.

106. Komatsu T, Tanaka Y, Kitagawa Y, Koide N, Naiki Y, Morita N, et al. Sendai Virus V Protein Inhibits the Secretion of Interleukin-1beta by Preventing NLRP3 Inflammasome Assembly. J Virol. United States; 2018;

107. Shaw ML, Cardenas WB, Zamarin D, Palese P, Basler CF. Nuclear Localization of the Nipah Virus W Protein Allows for Inhibition of both Virus- and Toll-Like Receptor 3-Triggered Signaling Pathways. J Virol [Internet]. 2005;79:6078–88. Available from: http://jvi.asm.org/cgi/doi/10.1128/JVI.79.10.6078-6088.2005

108. Satterfield BA, Cross RW, Fenton KA, Agans KN, Basler CF, Geisbert TW, et al. The immunomodulating v and W proteins of Nipah virus determine disease course. Nat Commun [Internet]. Nature Publishing Group; 2015;6:1–15. Available from: http://dx.doi.org/10.1038/ncomms8483

109. Park A, Yun T, Vigant F, Pernet O, Won ST, Dawes BE, et al. Nipah Virus C Protein Recruits Tsg101 to Promote the Efficient Release of Virus in an ESCRT-Dependent Pathway. PLoS Pathog. 2016;12:1–22.

110. Yamaguchi M, Kitagawa Y, Zhou M, Itoh M, Gotoh B. An anti-interferon activity shared by paramyxovirus C proteins: Inhibition of Toll-like receptor 7/9-dependent alpha interferon induction. FEBS Lett [Internet]. Federation of European Biochemical Societies; 2014;588:28–34. Available from: http://dx.doi.org/10.1016/j.febslet.2013.11.015

111. Patch JR, Crameri G, Wang L-F, Eaton BT, Broder CC. Quantitative analysis of Nipah virus proteins released as virus-like particles reveals central role for the matrix protein. Virol J. England; 2007;4:1.

112. Ciancanelli MJ, Basler CF. Mutation of YMYL in the Nipah virus matrix protein abrogates budding and alters subcellular localization. J Virol. United States; 2006;80:12070–8.

113. Bharaj P, Wang YE, Dawes BE, Yun TE, Park A, Yen B, et al. The Matrix Protein of Nipah Virus Targets the E3-Ubiquitin Ligase TRIM6 to Inhibit the IKKε Kinase-Mediated Type-I IFN Antiviral Response. PLoS Pathog. 2016;12:1–27.

114. Rawlinson SM, Zhao T, Rozario AM, Rootes CL, McMillan PJ, Purcell AW, et al. Viral regulation of host cell biology by hijacking of the nucleolar DNA-damage response. Nat Commun. England; 2018;9:3057.

115. Lieu KG, Marsh GA, Wang LF, Netter HJ. The non-pathogenic Henipavirus Cedar paramyxovirus phosphoprotein has a compromised ability to target STAT1 and STAT2. Antiviral Res [Internet]. Elsevier B.V; 2015;124:69–76. Available from: http://dx.doi.org/10.1016/j.antiviral.2015.09.017

116. Drexler JF, Corman VM, Gloza-Rausch F, Seebens A, Annan A, Ipsen A, et al. Henipavirus RNA in African bats. PLoS One. 2009;4:1–5.

117. Pernet O, Schneider BS, Beaty SM, Lebreton M, Yun TE, Park A, et al. Evidence for henipavirus spillover into human populations in Africa. Nat Commun [Internet]. Nature Publishing Group; 2014;5:1–10. Available from: http://dx.doi.org/10.1038/ncomms6342

118. Wu Z, Yang L, Yang F, Ren X, Jiang J, Dong J, et al. Novel Henipa-like virus, Mojiang Paramyxovirus, in rats, China, 2012. Emerg. Infect. Dis. United States; 2014. p. 1064–6.

119. Rissanen I, Ahmed AA, Azarm K, Beaty S, Hong P, Nambulli S, et al. Idiosyncratic Mojiang virus attachment glycoprotein directs a host-cell entry pathway distinct from genetically related henipaviruses. Nat Commun. England; 2017;8:16060.

120. Middleton DJ, Westbury HA, Morrissy CJ, van der Heide BM, Russell GM, Braun MA, et al. Experimental Nipah virus infection in pigs and cats. J Comp Pathol. England; 2002;126:124–36.

121. Marsh GA, Haining J, Hancock TJ, Robinson R, Foord AJ, Barr JA, et al. Experimental Infection of Horses with Hendra Virus/Australia/Horse/2008/Redlands. Emerg. Infect. Dis. 2011. p. 2232–8.

122. Weingartl H, Czub S, Copps J, Middleton D, Marszal P, Gren J, et al. Invasion of the Central Nervous System in a Porcine Host by Nipah Virus Invasion of the Central Nervous System in a Porcine Host by Nipah Virus. J Virol. 2005;79:7528–34.

123. Williamson MM, Hooper PT, Selleck PW, Gleeson LJ, Daniels PW, Westbury HA, et al. Transmission studies of Hendra virus (equine morbillivirus) in fruit bats, horses and cats. Aust Vet J. England; 1998;76:813–8.

124. F.J. T-V, W.J. S, P.E. R, T. M, C. B, T.G. K, et al. Histopathologic and immunohistochemical characterization of Nipah virus infection in the guinea pig. Vet Pathol [Internet]. 2008;45:576–85. Available from: http://www.embase.com/search/results?subaction=viewrecord&from=export&id=L352454393%5Cnhttp://dx.doi.org/10.1354/vp.45-4-576%5Cnhttp://sfx.library.uu.nl/utrecht?sid=EMBASE&issn=03009858&id=doi:10.1354%2Fvp.45-4-576&atitle=Histopathologic+and+immunohistoch

125. De Wit E, Munster VJ. Animal models of disease shed light on Nipah virus pathogenesis and transmission. J Pathol. 2015;235:196–205.

126. Rockx B, Brining D, Kramer J, Callison J, Ebihara H, Mansfield K, et al. Clinical Outcome of Henipavirus Infection in Hamsters Is Determined by the Route and Dose of Infection. J Virol [Internet]. 2011;85:7658–71. Available from: http://jvi.asm.org/cgi/doi/10.1128/JVI.00473-11

127. Wong KT, Grosjean I, Brisson C, Blanquier B, Fevre-Montange M, Bernard A, et al. A golden hamster model for human acute Nipah virus infection. Am J Pathol. United States; 2003;163:2127–37.

128. Bossart KN, Zhu Z, Middleton D, Klippel J, Crameri G, Bingham J, et al. A neutralizing human monoclonal antibody protects against lethal disease in a new ferret model of acute nipah virus infection. PLoS Pathog. United States; 2009;5:e1000642.

129. Pallister J, Middleton D, Crameri G, Yamada M, Klein R, Hancock TJ, et al. Chloroquine administration does not prevent Nipah virus infection and disease in ferrets. J Virol. United States; 2009;83:11979–82.

130. Rockx B, Bossart KN, Feldmann F, Geisbert JB, Hickey AC, Brining D, et al. A novel model of lethal Hendra virus infection in African green monkeys and the effectiveness of ribavirin treatment. J Virol. United States; 2010;84:9831–9.

131. Geisbert TW, Daddario-DiCaprio KM, Hickey AC, Smith MA, Chan Y-P, Wang L-F, et al. Development of an acute and highly pathogenic nonhuman primate model of Nipah virus infection. PLoS One. United States; 2010;5:e10690.

132. Dhondt KP, Mathieu C, Chalons M, Reynaud JM, Vallve A, Raoul H, et al. Type I Interferon Signaling Protects Mice From Lethal Henipavirus Infection. J Infect Dis [Internet]. 2013;207:142–51. Available from: https://academic.oup.com/jid/article-lookup/doi/10.1093/infdis/jis653

133. Dups J, Middleton D, Long F, Arkinstall R, Marsh GA, Wang LF. Subclinical infection without encephalitis in mice following intranasal exposure to Nipah virus-Malaysia and Nipah virus-Bangladesh. Virol J. 2014;11:1–5.

134. Dups J, Middleton D, Yamada M, Monaghan P, Long F, Robinson R, et al. A new model for Hendra virus encephalitis in the mouse. PLoS One. 2012;7:1–14.

135. Valbuena G, Halliday H, Borisevich V, Goez Y, Rockx B. A Human Lung Xenograft Mouse Model of Nipah Virus Infection. PLoS Pathog. 2014;10.

136. Escaffre O, Saito TB, Juelich TL, Ikegami T, Smith JK, Perez DD, et al. Contribution of human lung parenchyma and leukocyte influx to oxidative stress and immune systemmediated pathology following Nipah virus infection. J Virol. 2017;91:1–15.

137. Mire CE, Satterfield BA, Geisbert JB, Agans KN, Borisevich V, Yan L, et al. Pathogenic Differences between Nipah Virus Bangladesh and Malaysia Strains in Primates: Implications for Antibody Therapy. Sci Rep. 2016;6:1–16.

138. Baseler L, Scott DP, Saturday G, Horne E, Rosenke R, Thomas T, et al. Identifying Early Target Cells of Nipah Virus Infection in Syrian Hamsters. PLoS Negl Trop Dis. 2016;10:1–18.

139. Mathieu C, Guillaume V, Sabine A, Ong KC, Wong KT, Legras-Lachuer C, et al. Lethal nipah virus infection induces rapid overexpression of cxcl10. PLoS One. 2012;7.

140. Chang L-Y, Ali AM, Hassan S, AbuBakar S. Human neuronal cell protein responses to Nipah virus infection. Virol J [Internet]. 2007;4:54. Available from: http://virologyj.biomedcentral.com/articles/10.1186/1743-422X-4-54

141. Chang L-Y, Ali ARM, Hassan SS, AbuBakar S. Nipah virus RNA synthesis in cultured pig and human cells. J Med Virol. United States; 2006;78:1105–12.

142. Aljofan M, Saubern S, Meyer AG, Marsh G, Meers J, Mungall BA. Characteristics of Nipah virus and Hendra virus replication in different cell lines and their suitability for antiviral screening. Virus Res. 2009;142:92–9.

143. Lo MK, Miller D, Aljofan M, Mungall BA, Rollin PE, Bellini WJ, et al. Characterization of the antiviral and inflammatory responses against Nipah virus in endothelial cells and neurons. Virology [Internet]. Elsevier B.V.; 2010;404:78–88. Available from: http://dx.doi.org/10.1016/j.virol.2010.05.005

144. Escaffre O, Borisevich V, Vergara LA, Wen JW, Long D, Rockx B. Characterization of Nipah virus infection in a model of human airway epithelial cells cultured at an air–liquid interface. J Gen Virol. 2016;97:1077–86.

145. Anlar B. Subacute sclerosing panencephalitis and chronic viral encephalitis [Internet]. 1st ed. Handb. Clin. Neurol. Elsevier B.V.; 2013. Available from: http://dx.doi.org/10.1016/B978-0-444-52910-7.00039-8

146. Schneider-Schaulies S, Liebert UG, Segev Y, Rager-Zisman B, Wolfson M, ter Meulen V. Antibody-dependent transcriptional regulation of measles virus in persistently infected neural cells. J Virol. United States; 1992;66:5534–41.

147. Fujinami RS, Oldstone MB. Alterations in expression of measles virus polypeptides by antibody: molecular events in antibody-induced antigenic modulation. J Immunol. United States; 1980;125:78–85.

148. Reuter D, Schneider-Schaulies J. Measles virus infection of the CNS: Human disease, animal models, and approaches to therapy. Med Microbiol Immunol. 2010;199:261–71.

149. Fang YY, Song ZM, Wu T, Raha R. A, Kalvakolanu D V., Dhib-Jalbut S. Defective NF-κB activation in virus-infected neuronal cells is restored by genetic complementation. J Neurovirol. 2002;8:459–63.

150. Dhib-Jalbut S, Xia J, Rangaviggula H, Fang YY, Lee T. Failure of measles virus to activate nuclear factor-kappa B in neuronal cells: implications on the immune response to viral infections in the central nervous system. J Immunol. United States; 1999;162:4024–9.

151. Fang YY, Song ZM, Dhib-Jalbut S. Mechanism of measles virus failure to activate NF-kappaB in neuronal cells. J Neurovirol. United States; 2001;7:25–34.

152. Sato Y, Watanabe S, Fukuda Y, Hashiguchi T, Yanagi Y, Ohno S. Cell-to-cell measles virus spread between human neurons dependent on the hemagglutinin and the hyperfusogenic fusion protein. J Virol [Internet]. 2018;92:JVI.02166-17. Available from: http://jvi.asm.org/lookup/doi/10.1128/JVI.02166-17

153. Cattaneo R, Schmid A, Billeter MA, Sheppard RD, Udem SA. Multiple viral mutations rather than host factors cause defective measles virus gene expression in a subacute sclerosing panencephalitis cell line. J Virol. United States; 1988;62:1388–97.

154. Patterson JB, Cornu TI, Redwine J, Dales S, Lewicki H, Holz A, et al. Evidence that the hypermutated M protein of a subacute sclerosing panencephalitis measles virus actively contributes to the chronic progressive CNS disease. Virology. 2001;291:215–25.

155. Watanabe S, Ohno S, Shirogane Y, Suzuki SO, Koga R, Yanagi Y. Measles Virus Mutants Possessing the Fusion Protein with Enhanced Fusion Activity Spread Effectively in Neuronal Cells, but Not in Other Cells, without Causing Strong Cytopathology. J Virol [Internet]. 2015;89:2710–7. Available from: http://jvi.asm.org/lookup/doi/10.1128/JVI.03346-14

156. Millar EL, Rennick LJ, Weissbrich B, Schneider-Schaulies J, Duprex WP, Rima BK. The phosphoprotein genes of measles viruses from subacute sclerosing panencephalitis cases encode functional as well as non-functional proteins and display reduced editing. Virus Res [Internet]. Elsevier B.V.; 2016;211:29–37. Available from: http://dx.doi.org/10.1016/j.virusres.2015.09.016

157. Wong KT. Nipah and Hendra viruses: recent advances in pathogenesis ". 2010;5:129–31.

158. Satterfield BA, Cross RW, Fenton KA, Borisevich V, Agans KN, Deer DJ, et al. Nipah Virus C and W Proteins Contribute to Respiratory Disease in Ferrets. J Virol [Internet]. 2016;90:6326–43. Available from: http://jvi.asm.org/lookup/doi/10.1128/JVI.00215-16

159. Escaffre O, Borisevich V, Carmical JR, Prusak D, Prescott J, Feldmann H, et al. Henipavirus Pathogenesis in Human Respiratory Epithelial Cells. J Virol [Internet]. 2013;87:3284–94. Available from: http://jvi.asm.org/cgi/doi/10.1128/JVI.02576-12

160. Basler CF. Nipah and hendra virus interactions with the innate immune system. Curr Top Microbiol Immunol. Germany; 2012;359:123–52.

161. Kulkarni S, Volchkova V, Basler CF, Palese P, Volchkov VE, Shaw ML. Nipah Virus Edits Its P Gene at High Frequency To Express the V and W Proteins. J Virol [Internet]. 2009;83:3982–7. Available from: http://jvi.asm.org/cgi/doi/10.1128/JVI.02599-08

162. Parisien J-P, Bamming D, Komuro A, Ramachandran A, Rodriguez JJ, Barber G, et al. A shared interface mediates paramyxovirus interference with antiviral RNA

helicases MDA5 and LGP2. J Virol [Internet]. 2009;83:7252–60. Available from: 10.1128/JVI.00153-09%5Cnhttp://proxy-remote.galib.uga.edu/login?url=http://search.ebscohost.com/login.aspx?direct=true&db=a9h&AN=43405555&site=eds-live

163. Rodriguez JJ, Parisien J, Horvath CM. Nipah Virus Evasion of STAT 1,2 Transcription Factors. J Virol [Internet]. 2002;76:11476–83. Available from: http://www.pubmedcentral.nih.gov/articlerender.fcgi?artid=136769&tool=pmcentrez&rendertype=abstract

164. Rodriguez JJ, Wang L-F, Horvath CM. Hendra virus V protein inhibits interferon signaling by preventing STAT1 and STAT2 nuclear accumulation. J Virol [Internet]. 2003;77:11842–5. Available from: http://www.pubmedcentral.nih.gov/articlerender.fcgi?artid=229371&tool=pmcentrez&rendertype=abstract

165. Yoneda M, Guillaume V, Sato H, Fujita K, Georges-Courbot MC, Ikeda F, et al. The nonstructural proteins of Nipah virus play a key role in pathogenicity in experimentally infected animals. PLoS One. 2010;5:1–8.

166. Mathieu C, Guillaume V, Volchkova VA, Pohl C, Jacquot F, Looi RY, et al. Nonstructural Nipah Virus C Protein Regulates both the Early Host Proinflammatory Response and Viral Virulence. J Virol [Internet]. 2012;86:10766–75. Available from: http://jvi.asm.org/cgi/doi/10.1128/JVI.01203-12

167. Blank T, Prinz M. Type I interferon pathway in CNS homeostasis and neurological disorders. Glia. 2017;65:1397–406.

168. Detje CN, Lienenklaus S, Chhatbar C, Spanier J, Prajeeth CK, Soldner C, et al. Upon Intranasal Vesicular Stomatitis Virus Infection, Astrocytes in the Olfactory Bulb Are Important Interferon Beta Producers That Protect from Lethal Encephalitis. J Virol [Internet]. 2015;89:2731–8. Available from: http://jvi.asm.org/lookup/doi/10.1128/JVI.02044-14

169. Ireland DDC, Stohlman SA, Hinton DR, Atkinson R, Bergmann CC. Type I Interferons Are Essential in Controlling Neurotropic Coronavirus Infection Irrespective of Functional CD8 T Cells. J Virol [Internet]. 2008;82:300–10. Available from: http://jvi.asm.org/cgi/doi/10.1128/JVI.01794-07

170. Burdeinick-Kerr R, Wind J, Griffin DE. Synergistic Roles of Antibody and Interferon in Noncytolytic Clearance of Sindbis Virus from Different Regions of the Central Nervous System. J Virol [Internet]. 2007;81:5628–36. Available from: http://jvi.asm.org/cgi/doi/10.1128/JVI.01152-06

171. Samuel M a, Diamond MS. Alpha / Beta Interferon Protects against Lethal West Nile Virus Infection by Restricting Cellular Tropism and Enhancing Neuronal Survival Alpha / Beta Interferon Protects against Lethal West Nile Virus Infection by Restricting Cellular Tropism and Enhanci. J Virol. 2005;79:13350–61.

172. Staeheli P, Sentandreu M, Pagenstecher a, Hausmann J. Alpha/beta interferon promotes transcription and inhibits replication of borna disease virus in persistently infected cells. J Virol. 2001;75:8216–23.

173. Lin CC, Wu YJ, Heimrich B, Schwemmle M. Absence of a robust innate immune response in rat neurons facilitates persistent infection of Borna disease virus in neuronal tissue. Cell Mol Life Sci. 2013;70:4399–410.

174. Cavanaugh SE, Holmgren AM, Rall GF. Homeostatic interferon expression in neurons is sufficient for early control of viral infection. J Neuroimmunol [Internet]. Elsevier B.V.; 2015;279:11–9. Available from: http://dx.doi.org/10.1016/j.jneuroim.2014.12.012

175. Lindqvist R, Mundt F, Gilthorpe JD, Wölfel S, Gekara NO, Kröger A, et al. Fast type I interferon response protects astrocytes from flavivirus infection and virus-induced cytopathic effects. J Neuroinflammation [Internet]. Journal of Neuroinflammation; 2016;13:1–15. Available from: http://dx.doi.org/10.1186/s12974-016-0748-7

176. Li L, Ulrich R, Baumgärtner W, Gerhauser I. Interferon-stimulated genes-essential antiviral effectors implicated in resistance to Theiler's virus-induced demyelinating disease. J Neuroinflammation [Internet]. Journal of Neuroinflammation; 2015;12:1–14. Available from: http://dx.doi.org/10.1186/s12974-015-0462-x

177. Zhao L, Birdwell LD, Wu A, Elliott R, Rose KM, Phillips JM, et al. Cell-Type-Specific Activation of the Oligoadenylate Synthetase-RNase L Pathway by a Murine Coronavirus. J Virol [Internet]. 2013;87:8408–18. Available from: http://jvi.asm.org/cgi/doi/10.1128/JVI.00769-13

178. Kreit M, Paul S, Knoops L, De Cock A, Sorgeloos F, Michiels T. Inefficient Type I Interferon-Mediated Antiviral Protection of Primary Mouse Neurons Is Associated with the Lack of Apolipoprotein L9 Expression. J Virol [Internet]. 2014;88:3874–84. Available from: http://jvi.asm.org/cgi/doi/10.1128/JVI.03018-13

179. Cho H, Proll SC, Szretter KJ, Katze MG, Gale M, Diamond MS. Differential innate immune response programs in neuronal subtypes determine susceptibility to infection in the brain by positive-stranded RNA viruses. Nat Med [Internet]. Nature Publishing Group; 2013;19:458–64. Available from: http://dx.doi.org/10.1038/nm.3108

180. Lazear HM, Pinto AK, Vogt MR, Gale M, Diamond MS. Beta Interferon Controls West Nile Virus Infection and Pathogenesis in Mice. J Virol [Internet]. 2011;85:7186–94. Available from: http://jvi.asm.org/cgi/doi/10.1128/JVI.00396-11

181. Lindqvist R, Kurhade C, Gilthorpe JD, Överby AK. Cell-type- and region-specific restriction of neurotropic flavivirus infection by viperin. J Neuroinflammation. Journal of Neuroinflammation; 2018;15:1–11.

182. Tian B, Zhou M, Yang Y, Yu L, Luo Z, Tian D, et al. Lab-attenuated rabies virus causes abortive infection and induces cytokine expression in astrocytes by activating mitochondrial antiviral-signaling protein signaling pathway. Front Immunol. 2018;8:1–17.

183. Pfefferkorn C, Kallfass C, Lienenklaus S, Spanier J, Kalinke U, Rieder M, et al. Abortively Infected Astrocytes Appear To Represent the Main Source of Interferon Beta in the Virus-Infected Brain. J Virol [Internet]. 2016;90:2031–8. Available from: http://jvi.asm.org/lookup/doi/10.1128/JVI.02979-15

184. van den Pol AN, Ding S, Robek MD. Long-Distance Interferon Signaling within the Brain Blocks Virus Spread. J Virol [Internet]. 2014;88:3695–704. Available from: http://jvi.asm.org/cgi/doi/10.1128/JVI.03509-13

185. Hwang M, Bergmann CC. Alpha/Beta Interferon (IFN-alpha/beta) Signaling in Astrocytes Mediates Protection against Viral Encephalomyelitis and Regulates IFN-gamma-Dependent Responses. J Virol. United States; 2018;92.

186. Daniels BP, Jujjavarapu H, Durrant DM, Williams JL, Green RR, White JP, et al. Regional astrocyte IFN signaling restricts pathogenesis during neurotropic viral infection. J Clin Invest. 2017;127:843–56.

187. Drokhlyansky E, Göz Aytürk D, Soh TK, Chrenek R, O'Loughlin E, Madore C, et al. The brain parenchyma has a type I interferon response that can limit virus spread. Proc Natl Acad Sci [Internet]. 2017;114:E95–104. Available from: http://www.pnas.org/lookup/doi/10.1073/pnas.1618157114

188. Burdeinick-Kerr R, Govindarajan D, Griffin DE. Noncytolytic Clearance of Sindbis Virus Infection from Neurons by Gamma Interferon Is Dependent on Jak/Stat Signaling. J Virol [Internet]. 2009;83:3429–35. Available from: http://jvi.asm.org/cgi/doi/10.1128/JVI.02381-08

189. Burdeinick-kerr R, Griffin DE. Clearance of Sindbis Virus Infection from Neurons In Vitro Gamma Interferon-Dependent , Noncytolytic Clearance of Sindbis Virus Infection from Neurons In Vitro. 2005;79:5374–85.

190. Binder GK, Griffin DE. Interferon-γ-mediated site-specific clearance of alphavirus from CNS neurons. Science (80-). 2001;293:303–6.

191. Patterson CE, Lawrence DMP, Echols LA, Rall GF. Immune-mediated protection from measles virus-induced central nervous system disease is noncytolytic and gamma interferon dependent. J Virol [Internet]. 2002;76:4497–506. Available from: http://www.pubmedcentral.nih.gov/articlerender.fcgi?artid=155105&tool=pmcentrez&rendertype=abstract

192. Stubblefield Park SR, Widness M, Levine AD, Patterson CE. T Cell-, Interleukin-12-, and Gamma Interferon-Driven Viral Clearance in Measles Virus-Infected Brain Tissue. J Virol [Internet]. 2011;85:3664–76. Available from: http://jvi.asm.org/cgi/doi/10.1128/JVI.01496-10

193. O'Donnell LA, Conway S, Rose RW, Nicolas E, Slifker M, Balachandran S, et al. STAT1-Independent Control of a Neurotropic Measles Virus Challenge in

Primary Neurons and Infected Mice. J Immunol [Internet]. 2012;188:1915–23. Available from: http://www.jimmunol.org/cgi/doi/10.4049/jimmunol.1101356

194. O'Donnell LA, Henkins KM, Kulkarni A, Matullo CM, Balachandran S, Pattisapu AK, et al. Interferon Gamma Induces Protective Non-Canonical Signaling Pathways in Primary Neurons. J. Neurochem. 2015. p. 309–22.

195. Rose RW, Vorobyeva AG, Skipworth JD, Nicolas E, Rall GF. Altered Levels of STAT1 and STAT3 Influence the Neuronal Response to Interferon Gamma. J. Neuroimmunol. 2007. p. 145–56.

196. Ramana C V, Gil MP, Schreiber RD, Stark GR. Stat1-dependent and -independent pathways in IFN-gamma-dependent signaling. Trends Immunol. England; 2002;23:96–101.

197. Hausmann J, Pagenstecher A, Baur K, Richter K, Rziha H-J, Staeheli P. CD8 T cells require gamma interferon to clear borna disease virus from the brain and prevent immune system-mediated neuronal damage. J Virol [Internet]. 2005;79:13509–18. Available from: http://www.pubmedcentral.nih.gov/articlerender.fcgi?artid=1262614&tool=pmcentrez&rendertype=abstract

198. Richter K, Hausmann J, Staeheli P. Interferon-γ prevents death of bystander neurons during CD8 T cell responses in the brain. Am J Pathol. 2009;174:1799–807.

199. Geiger KD, Nash TC, Sawyer S, Krahl T, Patstone G, Reed JC, et al. Interferon-gamma protects against herpes simplex virus type 1-mediated neuronal death. Virology. 1997;238:189–97.

200. Geiger KD, Gurushanthaiah D, Howes EL, Lewandowski G a, Reed JC, Bloom FE, et al. Cytokine-mediated survival from lethal herpes simplex virus infection: role of programmed neuronal death. Proc Natl Acad Sci U S A. 1995;92:3411–5.

201. Liu T, Khanna KM, Carriere BN. Gamma Interferon Can Prevent Herpes Simplex Virus Type 1 Reactivation from Latency in Sensory Neurons. Society. 2001;75:11178–84.

202. Schijns VE, Van der Neut R, Haagmans BL, Bar DR, Schellekens H, Horzinek MC. Tumour necrosis factor-alpha, interferon-gamma and interferon-beta exert antiviral activity in nervous tissue cells. J Gen Virol. 1991;72:809–15.

203. van den Pol AN, Robek MD, Ghosh PK, Ozduman K, Bandi P, Whim MD, et al. Cytomegalovirus InducesInterferon-Stimulated Gene Expression and Is Attenuated by Interferon in the Developing Brain. J Virol [Internet]. 2007;81:332–48. Available from: http://jvi.asm.org/cgi/doi/10.1128/JVI.01592-06

204. Rodriguez M, Zoecklein LJ, Howe CL, Pavelko KD, Gamez JD, Nakane S, et al. Gamma interferon is critical for neuronal viral clearance and protection in a susceptible mouse strain following early intracranial Theiler's murine encephalomyelitis virus infection. J Virol. United States; 2003;77:12252–65.

205. Chesler DA, Dodard C, Lee GY, Levy DE, Reiss CS. Interferon-γ-induced inhibition of neuronal vesicular stomatitis virus infection is STAT1 dependent. J Neurovirol. 2004;10:57–63.

206. Burdeinick-Kerr R, Griffin DE. Gamma interferon-dependent, noncytolytic clearance of sindbis virus infection from neurons in vitro. J Virol. United States; 2005;79:5374–85.

207. Rall GF, Manchester M, Daniels LR, Callahan EM, Belman AR, Oldstone MB. A transgenic mouse model for measles virus infection of the brain. Proc Natl Acad Sci U S A. United States; 1997;94:4659–63.

208. Ohno S, Ono N, Seki F, Takeda M, Kura S, Tsuzuki T, et al. Measles virus infection of SLAM (CD150) knockin mice reproduces tropism and immunosuppression in human infection. J Virol. United States; 2007;81:1650–9.

209. Seok J, Warren HS, Cuenca AG, Mindrinos MN, Baker H V., Xu W, et al. Genomic responses in mouse models poorly mimic human inflammatory diseases. Proc Natl Acad Sci [Internet]. 2013;110:3507–12. Available from: http://www.pnas.org/lookup/doi/10.1073/pnas.1222878110

210. Mestas J, Hughes CCW. Of Mice and Not Men: Differences between Mouse and Human Immunology. J Immunol [Internet]. 2004;172:2731–8. Available from: http://www.jimmunol.org/cgi/doi/10.4049/jimmunol.172.5.2731

211. Oberheim NA, Takano T, Han X, He W, Lin JHC, Wang F, et al. Uniquely Hominid Features of Adult Human Astrocytes. J Neurosci [Internet]. 2009;29:3276–87. Available from: http://www.jneurosci.org/cgi/doi/10.1523/JNEUROSCI.4707-08.2009

212. Jordan PM, Cain LD, Wu P. Astrocytes enhance long-term survival of cholinergic neurons differentiated from human fetal neural stem cells. J Neurosci Res. United States; 2008;86:35–47.

213. Faissner S, Ambrosius B, Schanzmann K, Grewe B, Potthoff A, Münch J, et al. Cytoplasmic HIV-RNA in monocytes determines microglial activation and neuronal cell death in HIV-associated neurodegeneration. Exp Neurol [Internet]. Elsevier Inc.; 2014;261:685–97. Available from: http://dx.doi.org/10.1016/j.expneurol.2014.08.011

214. Hill E, Nagel D, Parri R, Coleman M. Stem cell-derived astrocytes: are they physiologically credible? J Physiol. 2016;594:6595–606.

215. Grigoryan S, Kinchington PR, Yang IH, Selariu A, Zhu H, Yee M, et al. Retrograde axonal transport of VZV: Kinetic studies in hESC-derived neurons. J Neurovirol. 2012;18:462–70.

216. Markus A, Grigoryan S, Sloutskin A, Yee MB, Zhu H, Yang IH, et al. Varicella-Zoster Virus (VZV) Infection of Neurons Derived from Human Embryonic Stem Cells: Direct Demonstration of Axonal Infection, Transport of VZV, and Productive Neuronal Infection. J Virol [Internet]. 2011;85:6220–33. Available from: http://jvi.asm.org/cgi/doi/10.1128/JVI.02396-10

217. Pugazhenthi S, Nair S, Velmurugan K, Liang Q, Mahalingam R, Cohrs RJ, et al. Varicella-Zoster Virus Infection of Differentiated Human Neural Stem Cells. J Virol [Internet]. 2011;85:6678–86. Available from: http://jvi.asm.org/cgi/doi/10.1128/JVI.00445-11

218. Markus A, Lebenthal-Loinger I, Yang IH, Kinchington PR, Goldstein RS. An In Vitro Model of Latency and Reactivation of Varicella Zoster Virus in Human Stem Cell-Derived Neurons. PLoS Pathog. 2015;11:1–22.

219. Lee KS, Zhou W, Scott-McKean JJ, Emmerling KL, Cai G yun, Krah DL, et al. Human Sensory Neurons Derived from Induced Pluripotent Stem Cells Support Varicella-Zoster Virus Infection. PLoS One. 2012;7.

220. McGrath EL, Rossi SL, Gao J, Widen SG, Grant AC, Dunn TJ, et al. Differential Responses of Human Fetal Brain Neural Stem Cells to Zika Virus Infection. Stem Cell Reports. 2017;8:715–27.

221. Lancaster MA, Renner M, Martin C-A, Wenzel D, Bicknell LS, Hurles ME, et al. Cerebral organoids model human brain development and microcephaly. Nature [Internet]. Nature Publishing Group, a division of Macmillan Publishers Limited. All Rights Reserved.; 2013;501:373. Available from: http://dx.doi.org/10.1038/nature12517

222. Tang H, Hammack C, Ogden SC, Wen Z, Qian X, Li Y, et al. Zika Virus Infects Human Cortical Neural Progenitors and Attenuates Their Growth. Cell Stem Cell. United States; 2016;18:587–90.

223. Garcez PP, Loiola EC, Madeiro da Costa R, Higa LM, Trindade P, Delvecchio R, et al. Zika virus impairs growth in human neurospheres and brain organoids. Science. United States; 2016;352:816–8.

224. Zhang B, He Y, Xu Y, Mo F, Mi T, Shen QS, et al. Differential antiviral immunity to Japanese encephalitis virus in developing cortical organoids. Cell Death Dis [Internet]. Springer US; 2018; Available from: http://dx.doi.org/10.1038/s41419-018-0763-y

225. Dionne KR, Galvin JM, Schittone SA, Clarke P, Tyler KL. Type I interferon signaling limits reoviral tropism within the brain and prevents lethal systemic infection. J Neurovirol. 2011;17:314–26.

226. Ehrengruber MU, Lundstrom K, Schweitzer C, Heuss C, Schlesinger S, Gahwiler BH. Recombinant Semliki Forest virus and Sindbis virus efficiently infect neurons in hippocampal slice cultures. Proc Natl Acad Sci U S A. United States; 1999;96:7041–6.

227. Wu P, Tarasenko YI, Gu Y, Huang L-YM, Coggeshall RE, Yu Y. Region-specific generation of cholinergic neurons from fetal human neural stem cells grafted in adult rat. Nat Neurosci [Internet]. 2002;5:1271–8. Available from: http://www.nature.com/articles/nn974

228. Cai Y, Wu P, Ozen M, Yu Y, Wang J, Ittmann M, et al. Gene expression profiling and analysis of signaling pathways involved in priming and differentiation of human neural stem cells. Neuroscience. 2006;138:133–48.

229. Tarasenko YI, Yu Y, Jordan PM, Bottenstein J, Wu P. Effect of growth factors on proliferation and phenotypic differentiation of human fetal neural stem cells. J Neurosci Res. 2004;78:625–36.

230. Adams KV, Morshead CM. Neural stem cell heterogeneity in the mammalian forebrain. Prog Neurobiol [Internet]. Elsevier; 2018;0–1. Available from: http://linkinghub.elsevier.com/retrieve/pii/S0301008217301831

231. Yun T, Park A, Hill TE, Pernet O, Beaty SM, Juelich TL, et al. Efficient Reverse Genetics Reveals Genetic Determinants of Budding and Fusogenic Differences between Nipah and Hendra Viruses and Enables Real-Time Monitoring of Viral Spread in Small Animal Models of Henipavirus Infection [Internet]. J. Virol. 2015. Available from: http://jvi.asm.org/lookup/doi/10.1128/JVI.02583-14

232. Herculano-Houzel S. The glia/neuron ratio: how it varies uniformly across brain structures and species and what that means for brain physiology and evolution. Glia. United States; 2014;62:1377–91.

233. Costello DA, Lynch MA. Toll-like receptor 3 activation modulates hippocampal network excitability, via glial production of interferon-?? Hippocampus. 2013;23:696–707.

234. Gesuete R, Packard AEB, Vartanian KB, Conrad VK, Stevens SL, Bahjat FR, et al. Poly-ICLC preconditioning protects the blood-brain barrier against ischemic injury in vitro through type i interferon signaling. J Neurochem. 2012;123:75–85.

235. Savarin C, Bergmann CC, Hinton DR, Stohlman SA. MMP-independent role of TIMP-1 at the blood brain barrier during viral encephalomyelitis. ASN Neuro. United States; 2013;5:e00127.

236. Groters S, Alldinger S, Baumgartner W. Up-regulation of mRNA for matrix metalloproteinases-9 and -14 in advanced lesions of demyelinating canine distemper leukoencephalitis. Acta Neuropathol. Germany; 2005;110:369–82.

237. Toft-Hansen H, Buist R, Sun X-J, Schellenberg A, Peeling J, Owens T. Metalloproteinases control brain inflammation induced by pertussis toxin in mice overexpressing the chemokine CCL2 in the central nervous system. J Immunol. United States; 2006;177:7242–9.

238. Buhler LA, Samara R, Guzman E, Wilson CL, Krizanac-Bengez L, Janigro D, et al. Matrix metalloproteinase-7 facilitates immune access to the CNS in experimental autoimmune encephalomyelitis. BMC Neurosci. England; 2009;10:17.

239. Conant K, McArthur JC, Griffin DE, Sjulson L, Wahl LM, Irani DN. Cerebrospinal fluid levels of MMP-2, 7, and 9 are elevated in association with human immunodeficiency virus dementia. Ann Neurol. United States; 1999;46:391–8.

240. Gardner J, Ghorpade A. Tissue inhibitor of metalloproteinase (TIMP)-1: the TIMPed balance of matrix metalloproteinases in the central nervous system. J Neurosci Res. United States; 2003;74:801–6.

241. Morrey JD, Siddharthan V, Wang H. Neurological approaches for investigating West Nile virus disease and its treatment in rodents. Antiviral Res [Internet].

Elsevier B.V.; 2013;100:535–45. Available from: http://dx.doi.org/10.1016/j.antiviral.2013.09.010

242. Salimi H, Cain MD, Klein RS. Encephalitic Arboviruses: Emergence, Clinical Presentation, and Neuropathogenesis. Neurotherapeutics [Internet]. Neurotherapeutics; 2016;13:514–34. Available from: http://dx.doi.org/10.1007/s13311-016-0443-5

243. De Miranda J, Yaddanapudi K, Hornig M, Lipkin WI. Astrocytes recognize intracellular polyinosinic-polycytidylic acid via MDA-5. FASEB J [Internet]. The Federation of American Societies for Experimental Biology; 2009;23:1064–71. Available from: http://www.ncbi.nlm.nih.gov/pmc/articles/PMC2660646/

244. Banisadr G, Gosselin R-D, Mechighel P, Kitabgi P, Rostene W, Parsadaniantz SM. Highly regionalized neuronal expression of monocyte chemoattractant protein-1 (MCP-1/CCL2) in rat brain: evidence for its colocalization with neurotransmitters and neuropeptides. J Comp Neurol. United States; 2005;489:275–92.

245. Park J, Wetzel I, Marriott I, Dreau D, D'Avanzo C, Kim DY, et al. A 3D human triculture system modeling neurodegeneration and neuroinflammation in Alzheimer's disease. Nat Neurosci. United States; 2018;21:941–51.

246. Metcalf TU, Baxter VK, Nilaratanakul V, Griffin DE. Recruitment and Retention of B Cells in the Central Nervous System in Response to Alphavirus Encephalomyelitis. J Virol [Internet]. 2013;87:2420–9. Available from: http://jvi.asm.org/cgi/doi/10.1128/JVI.01769-12

247. Michlmayr D, McKimmie CS, Pingen M, Haxton B, Mansfield K, Johnson N, et al. Defining the Chemokine Basis for Leukocyte Recruitment during Viral Encephalitis. J Virol [Internet]. 2014;88:9553–67. Available from: http://jvi.asm.org/cgi/doi/10.1128/JVI.03421-13

248. Liu MT, Chen BP, Oertel P, Buchmeier MJ, Armstrong D, Hamilton TA, et al. Cutting Edge: The T Cell Chemoattractant IFN-Inducible Protein 10 Is Essential in Host Defense Against Viral-Induced Neurologic Disease. J Immunol [Internet]. 2000;165:2327–30. Available from: http://www.jimmunol.org/cgi/doi/10.4049/jimmunol.165.5.2327

249. Wuest TR, Carr DJJ. Dysregulation of CXCR3 Signaling due to CXCL10 Deficiency Impairs the Antiviral Response to Herpes Simplex Virus 1 Infection. J Immunol [Internet]. 2008;181:7985–93. Available from: http://www.jimmunol.org/cgi/doi/10.4049/jimmunol.181.11.7985

250. Glass WG, McDermott DH, Lim JK, Lekhong S, Yu SF, Frank WA, et al. CCR5 deficiency increases risk of symptomatic West Nile virus infection. J Exp Med [Internet]. 2006;203:35 LP-40. Available from: http://jem.rupress.org/content/203/1/35.abstract

251. Smith PM, Wolcott RM, Chervenak R, Jennings SR. Control of acute cutaneous herpes simplex virus infection: T cell-mediated viral clearance is dependent upon interferon-gamma (IFN-gamma). Virology. United States; 1994;202:76–88.

252. Reed C, Lin K, Wilhelmsen C, Friedrich B, Nalca A, Keeney A, et al. Aerosol Exposure to Rift Valley Fever Virus Causes Earlier and More Severe Neuropathology in the Murine Model, which Has Important Implications for Therapeutic Development. PLoS Negl Trop Dis. 2013;7.

253. Dodd KA, McElroy AK, Jones TL, Zaki SR, Nichol ST, Spiropoulou CF. Rift Valley Fever Virus Encephalitis Is Associated with an Ineffective Systemic Immune Response and Activated T Cell Infiltration into the CNS in an Immunocompetent Mouse Model. PLoS Negl Trop Dis. 2014;8.

254. Georges-Courbot M, Contamin H, Faure C, Loth P, Leyssen P, Neyts J, et al. Poly (I)-Poly (C(12)U) but Not Ribavirin Prevents Death in a Hamster Model of Nipah Virus Infection. Am Soc Microbiol [Internet]. 2006;50:1768–72. Available from: http://aac.asm.org/content/50/5/1768.full.pdf+html

255. Hyatt AD, Zaki SR, Goldsmith CS, Wise TG, Hengstberger SG. Ultrastructure of Hendra virus and Nipah virus within cultured cells and host animals. Microbes Infect. 2001;3:297–306.

256. Borisevich V, Ozdener MH, Malik B, Rockx B. Hendra and Nipah Virus Infection in Cultured Human Olfactory Epithelial Cells. mSphere. United States; 2017;2.

257. Paul S, Ricour C, Sommereyns C, Sorgeloos F, Michiels T. Type I interferon response in the central nervous system. Biochimie. 2007;89:770–8.

258. Fantetti KN, Gray EL, Ganesan P, Kulkarni A, O'Donnell LA. Interferon gamma protects neonatal neural stem/progenitor cells during measles virus infection of the brain. J Neuroinflammation [Internet]. Journal of Neuroinflammation; 2016;13:1–17. Available from: http://dx.doi.org/10.1186/s12974-016-0571-1

259. Ganesan P, Chandwani MN, Creisher PS, Bohn L, O'Donnell LA. The neonatal anti-viral response fails to control measles virus spread in neurons despite interferon-gamma expression and a Th1-like cytokine profile. J Neuroimmunol [Internet]. Elsevier; 2018;316:80–97. Available from: https://doi.org/10.1016/j.jneuroim.2017.12.018

260. Habjan M, Pichlmair A, Elliott RM, Overby AK, Glatter T, Gstaiger M, et al. NSs Protein of Rift Valley Fever Virus Induces the Specific Degradation of the Double-Stranded RNA-Dependent Protein Kinase. J Virol [Internet]. 2009;83:4365–75. Available from: http://jvi.asm.org/cgi/doi/10.1128/JVI.02148-08

261. Verbruggen P, Ruf M, Blakqori G, Overby AK, Heidemann M, Eick D, et al. Interferon antagonist NSs of La Crosse virus triggers a DNA damage response-like degradation of transcribing RNA polymerase II. J Biol Chem. United States; 2011;286:3681–92.

262. Chang L-Y, Ali ARM, Hassan SS, AbuBakar S. Human neuronal cell protein responses to Nipah virus infection. Virol J [Internet]. 2007;4:54. Available from: http://www.virologyj.com/content/4/1/54

263. Ong KC, Wong KT. Henipavirus encephalitis: Recent developments and advances. Brain Pathol. 2015;25:605–13.

264. Rockx B, Winegar R, Freiberg AN. Recent progress in henipavirus research: Molecular biology, genetic diversity, animal models. Antiviral Res [Internet]. Elsevier B.V.; 2012;95:135–49. Available from: http://dx.doi.org/10.1016/j.antiviral.2012.05.008

265. Olson JG, Rupprecht C, Rollin PE, An US, Niezgoda M, Clemins T, et al. Antibodies to Nipah-like virus in bats (Pteropus lylei), Cambodia. Emerg Infect Dis. United States; 2002;8:987–8.

266. Mire CE, Geisbert JB, Agans KN, Feng Y-R, Fenton KA, Bossart KN, et al. A recombinant Hendra virus G glycoprotein subunit vaccine protects nonhuman primates against Hendra virus challenge. J Virol. United States; 2014;88:4624–31.

267. Broder CC. Passive immunization and active vaccination against Hendra and Nipah viruses. Dev Biol (Basel). Switzerland; 2013;135:125–38.

268. Cartwright D. Hendra virus vaccine trial reveals no ill-effects [Internet]. Sydney Morning Her. 2016. Available from: https://www.smh.com.au/national/queensland/hendra-virus-vaccine-trial-reveals-no-illeffects-20160628-gpt9nk.html

269. Chong HT, Kamarulzaman A, Tan CT, Goh KJ, Thayaparan T, Kunjapan SR, et al. Treatment of acute Nipah encephalitis with ribavirin. Ann Neurol. United States; 2001;49:810–3.

270. Freiberg AN, Worthy MN, Lee B, Holbrook MR. Combined chloroquine and ribavirin treatment does not prevent death in a hamster model of Nipah and Hendra virus infection. J Gen Virol. England; 2010;91:765–72.

271. Lo MK, Jordan R, Arvey A, Sudhamsu J, Shrivastava-Ranjan P, Hotard AL, et al. GS-5734 and its parent nucleoside analog inhibit Filo-, Pneumo-, and Paramyxoviruses. Sci Rep. England; 2017;7:43395.

272. Siegel D, Hui HC, Doerffler E, Clarke MO, Chun K, Zhang L, et al. Discovery and Synthesis of a Phosphoramidate Prodrug of a Pyrrolo[2,1-f][triazin-4-amino] Adenine C-Nucleoside (GS-5734) for the Treatment of Ebola and Emerging Viruses. J Med Chem. United States; 2017;60:1648–61.

273. Hotard AL, He B, Nichol ST, Spiropoulou CF, Lo MK. 4’-Azidocytidine (R1479) inhibits henipaviruses and other paramyxoviruses with high potency. Antiviral Res. Netherlands; 2017;144:147–52.

274. Furuta Y, Takahashi K, Fukuda Y, Kuno M, Kamiyama T, Kozaki K, et al. In vitro and in vivo activities of anti-influenza virus compound T-705. Antimicrob Agents Chemother. United States; 2002;46:977–81.

275. Koszalka P, Tilmanis D, Hurt AC. Influenza antivirals currently in late-phase clinical trial. Influenza Other Respi Viruses. England; 2017;11:240–6.

276. Sangawa H, Komeno T, Nishikawa H, Yoshida A, Takahashi K, Nomura N, et al. Mechanism of action of T-705 ribosyl triphosphate against influenza virus RNA polymerase. Antimicrob Agents Chemother. 2013;57:5202–8.

277. Delang L, Segura Guerrero N, Tas A, Querat G, Pastorino B, Froeyen M, et al. Mutations in the chikungunya virus non-structural proteins cause resistance to favipiravir (T-705), a broad-spectrum antiviral. J Antimicrob Chemother. England; 2014;69:2770–84.

278. Yamada K, Noguchi K, Komeno T, Furuta Y, Nishizono A. Efficacy of Favipiravir (T-705) in Rabies Postexposure Prophylaxis. J Infect Dis. United States; 2016;213:1253–61.

279. Sissoko D, Laouenan C, Folkesson E, M'Lebing A-B, Beavogui A-H, Baize S, et al. Experimental Treatment with Favipiravir for Ebola Virus Disease (the JIKI Trial): A Historically Controlled, Single-Arm Proof-of-Concept Trial in Guinea. PLoS Med. United States; 2016;13:e1001967.

280. Jochmans D, van Nieuwkoop S, Smits SL, Neyts J, Fouchier RAM, van den Hoogen BG. Antiviral Activity of Favipiravir (T-705) against a Broad Range of Paramyxoviruses In Vitro and against Human Metapneumovirus in Hamsters. Antimicrob Agents Chemother. United States; 2016;60:4620–9.

281. Safronetz D, Rosenke K, Westover JB, Martellaro C, Okumura A, Furuta Y, et al. The broad-spectrum antiviral favipiravir protects guinea pigs from lethal Lassa virus infection post-disease onset. Sci Rep. England; 2015;5:14775.

282. Scharton D, Bailey KW, Vest Z, Westover JB, Kumaki Y, Van Wettere A, et al. Favipiravir (T-705) protects against peracute Rift Valley fever virus infection and reduces delayed-onset neurologic disease observed with ribavirin treatment. Antiviral Res. Netherlands; 2014;104:84–92.

283. Oestereich L, Rieger T, Neumann M, Bernreuther C, Lehmann M, Krasemann S, et al. Evaluation of antiviral efficacy of ribavirin, arbidol, and T-705 (favipiravir) in a mouse model for Crimean-Congo hemorrhagic fever. PLoS Negl Trop Dis. United States; 2014;8:e2804.

284. Gowen BB, Juelich TL, Sefing EJ, Brasel T, Smith JK, Zhang L, et al. Favipiravir (T-705) inhibits Junin virus infection and reduces mortality in a guinea pig model of Argentine hemorrhagic fever. PLoS Negl Trop Dis. United States; 2013;7:e2614.

285. Gowen BB, Sefing EJ, Westover JB, Smee DF, Hagloch J, Furuta Y, et al. Alterations in favipiravir (T-705) pharmacokinetics and biodistribution in a hamster model of viral hemorrhagic fever. Antiviral Res. Netherlands; 2015;121:132–7.

286. Oestereich L, Ludtke A, Wurr S, Rieger T, Munoz-Fontela C, Gunther S. Successful treatment of advanced Ebola virus infection with T-705 (favipiravir) in a small animal model. Antiviral Res. Netherlands; 2014;105:17–21.

287. Tani H, Fukuma A, Fukushi S, Taniguchi S, Yoshikawa T, Iwata-Yoshikawa N, et al. Efficacy of T-705 (Favipiravir) in the Treatment of Infections with Lethal Severe Fever with Thrombocytopenia Syndrome Virus. mSphere. United States; 2016;1.

288. DeBuysscher BL, Scott D, Marzi A, Prescott J, Feldmann H. Single-dose live-attenuated Nipah virus vaccines confer complete protection by eliciting antibodies directed against surface glycoproteins. Vaccine. Netherlands; 2014;32:2637–44.

289. Lo MK, Bird BH, Chattopadhyay A, Drew CP, Martin BE, Coleman JD, et al. Single-dose replication-defective VSV-based Nipah virus vaccines provide protection from lethal challenge in Syrian hamsters. Antiviral Res. Netherlands; 2014;101:26–9.

290. Guillaume V, Contamin H, Loth P, Grosjean I, Courbot MCG, Deubel V, et al. Antibody prophylaxis and therapy against Nipah virus infection in hamsters. J Virol. United States; 2006;80:1972–8.

291. Porotto M, Rockx B, Yokoyama CC, Talekar A, Devito I, Palermo LM, et al. Inhibition of Nipah virus infection in vivo: targeting an early stage of paramyxovirus fusion activation during viral entry. PLoS Pathog. United States; 2010;6:e1001168.

292. Park A, Yun T, Hill TE, Ikegami T, Juelich TL, Smith JK, et al. Optimized P2A for reporter gene insertion into nipah virus results in efficient ribosomal skipping and wild-type lethality. J Gen Virol. 2016;97:839–43.

293. Sidwell RW, Barnard DL, Day CW, Smee DF, Bailey KW, Wong M-H, et al. Efficacy of orally administered T-705 on lethal avian influenza A (H5N1) virus infections in mice. Antimicrob Agents Chemother. United States; 2007;51:845–51.

294. Bossart KN, Geisbert TW, Feldmann H, Zhu Z, Feldmann F, Geisbert JB, et al. A neutralizing human monoclonal antibody protects african green monkeys from hendra virus challenge. Sci Transl Med. United States; 2011;3:105ra103.

295. Pessi A, Langella A, Capito E, Ghezzi S, Vicenzi E, Poli G, et al. A general strategy to endow natural fusion-protein-derived peptides with potent antiviral activity. PLoS One. United States; 2012;7:e36833.

296. Gowen BB, Smee DF, Wong M-H, Hall JO, Jung K-H, Bailey KW, et al. Treatment of late stage disease in a model of arenaviral hemorrhagic fever: T-705 efficacy and reduced toxicity suggests an alternative to ribavirin. PLoS One. United States; 2008;3:e3725.

297. Gowen BB, Westover JB, Miao J, Van Wettere AJ, Rigas JD, Hickerson BT, et al. Modeling Severe Fever with Thrombocytopenia Syndrome Virus Infection in Golden Syrian Hamsters: Importance of STAT2 in Preventing Disease and Effective Treatment with Favipiravir. J Virol. United States; 2017;91.

298. Kiso M, Takahashi K, Sakai-Tagawa Y, Shinya K, Sakabe S, Le QM, et al. T-705 (favipiravir) activity against lethal H5N1 influenza A viruses. Proc Natl Acad Sci U S A. United States; 2010;107:882–7.

Vita

Brian Erik Dawes was born in Colorado Springs, CO on June 28th, 1990 to Gary and Mary Dawes. He married Sofia Fanourakis on July 1st, 2018. Brian graduated from Hendersonville High School in Hendersonville, TN in 2008. Brian then attended the University of Illinois at Urbana-Champaign, Urbana, IL. As an undergraduate he performed research on host resistance to *Yersinia pestis* with Dr. Richard Tapping, Ph.D. Brian graduated in 2012 with his B.S. in molecular and cellular biology *magna cum laude*. Brian then matriculated into the University of Texas Medical Branch, Galveston, TX, in the M.D./Ph.D. combined degree program in 2012. After completing the first two years of medical school Brian joined the lab of Dr. Alexander Freiberg, Ph.D. where he performed his Ph.D. studies on the neuropathogenesis of La Crosse virus and Nipah virus using human neural stem cell derived neuron/astrocyte co-cultures. In addition, Brian studied performed research on the efficacy of favipiravir as an antiviral against Nipah virus infection which was published in the online peer-reviewed journal *Scientific Reports*.

Education

B.S., Molecular and Cellular Biology, University of Illinois at Urbana-Champaign

Peer Reviewed Publications

Dawes BE, Kalveram B, Ikegami T, Juelich T, Smith JK, Zhang L, Park A, Lee B, Komeno T, Furuta Y, Freiberg AN. Favipiravir (T-705) protects against Nipah virus infection in the hamster model. Sci Rep. 2018 May 15;8(1):7604

Bharaj P, Atkins C, Luthra P, Giraldo MI, **Dawes BE**, Miorin L, Johnson JR, Krozan NJ, Basler CF, Freiberg AN, Rajsbaum R. The host E3-Ubiquitin ligase TRIM6 ubiquitinates the Ebola virus VP35 protein and promotes virus replication. J Virol. 2017 Jul 5. pii: JVI.00833-17. doi: 10.1128/JVI.00833-17

Bharaj P, Wang YE, **Dawes BE**, Yun TE, Park A, Yen B, Basler CF, Freiberg AN, Lee B, Rajsbaum R. The Matrix Protein of Nipah Virus Targets the E3-Ubiquitin Ligase TRIM6 to Inhibit the IKKε Kinase-Mediated Type-I IFN Antiviral Response. PLoS Pathog. 2016 Sep 13;12(9):e1005880

Dawes BE, Smalley C, Tiner B, Beasley D, Milligan G, Reece L, Hombach J, Barrett A. Research and development of Zika virus vaccines. NPJ Vaccines. 2016 July 28; 1:16007.

S Satterfield BA, **Dawes BE**, Milligan GN. Status of vaccine research and development of vaccines for Nipah virus. Vaccine. 2016 Jun 3;34(26):2971-5. doi: 10.1016/j.vaccine.2015.12.075

Park A, Yun T, Vigant F, Pernet O, Won ST, **Dawes BE**, Bartkowski W, Freiberg AN, Lee B. Nipah Virus C Protein Recruits Tsg101 to Promote the Efficient Release of Virus in an ESCRT-Dependent Pathway. PLoS Pathog. 2016 May 20;12(5):e1005659

Abstracts

Dawes B.E., Gao J., Wu P., Freiberg AN., *Responses of Human Neuronal Cells to Nipah Virus Infection.* Poster Presentation at the Cell Symposium for Emerging and Re-emerging Viruses, Arlington, VA, Oct 2, 2017

Dawes B., Gao J., Wu P., Freiberg A., *Infection of Human Neuronal Stem Cell Derived Neuron/Astrocyte Co-Cultures with Henipaviruses*. Oral Presentation at the 35th Annual Meeting of the American Society of Virology; Jun 20, 2016; Blacksburg, VA

Dawes B., Gao J., Wu P., Freiberg A., *Infection of Human Neuronal Stem Cell Derived Neuron/Astrocyte Co-Cultures with La Crosse Virus*. Oral Presentation at the 34th Annual Meeting of the American Society of Virology; Jul 11, 2015; London, ON, Canada

Dawes B., Zhang L., Komeno T., Furuta Y., Freiberg A., *T-705 (favipiravir) activity against Henipaviruses*. Oral Presentation at the 34th Annual Meeting of the American Society of Virology; Jul 12, 2015; London, ON, Canada

Permanent address: 1455 Louisiana Ave. Apt 3202, League City, Texas 77573

This dissertation was typed by Brian Erik Dawes.